THE DESIGN AND APPLICATION OF PEPTIDES AND SYNTHETIC RECEPTORS TO CHEMICAL BIOLOGY

Effrat Libby Fayer

A dissertation submitted to the faculty of the University of North Carolina at Chapel Hill in partial fulfillment of the requirements for the degree of Doctor of Philosophy in the Department of Chemistry (Organic) in the College of Arts & Sciences

Chapel Hill
2016

Approved by:

Marcey Waters

Nancy Allbritton

Michel Gagné

Jeffrey Johnson

Kevin Weeks

ABSTRACT

Effrat Libby Fayer: The Design and Application of Peptides and Synthetic Receptors to Chemical Biology
(Under the direction of Marcey Waters)

The need for chemical tools to probe biological process has become increasingly apparent in the last decade. The work presented here focused on developing such tools, taking on two different paths of development-one using supramolecular chemistry to aid in proteomics, a highly popular focus of research, and the other making use of peptides to create reporters with the ability to probe enzyme activity in cells.

Posttranslational Modifications (PTMs) of proteins are implicated in a wide range of biological processes, including gene transcription, DNA replication and repair, mitosis, and meiosis.[1] Consequently, their dysregulation is linked to various diseases, including cancer, asthma, and diabetes, among others, and can thus serve as valuable diagnostic indicators of disease progression.[1,2] Due to these biological ramifications, there is great interest in mapping where, when, why, and how PTMs are installed and their subsequent downstream effects, though this is often hampered by their presence in complex mixtures, consisting of mostly un-modified proteins/peptides.

Using synthetic supramolecular receptors developed in our lab,[3] an affinity chromatography based method is described here that allows for the separation/enrichment of posttranslationally methylated peptides from such mixtures. This takes advantage of the receptor's greater affinity towards methylated lysine over its non-methylated counterpart. When

attached to a solid support, the receptors can be used to make a column, through which peptides will travel at different rates based on the methylation states of lysine residues. This allows for the separation of these peptides, drastically simplifying their detection and analysis.

Just as important as PTMs are the enzymes that install them. Dysregulation of various enzymatic pathways is implicated in many diseases. The ability to monitor enzyme activity within cells is becoming increasingly important, for promoting further discovery, as well as to enable early detection and patient monitoring during treatment. The use of peptide substrates for such assays is extremely advantageous, as they are the best mimics of the enzymes' natural substrates. Furthermore, the ease of synthesizing peptides allows them to be easily modified for specialized function and detection, making them applicable to multiple types of assays.[4] While they work quite well for *in vitro* assays, they are incompatible with the cytosolic environment, as they are rapidly destroyed by cytosolic peptidases.[5]

In this dissertation, a variety of approaches towards increasing the lifetime of peptides in cytosolic environment were tested. Kinase substrates were selected as test peptides due to their role in a diverse set of vital processes, and their importance in current drug development efforts. For the most successful method, the rates of proteolytic degradation in cell lysates and *in vitro* phosphorylation were measured and analyzed using capillary electrophoresis paired with laser induced fluorescence (CE-LIF). Comparison to unmodified substrate peptides was used to assess the effect of dimerization on protease resistance and substrate efficacy. Finally, a dimerized Abl kinase substrate was used to monitor phosphorylation in living cells, demonstrating the utility of this method for intracellular assays. We find that N-terminal dimerization provides comparable half-lives to the best previously reported methods, with significantly greater synthetic

accessibility, suggesting that this is a promising new method for developing peptide-based intracellular probes.

ACKNOWLEDGEMENTS

First and foremost, I would like to thank Marcey Waters for all of her guidance throughout my time here. The environment you created in the lab and the relationship you choose to have with your students served as major factors when I chose to join this lab, and I never regretted it for a minute. I'd like to also thank my committee members, both for this defense and oral examination: Nancy Allbritton, Mike Gagné, Jeff Johnson, Kevin Weeks, and Dave Nicewicz. Your willingness to take the time to help me complete this is very much appreciated.

I'd also like to thank the members of our lab. Nick and Brendan, for having endless patience whenever I needed advice or had random questions, during their time here, and still now. Kai, for spending her last weeks here teaching me how to carry her work on. Lauren for letting me talk her ear off endlessly about anything and everything, and all other lab members who helped create a warm, fun environment to work in. I would also like to thank members of the Allbritton lab, especially Angie and Emilie, for teaching me whenever my research reached points outside of my field of expertise, more biological and/or analytical than I ever expected, and significantly expanding the scope of my knowledge.

I would especially like to thank Amber for being a great friend outside of lab and helping to keep us both balanced during our time here. I would also like to thank Sarah, for doing the same thing for me all the way from France.

TABLE OF CONTENTS

LIST OF TABLES

LIST OF FIGURES

LIST OF SCHEMES

LIST OF ABBREVIATIONS

Ac	Acetal
ACN, CH_3CN	Acetonitrile
ADP	Adenosine Diphosphate
Alloc	Allyloxycarbonyl
APN	Aminopeptidase N
Arg,R	Argenine
$aRMe_2$	Asymmetric Dimethyl Argenine
$sRMe_2$	Symmetric Dimethyl Argenine
ATP	Adenosine Triphosphate
CB[x]	Cucurbit[x]uril
CE	Capillary Electrophoresis
CX4	Calix[4]arene
DBU	1,8-Diazabicyclo[5.4.0]undec-7-ene
DCC	Dynamic Combinatorial Chemistry
DCC	*N*,*N*′-Dicyclohexylcarbodiimide
DCM	Dichloromethane
DIC	*N*,*N*′-Diisopropylcarbodiimide
DIPEA	*N*,*N*′-Diisopropylethylamine
DMEM	Dulbecco's Modified Eagle Medium
DMF	Dimethylformamide
DMSO	Dimethyl Sulfoxide
DNA	Deoxyribonucleic Acid

DPPA	Diphenylphosphoryl Azide
EDTA	Ethylenediaminetetraacetic acid
ELISA	Enzyme-Linked Immunosorbent Assay
EtOAc	Ethyl Acetate
FAM	Carboxyfluorescein
FBS	Fetal Bovine Serum
Fmoc	Fluorenylmethyloxycarbonyl
FRET	Förester Resonance Energy Transfer
HBTU	N,N,N′,N′-Tetramethyl-O-(1H-benzotriazol-1-yl)uranium hexafluorophosphate
HCTU	N,N,N′,N′-Tetramethyl-O-(6-chloro-1H-benzotriazol-1-yl)uranium hexafluorophosphate
HOBt	Hydroxybenzotriazole
HP1	Heterochromatin Protein 1
HR ESI-MS	High Resolution Electrospray Ionization Mass Spectrometry
HTS	High Throughput Screening
IMAC	Immobilized Metal Affinity Chromatography
ITC	Isothermal Titration Calorimetry
ivDde	1-(4,4-dimethyl-2,6- dioxocyclohex-1-ylidene-3-methylbutyl
$K(Me)_{1/2/3}$	Mono/Di/Trimethyl Lysine
K_d	Dissociation Constant
LAP	Leucine Aminopeptidase
LC	Liquid Chromatography
L-Htc	7- (S)-hydroxy-1,2,3,4-tetrahydroisoquinoline-3-carboxylic acid

LIF	Laser Induced Fluorescence
Lys, K, KMe_0	Lysine
MALDI	Matrix-Assisted Laser Desorption Ionization
MeOH	Methanol
MOAC	Metal Oxide Affinity Chromatography
MPER	Mammalian Protein Extraction Reagent
MS	Mass Spectrometry
MSH	Melanocyte-Stimulating Hormone
NH_4OAc	Ammonium Acetate
NHS	N-hydroxysuccinamide
NMM	N-Methylmorpholine
NMR	Nuclear Magnetic Resonance
O-GlcNac	O-linked β-N-acetylglucosamine
PBS	Phosphate Buffered Saline
PEG	Polyethylene Glycol
Phe	Phenylalanine
PKB	Protein Kinase B
PKC	Protein Kinase C
PNGase F	Peptide-N-Glycosidase F
POP	Prolyl Oligopeptidase
PTK	Protein Tyrosine Kinase
PTM	Posttranslational Modification
PyBOP	Benzotriazol-1-yl-oxytripyrrolidinophosphonium hexafluorophosphate

QD	Quantum Dot
RP-HPLC	Reversed-Phase High-Performance Liquide Chromatography
SAM	S-adenosyl-L-methionine
SDS	Sodium Dodecyl Sulfate
SP	Substance P
TCEP	Tris(2-carboxyethyl)phosphine
TFA	Trifluoroacetic Acid
THF	Tetrahydrofuran
TIPS	Triisopropylsilane
TLC	Thin Layer Chromatography
TOP	Thimet Oligopeptidase
TPPII	Tripeptidylpeptidase II
Trt	Trityl
TUBEs	Tandem-Repeat Ubiquitin-Binding Entities

Chapter I. The Use of Peptides as Reporters to Monitor Enzymatic Activity

1. Introduction

The understanding of disease has evolved markedly over the last two centuries. With the rapid advancements in analytics and the mapping of the human genome and proteome, scientists have gone from merely treating external symptoms to the point of understanding them on the molecular level. Dysregulated enzymes are now known to be notorious culprits in the causation and progression of many diseases, and with this knowledge at hand, it has become increasingly important to develop biosensors that allow us to monitor their activity. Such tools are extremely useful for fundamental studies, allowing scientists to tackle questions concerning the function of enzymes, as well as subsequent use of that knowledge to develop mimics or derivatives for the purpose of binding and/or catalysis. Drug discovery also heavily relies on the toolbox of probes for high throughput screening (HTS) of drug candidates and subsequent analysis of their therapeutic efficacy.[6] An expansion of the toolbox is foreseen to extend its use into biomedical applications, including diagnostic assays and monitoring of disease progression and response to therapeutics in patients. This area of research has recently sparked the interest of the scientific community and the addition of new analytical techniques has advanced at a rapid pace. In this chapter, examples of biosensors used to monitor enzyme activity will be discussed, focusing on peptide-based probes.

2. Peptides as substrates for the detection of enzymatic activity

Enzymatic activity is traditionally analyzed by radiolabeling, where incorporation of a radioactive moiety into a substrate is quantified by scintillation counting, or by a number of antigenic approaches, such as Western blotting, enzyme-linked immunosorbent assay (ELISA), and immunohistochemistry. Aside from radiolabeling, which has the obvious problem of having to handle radioactive waste, these methods all rely on antibodies for recognition. This can be seen as a disadvantage since they are expensive and difficult to produce, and batch to batch variability can be the source of misleading results.[7] The post reaction analysis required with these methods is also quite time consuming, and while they can provide significant information, they give only indirect measurement of catalytic activity, and are not able to provide real-time kinetic data.[8] For investigating cell lysates, all of the above methods suffer from the additional disadvantage of requiring a large number of cells. In the context of biomedical applications, this can become problematic, as obtaining large samples from patients can be challenging, and even detrimental to the patient.

The use of peptide-based reporters for enzymatic assays has begun to overcome some of the aforementioned limitations. Peptides are excellent mimics of the enzymes' natural substrates, making them particularly effective as probes for enzymatic activity. They can be designed with high affinity and specificity to the enzyme of interest, or alternatively, as non-selective substrates for an enzyme family, if so desired.[4] Peptides further carry the advantage of being easy to synthesize and modify, by hand or by automated synthesis, and cost effective. Finally, peptide substrates can provide a direct readout, allowing one to monitor enzyme reactions in real-time. Numerous approaches have been developed to pair such substrates with a detectable readout, including the use of electrochemical,[9–16] colorimetric,[17] and element mass spectrometry[18] output, though those will not be discussed here (for further examples, see Liu et al.[19] and Pavan et al.[20]).

Instead, the focus here will be on using fluorescent peptide-based reporters. The addition of a fluorophore to a peptide substrate allows for rapid sensitive detection that can be visualized and quantified by various types of instrumentation, including fluorescence microscopy, liquid chromatography with fluorescence detection, and capillary electrophoresis paired with laser induced fluorescence (CE-LIF). Within that category alone, a number of approaches have already been taken in translating enzyme activity into readable output. A few of the most popular ones are described below, followed by the work being done to apply those to intracellular assays.

2.1.Approaches to reading fluorescent peptide-based probes

The use of solvatochromic fluorophores conjugated to peptide substrates has been extremely popular in kinase assays. [21] Solvatochromic fluorophores are ones whose spectroscopic properties change in response to changes in the polarity of their surrounding environment. When placed in proximity to a target residue on a peptide substrate, modification of the peptide by an enzyme, or a subsequent event, such as recruitment of a reader protein (Figure 1), can lead to a change in fluorescence. Examples of this can be seen in probes developed for PKC,[22] Src, [23] and cyclin-dependent kinase activity.[24]

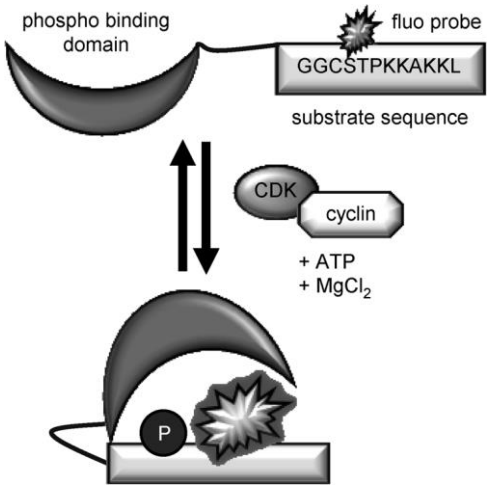

*Figure 1. Quench-based kinase assay dependent on the recruitment of a reader protein. Reproduced with permission from Wiley: ChemBioChem **2014**, No. 15, 2298.*

Another method used quite commonly is one based on restoring the fluorescence of a quenched fluorophore. This approach has been seen in kinase as well as protease assays. In the latter, a self-quenching fluorophore must be placed at several residues on a peptide substrate in close proximity,[25] or ones that come in close proximity due to secondary structure.[26] Upon enzymatic cleavage of the peptide substrate, the local concentration

of the fluorophore decreases, and fluorescence intensity increases in turn. In kinase assays, quenching-based fluorescent assays can take multiple forms. Tyrosine and tryptophan, both viable phosphorylation sites, are known to quench a variety of organic fluorophores through π-π interactions.[27,28] Phosphorylation can disrupt the stacking and result in a fluorescence enhancement (Figure 2). Alternatively, the Lawrence lab developed the "deep-quench" method, which they used to monitor PKA activity.[29,30] In this construct, the fluorophore is quenched by a molecule in solution. Upon phosphorylation, the corresponding phospho-peptide binds to a phospho-recognition domain thereby effectively shielding the fluorophore from the quencher in solution and restoring fluorescence. In a more recently reported form of this biosensor, a positively charged fluorescent peptide was quenched by a negatively charged quencher. Upon phosphorylation, the quencher was released due to electrostatic repulsion, leading to increased fluorescence.[31]

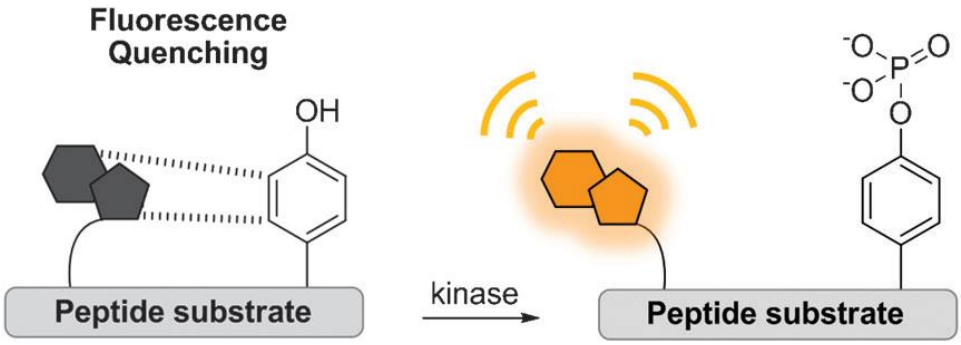

Figure 2. Quench-based kinase assay. The fluorophore is quenched by tyrosine, and upon phosphorylation, fluorescence is restored. Reproduced from Chem. Soc. Rev. ***2012****, 41 (5), 1652 with permission of The Royal Society of Chemistry.*

Förster resonance energy transfer (FRET) is perhaps one of the most common detection methods among all biosensors. A donor-acceptor pair conjugated onto opposite ends of a peptide substrate (within Förester radius), and upon enzymatic cleavage, the donor-acceptor pair are separated, leading to a detectable change in fluorescence (Figure 3). This FRET-quenching approach has been used to assay a multitude of proteases, including bacillus anthracis protease,[32]

MMP-9,[33] and HIV protease.[34] Apart from fluorescent dye molecules, much attraction has been paid to utilizing semiconductor quantum dots (QDs) to develop peptide-based FRET protease sensors.[35] Particle size and surface modification control the absorbance and emission of QDs, allowing one to adjust them to match various fluorescent dyes. Several groups have successfully used QD-conjugated peptides to monitor the activity of various proteases, such as caspases,[36] and *Botulinum* neurotoxin A.[37] Impressively, QD-FRET methods are already being applied to microchip detection platforms, and are believed to have great potential for commercialization. [38]

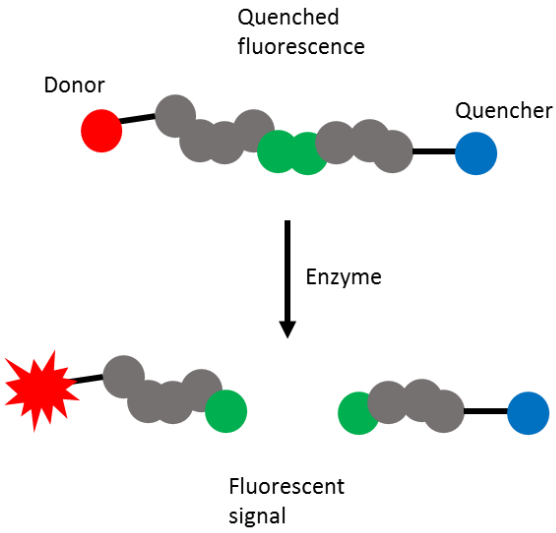

Figure 3. FRET-based protease assay.[166]

All of the methods discussed above are based on monitoring changes in fluorescence. Another option is to pair fluorescence detection with a separation method, thereby observing the modified and un-modified peptide substrate simultaneously throughout an enzymatic reaction. The Allbritton group, in collaboration with the Lawrence group, reported the detection of several enzymes using capillary electrophoresis paired with laser induced fluorescence (CE-LIF). Using this technique, modified and un-modified peptide substrate are separated due to the difference in their electrophoretic mobility. They applied this method to monitoring the activity of several enzymes, including Abl,[39] PKB,[40] PKT,[41] and PTP.[42] This method can also be applied to monitoring protease activity, as the fragmentation products can be separated from the un-degraded substrate, and even from each other.[43,44]

2.2.Using peptides to monitor intracellular enzymatic activity

While the number of peptide-based probes developed for *in vitro* detection of enzyme activity is vast, the examples of such probes used intracellularly are much fewer. Peptides are generally incompatible with the cytosolic environment, as they are rapidly metabolized by cytosolic peptidases.[5] A limited number of aminopeptidases and endopeptidases are known to exist free in the cytosol of cells, including tripeptidylpeptidase II (TPPII),[45–47] thimet oligopeptidase (TOP),[48] prolyl oligopeptidase (POP),[49] and leucine aminopeptidase (LAP).[50,51] A common feature of these peptidases is a narrow cleft that contains the catalytic site, and evidence suggests that it is the N-terminus of peptides that initially enters the cleft.[49,52–55] Several methods in the literature have taken advantage of these features to create longer-living peptides, for use as enzymatic reporters, as well as drug candidates.[56] A few such approaches are discussed below. Note that this is a limited overview, and other notable methods (commonly used in the pharmaceutical industry), such as PEGylation[57,58] and conjugation of macromolecules,[59–61] will not be covered here.

2.2.1. Peptidomimetics

The incorporation of non-canonical amino acids or amino acid analogues into peptide regions important for enzymatic activity is expected to strongly affect their efficacy as substrates. This holds true with proteases as well. β and γ-amino acids, N-methylated amino acids, and even D-amino acids have been shown to increase a peptide's resistance to proteolysis.[62,63] For example, Hamamoto et al. demonstrated this in their development of a small antimicrobial peptide. Partial incorporation of D-amino acids made the peptide, though short and cationic, more resistant to trypsin degradation than its L-amino acids counterpart.[64] Tugyi et al. also demonstrated that the stability of peptide immunogens was increased by incorporation of D-Thr and D-Pro at several sites.[65] This has been further iterated in our lab, when a β-hairpin made of

all D-amino acids was found to remain completely intact even after 24 hours of incubation with pronase E, showing no degradation at all. However, an unstructured L-amino acid peptide attached to the C-terminus of the D-beta-hairpin was degraded rapidly, suggesting that D-amino acids do not prevent threading into the catalytic cleft of the enzymes.[66] The use of β- and γ-amino acids was also found to successfully increase resistance in peptides. Separate work done by the Seebach and Gellman labs showed peptides made entirely of β- and γ- amino acids are resistant to proteolysis by a number of different proteases.[67–69] More significant modifications to the peptide backbone to enhance resistance are also seen in the literature, including ester linkages, peptoids, oligoureas, and azapeptides.[57,70–72]

In order to use such peptides as enzymatic substrates, they must maintain the ability to be recognized by the target enzyme. One can infer that residues important for catalytic activity must therefore remain unmodified. Optimal results can be achieved by careful analysis of cleavage sites, followed by modifications at those sites alone. Proctor and co-workers used this approach to develop protease resistant peptide probes for kinase activity. After incubation of a peptide substrate in cytosolic lysate, the degradation products were analyzed using CE-LIF. Cleavage sites were identified and the residues substituted with non-native amino acids. Through an iterative design process, they were able to attain a 15-fold increase in the half-life of an Abl substrate peptide,[39] and a 4.6-fold increase in a PKB substrate peptide, which was then used as a reporter to measure PKB activity in a single cell.[40] In another example, Turner et al. showed that placing 7- (S)-hydroxy-1,2,3,4-tetrahydroisoquinoline-3-carboxylic acid (L- Htc) in the place of tyrosine in a PTK substrate peptide was enough to double the half-life in cell lysates, allowing it to be used as an intracellular reporter.[41] Though effective, this method requires multiple rounds of iterative design for each peptide, which can be extremely time consuming and costly.

Additionally, each modification made to a peptide can also affect its efficacy as a substrate for the enzyme of interest, and so a delicate balance must be maintained.

2.2.2. Secondary Structure

Research has shown that well-folded peptides have longer lifetimes in cytosolic environments than those of their unstructured counterparts. This is believed to be due to the fact that in their folded form, peptides are too large to enter the narrow catalytic cleft of cytosolic proteases, thereby limiting their degradation. Work from our lab has shown evidence to that effect. A series of β-hairpins composed of entirely natural amino acids were synthesized and the rate of degradation in α-chemotrypsin, trypsin, and pronase E were measured. As was expected, a direct correlation between the fraction folded and the stability of a peptide was seen, reaching up to a 42-fold increase in half-life for the best folded β-hairpin.[73] Taking advantage of this correlation, along with the evidence that cytosolic proteases thread peptides in through the N-terminus,[49,52–55] our group further showed that the inclusion of a small β-turn at the N-terminus of a linear peptide can extend its lifetime in cytosolic environment up to 10-fold.[74] The protected peptide, a known Abl substrate, maintained its biological activity, and was successfully phosphorylated by the Abl kinase.[74]

Cyclic peptides have also exhibited substantial resistance to proteolysis.[75–78] Such peptides are bulky (preventing entrance to proteases' catalytic cleft), lack an N-terminus (preventing recognition by aminopeptidases), and unlike β-hairpins, which sample both a folded and un-folded form in solution, they are permanently locked in that conformation. Examples of that can be seen in nature; naturally occurring cyclic peptides such as Gramicidin and Polymyxin B are metabolically stable, allowing them to be used as therapeutic agents.[79] Inspired by some of these natural products, the ability to impart that stability on synthetic peptides via cyclization has been

extensively investigated in the literature. In a paper published in 1996, Kyb et al. synthesized various cyclic analogues of Substance P (SP), a member of the tachykinin neuropeptide family, and studied the effect of cyclization on its properties. Cyclized peptides, though with varying biological activity, consistently showed increased metabolic stability, with up to 80% remaining after 2 hour incubation in parotid gland slices (compared to 50% of the linear peptide within 6 minutes).[80] In a more recent example, Hess et al. explored the effect of structural and conformational modifications on the intestinal permeability and metabolic stability of hydrophilic peptides. A library of 18 cyclic peptides was screened, and in all cases, cyclization dramatically reduced proteolysis by brush border enzymes.[81] They carried out the same tests on a tetrapeptide derived from melanocyte-stimulating hormone (αMSH), a peptide with potential as a therapeutic agent for treating obesity. As in the prior case, they found that cyclized analogues all displayed improved metabolic stability.[82]

Although cyclization remains the most effective way to protect peptides from proteolytic degradation, this method does not come without its challenges. Cyclization of peptides is not always feasible, whether it's due to a lack of suitable side chain functionalities, or because of the importance of such functionality for bioactivity. Furthermore, the conformational constraints that help maintain metabolic stability can also render a peptide inactive, locking it in a conformation that is unfavorable for binding/catalysis.[83] In collaboration with the Allbritton group, our group, in an extension of the work described above, cyclized the β-turns at the N-terminus of an Abl substrate peptide, thereby leaving the substrate region linear and the substrate efficacy un-affected. This showed up to a 4-fold increase in lifetime over its non-cyclized counterpart (40-fold increase over the linear peptide alone). This peptide was then used in an intracellular Abl kinase assay. This was not previously possible with the unprotected substrate, as it degraded too

quickly.[74] However, even in this best case scenario, the synthesis of cyclized peptides is no trivial task, as is evident by the constant efforts to improve and develop new methods of cyclization.[84]

3. Purpose of this work

As is evident by the above discussion, despite the great advantages of using peptides as reporters, incorporating them into intracellular assays is challenging, as they get rapidly degraded by proteases. While some methods exist to prevent that, none go without affecting the efficacy/bioactivity of the peptide in question, and the most commonly used ones are also synthetically and/or financially draining. To further the use of these probes, a generalizable and synthetically simple method is needed to make them more stable in cytosolic environment. Described below is the work done to develop a technique for increasing the protease resistance of peptides, thereby allowing their effective use in intracellular enzymatic assays. A variety of protecting strategies were tested for their ability to prevent or slow down proteolytic degradation of a linear peptide. The most successful method was then applied to several different peptides, and their efficacy as enzymatic substrates was evaluated. One of the protected peptides was then carried forward to use as a substrate in an intracellular phosphorylation assay (Figure 4).

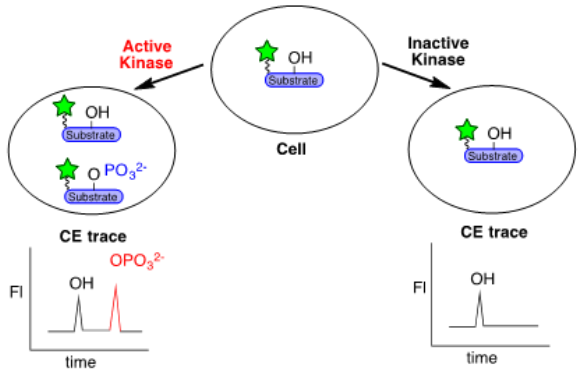

Figure 4. Intracellular phosphorylation assay analyzed by CE-LIF using a fluorescent peptide substrate.

Chapter II. Design, Synthesis, and Characterization of Protected Peptides (Protectides) for Kinases

1. Introduction

To address the limitations in intracellular enzyme assays described in chapter one, we aimed to develop protected peptide substrates, which we call "protectides". Our design focused on the three characteristics known to be common among cytosolic proteases: narrow catalytic cleft, highly charged surface area, and threading of peptides in an N- to C-terminus manner.[49,52–55] We reasoned that entrance into the catalytic clefts can be prevented through sterics, by addition of bulky groups, or electrostatic repulsion, by incorporating negative charge into peptides, at the N-terminus. To begin our work on developing a protection method, a peptide sequence on which to test protecting groups was needed. We envisioned ultimately using our protecting strategy on a peptide substrate in an enzymatic assay. It was therefore ideal to test possible protecting groups (termed "protectides") directly on the substrate in mind. We decided to demonstrate our work on kinase substrates. Kinases are a superfamily of enzymes that are responsible for the phosphorylation of tyrosine, threonine, and serine. They play an important role in a large set of vital processes, including cell differentiation, gene expression, and apoptosis.[85] The involvement of these enzymes in so many aspects of cell function makes cells extremely vulnerable to any alterations in their function, be it due to mutations, or overexpression. Dysregulation of kinases is in fact implicated in a wide range of diseases, including, but not limited to, diabetes, infectious disease, cardiovascular disorders, and cancer.[86] Kinase inhibitors are currently among the most

heavily investigated drugs,[87] motivating the development of robust probes for intracellular kinase assays.

2. Analysis of an Unprotected Kinase Substrate

Many peptide sequences are known to function as kinase substrates, and the choice of one for these purposes was rather arbitrary. We initially decided to use the sequence RKRDRLGTLGI-NH_2, reported by Kunkel et al. to be a selective PKB substrate.[88] The synthesis of this peptide, however, turned out to be quite problematic due to aspartamide formation, and the desired peptide was never isolated. This was quickly abandoned in favor of another PKB substrate peptide, GRPRAATFAEG-NH_2, previously used by our collaborators in the Allbritton lab.[89] This peptide was cleanly synthesized by hand or by an automated synthesizer, and despite the low overall charge, it did not present any solubility problems at the concentrations needed for this work. The control peptide **1** was simply capped with (5,6)-carboxyfluorescein ((5,6)-FAM) at the N-terminus for visualization (Figure 5) and served as the standard for comparison for all of the studies described below.

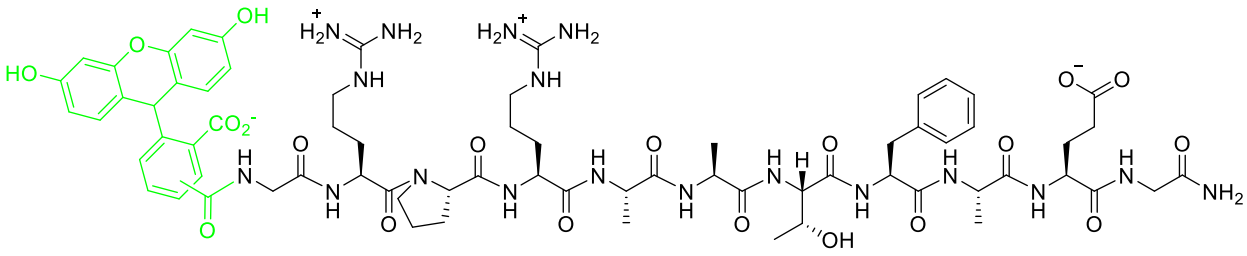

*Figure 5. Control peptide **1**. The substrate is in black, and the fluorophore is shown in green.*

The stability of peptide **1** in the presence of cytosolic peptidases was tested by incubating in HeLa cell lysates at 37 °C. Aliquots were removed and quenched with equal amount of hydrochloric acid at various time points and the amount of intact peptide left was determined by

capillary electrophoresis paired with laser induced fluorescence (CE-LIF) (Figure 6). Based on peak integrations relative to an added internal standard ((5,6)-FAM), the half-life of the peptide, the point at which 50% remained un-degraded, was found to be 15±2 minutes.

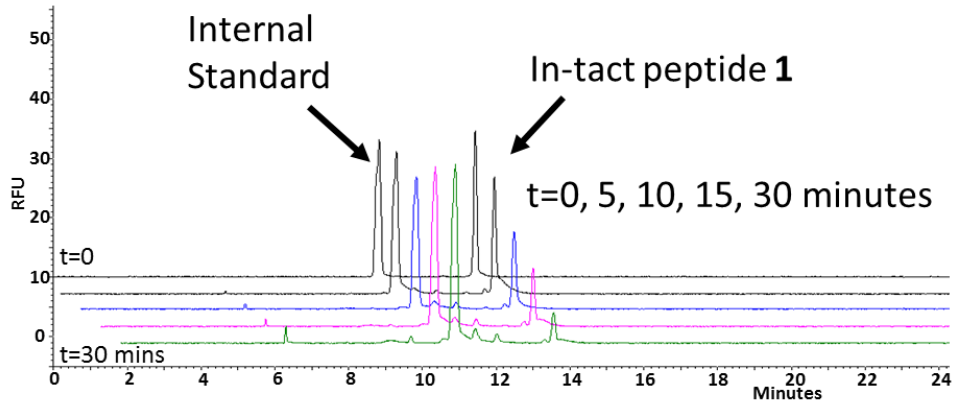

*Figure 6. Electropherogram from a degradation assay of control peptide **1**.*

Throughout the rest of this chapter, various protecting methods, or "protectides", are evaluated. All protected peptides consist of the substrate sequence, shown in black, a PEG spacer, shown in red, a fluorophore conjugated to a lysine residue, shown in green, and a protecting moiety, shown in blue (Figure 7). All peptides, unless otherwise stated, were synthesized via standard Fmoc solid phase chemistry, and all were amidated at the C-terminus. Peptide characterization was done using HR ESI-MS or LC-MS.

Protecting Group-K(FAM)-PEG-GRPRAATFAEG-NH_2

General structure of protected peptide

Figure 7. General design of peptide constructs. The PKB substrate is in black, the spacer in red, the lysine conjugated fluorophore in green, and the protecting group in blue.

3. Beta-Hairpins as "Protectides"

Previous work in our lab has shown that appending small β-turn structures to the N-terminus of a linear peptide can extend its lifetime in cytosolic environment, [74] presumably due to the

steric bulk preventing entrance into the narrow catalytic clefts of proteases. With this knowledge at hand, we set out to examine the effect of attaching more highly folded and "click-cyclized" β-hairpins to the N-terminus of a substrate peptide to see whether longer half-lives were achievable with this method. Three peptide sequences known to fold well were adapted from the literature and modified for our purposes: Ac-WIpOOWTGPS (ACAP1), Ac-WVWVpOOKIWTG (ACAP2),[90,91] and Ac-RK(N_3)VKVpGOWIG(propargyl)Q (NHB).[92] ACAP1 and ACAP2 were designed by Andersen et al. with a unique capping motif that enhances folding and minimizes terminal fraying of β-hairpins. This capping motif, "acyl-W-loop-WTG", confers additional stability through a face-to-edge Trp-Trp interaction, hydrogen bonding of the Thr residue with the N-terminal acyl group and the H_N of Gly, and a CH-π interaction between the N-terminal Trp and C-terminal Gly (Figure 8).[91] Since the incorporation of noncanonical amino acids is known to increase protease resistance,[40,62] ornithines were incorporated in ACAP1 and ACAP2 at positions that were shown to be unimportant for folding. NHB, designed by Park and Waters, was shown to be amenable to cyclization via click reaction, and in its cyclized form, showed no degradation after 48 hours of incubation with Pronase E.[92] We thus chose to investigate its effect, in both the cyclized and un-cyclized form, on the PKB substrate. The PKB substrate was synthesized with each one of these hairpins appended to its N-terminus (peptides **2**-**4**, Figure 9) in a linear manner. The peptides' half-lives in HeLa cytosolic lysate was then measured using CE-LIF for analysis.

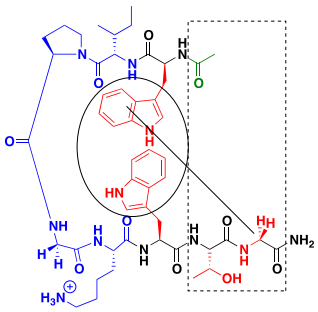

Figure 8. An example peptide highlighting the noncovalent interactions of the Andersen capping motif.

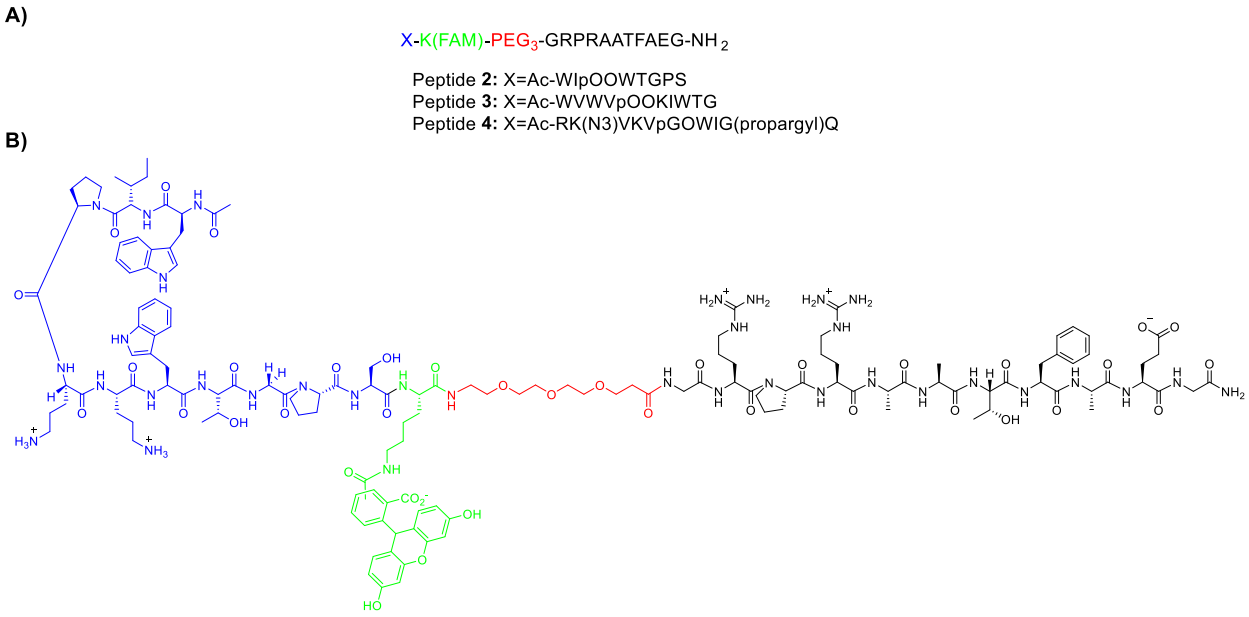

Figure 9. (A) Protected peptides 2-4. (B) Structure of peptide 2. The PKB substrate is in black, the PEG spacer in red, the lysine-conjugated FAM in green, and the protecting β-hairpin in blue.

When appended to a β-hairpin, up to a 3-fold increase in half-life relative to peptide **1** was seen. Peptides **2** and **3** were within error of each other, with peptide **2** having a half-life of 26±3 minutes, and peptide **3** 30±5 minutes. Peptide **4**, in its unclicked form, showed the greatest improvement over the control peptide, with a half-life of 45±7 minutes (Figure 10 & Table 1). Since cyclized peptides are known to dramatically improve metabolic stability,[75–78] it was postulated that cyclization of peptide **4** would further enhance the lifetime of the protected substrate. Attempts at cyclizing peptide **4** (using the procedure outlined by Park & Waters[92]), however, proved futile, only further illustrating the impracticality of relying on peptide cyclization for protection.

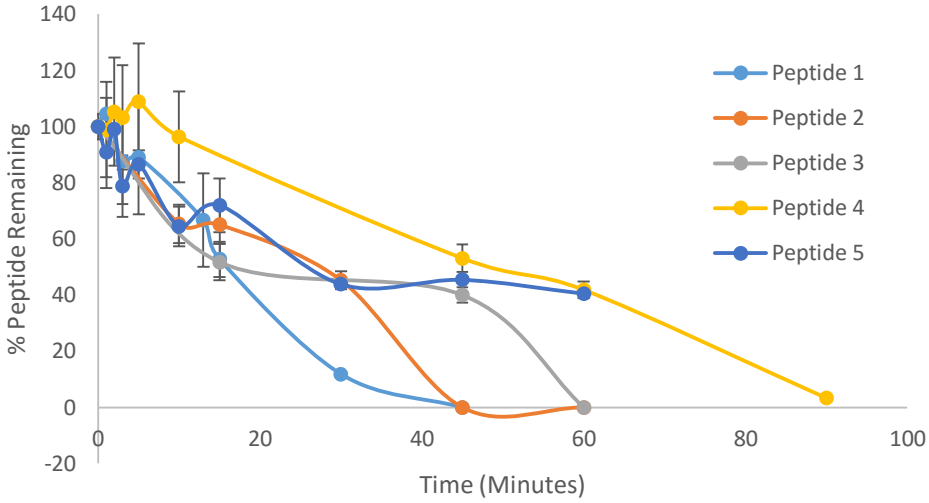

*Figure 10.Degradation of peptides **1**-**5** in HeLa cytosolic Lysate. Error bars represent the standard deviation from three trials.*

*Table 1. Half-lives of peptides **1**-**5** in HeLa cytosolic lysates.[a]*

Peptide	**$t_{1/2}$ (minutes)**
Peptide **1**	15±1
Peptide **2**	26±3
Peptide **3**	30±5
Peptide **4**	45±7
Peptide **5**	25±2

[a] Error was determined based on the standard deviation from three runs.

We chose to also test the effect of adding "protection" on the C-terminus of a peptide. Since the addition of another β-hairpin on the C-terminus of the peptide would have been far more synthetically challenging, we chose to take advantage of the negatively charged surface of cytosolic proteases,[5,48] and hoped that the addition of negative residues to the C-terminus of the peptide would help by creating electrostatic repulsion between the peptide and the catalytic cleft of peptidases. This hypothesis was tested on peptide **3**. We initially attempted to synthesize it with four glutamic acid residues added to the C-terminus. However, this peptide was never successfully isolated. Sequential reduction of the number of residues added was finally successful, as the peptide was made and isolated with two glutamic acids added (peptide **5**, Figure 11). This additional modification of the C-terminus, however, did not appear to have an

effect on the peptide's stability, as its half-life remained within error of peptide **3** (Figure 10 & Table 1).

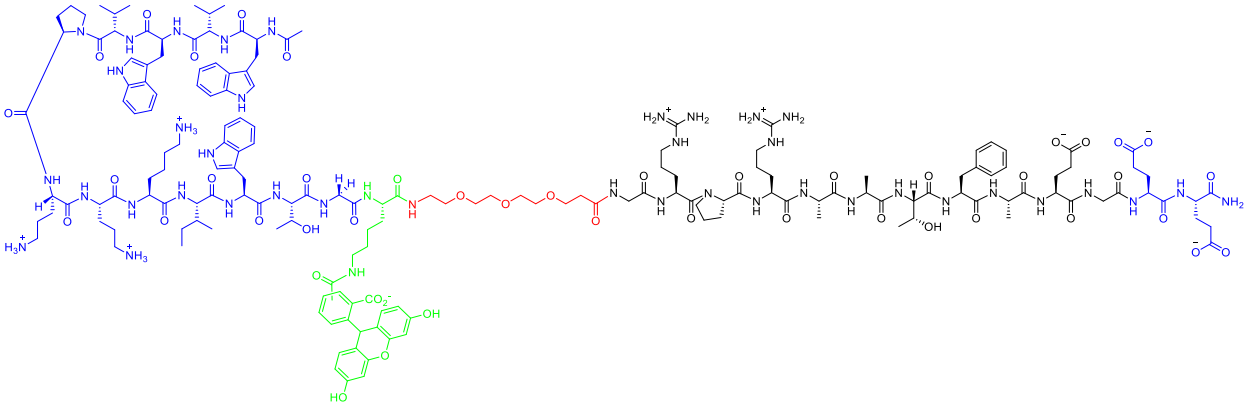

*Figure 11. Peptide **5**. Protected by a β-hairpin at the N-terminus and two glutamic acid residues at the C-terminus.*

4. Supramolecular "Protectide"

In 2011, Urbach demonstrated the ability of a synthetic cucurbit[7]uril (CB[7]) to bind the 4-*tert*-butyl and 4-amino-methyl derivatives of phenylalanine with sub-micromolar dissociation constants (K_d). Binding was shown to be promoted by the positive cooperativity between the N-terminal ammonium group and the side chain ammonium group in the case of aminomethyl phenylalanine (Figure 12). Placement of these residues at the N-terminus of tripeptides did not reduce the affinity, and in some cases even improved it due to additional cooperativity by the peptide backbone.[93] In 2013, Urbach et al. reported the use of CB[7] to inhibit the degradation of a peptide by aminopeptidase N (APN), a non-specific exopeptidase. In the presence of CB[7], digestion of a peptide stopped upon reaching a Phe or (4-aminomethyl)Phe residue, and the remaining peptide was stable for at least 24 hours (Figure 13).

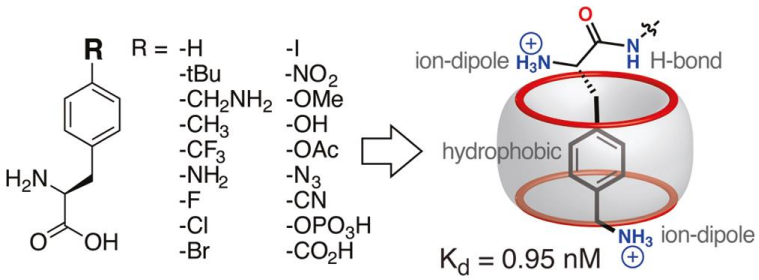

Figure 12. Binding of Urbach's Cucurbit[7]uril to various phenylalanine derivatives. Reprinted with permission from J. Am. Chem. Soc. 2011, 133 (42), 17087. Copyright 2011 American Chemical Society.

The extent of protection of an N-terminal residue was found to directly correlate to its binding affinity to CB[7].[94] This study, however was done in the presence of a single, purified peptidase. We decided to see if this approach could be extended to multiple peptidases, such as those in the cytosol of a cell. Based on the above results, we speculated that placement of a Phe or (4-aminomethyl)Phe residue at the N-terminus of our peptide substrate could inhibit degradation by aminopeptidases. Since (4-aminomethyl)Phe is known to have a higher affinity towards CB[7],[93,94] we chose to test this hypothesis by appending it to the N-terminus of our peptide.

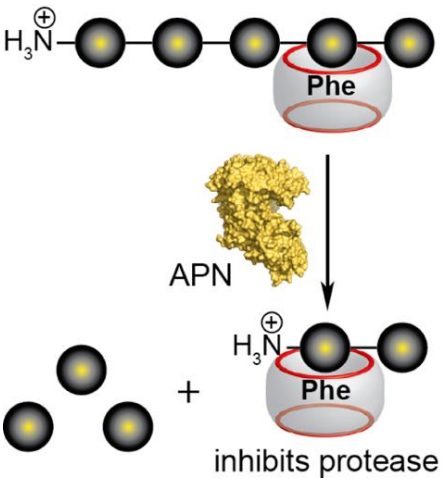

*Figure 13. Schematic illustration of the inhibition of APN-mediated peptide digestion at a Phe residue using CB[7]. Reprinted with permission from J. Am. Chem. Soc. **2013**, 135 (31), 11414. Copyright 2013 American Chemical Society.*

Attempts were made to synthesize the peptide with a free N-terminus to get maximal binding (K_d~1.88 nM),[94] but the peptide was never successfully isolated, or even detected in crude mixtures. We instead used the Ac-capped peptide (peptide **6**, Figure 14), as CB[7] displays strong binding to peptides containing (4-aminomethyl)Phe as an internal residue as well (K_d~510 nM).[93]

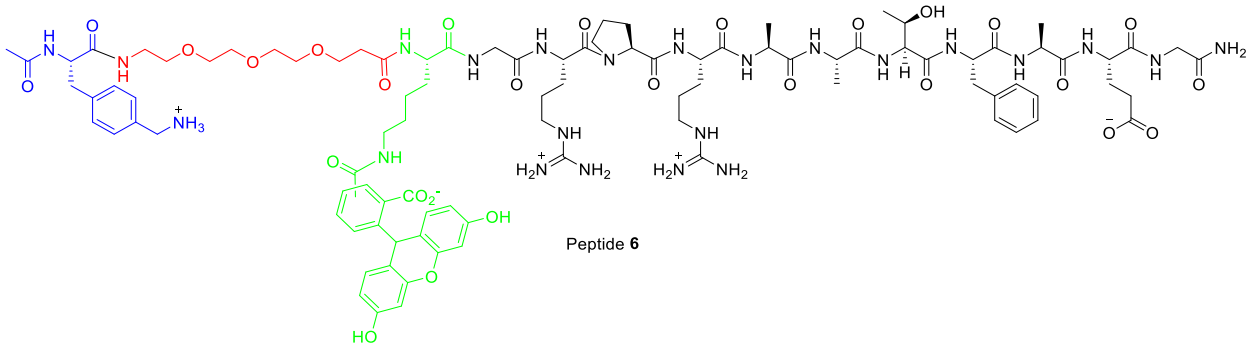

*Figure 14. Peptide **6**.*

The stability of peptide **6** was assessed with and without CB[7] (commercially available) in the same manner described above, using CE-LIF for analysis. In the absence of CB[7], the peptide was found to be 50% degraded within 5±0.4 minutes. In the presence of 2-fold excess of CB[7] (20 μM), the half-life of the peptide was 20±1 minutes, representing a 4-fold increase (Figure 15). It is possible that while the cucurbituril is large enough to block entrance into the catalytic cleft of the peptidase APN, it is not large enough to do so for some other peptidases found in the cytosol, as size differences do exist. Additionally, despite the strong binding affinity, it is still a reversible process, just like the folding of β-hairpins, and the peptide could thread into the proteolytic cleft while sampling the off state. While the concentrations used were well above the reported K_d, it is important to note that these assays were carried out in PBS, and not in ammonium phosphate buffer as was reported in the literature.[94] The difference in buffer, and especially the presence of such high concentrations of salts (and of course everything else

present in cell lysates), could have a profound effect on the binding properties of CB[7], though this was not investigated further.

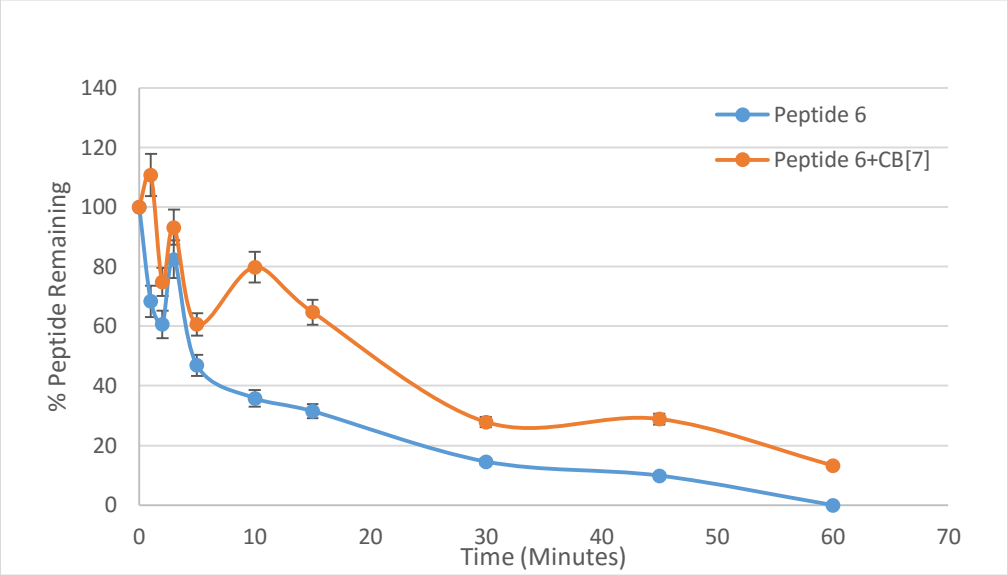

*Figure 15. Degradation of peptide **6**, with and without CB[7], in HeLa cytosolic lysates. Error bars represent the standard deviation of three runs.*

5. Aryl Cap as "Protectide"

With the above results at hand, it was deemed best to move away from using reversible processes for protection and focus on covalent attachment of protecting groups. In another article published by Urbach and Ramalingam, they outlined the synthesis of 2 rotaxanes, each comprising a viologen core threaded through a similar, this time cucurbit[8]uril macrocycle (CB[8]), and stoppered by tetraphenylmethane groups (Figure 16).[95] Since the tetraphenylmethane unit is large

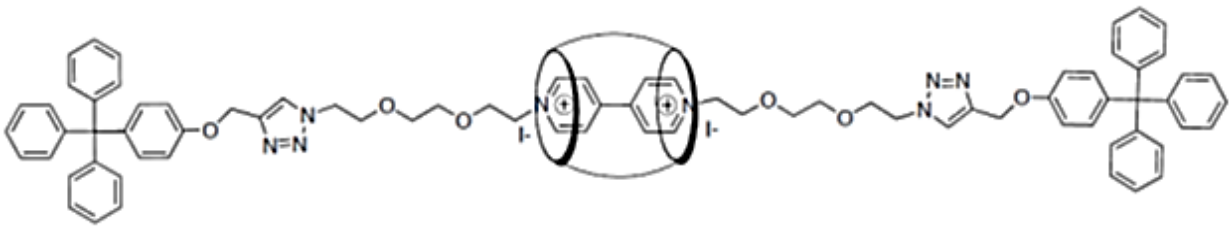

*Figure 16. Urbach's rotaxane, stoppered by tetraphenylmethane groups. Reprinted with permission from Org. Lett. **2011**, 13 (18), 4898. Copyright 2011 American Chemical Society.*

enough to stopper the rotaxane, it was our hope that it would be large enough to act as a barrier

to sterically restrict access of our substrates into the catalytic cleft of cytosolic peptidases, thereby increasing the lifetime of the peptide substrates. Based on structural analysis of several peptidases found in the cytosol, the tetraphenylmethane is larger than the entrance to the catalytic site in some. Thus with its large size, unnatural structure, and unnatural linker to the peptide, we hypothesized that is could hinder the recognition of the peptidic substrate by the peptidase, thereby reducing threading into the catalytic cleft and extending its lifetime.

To test this hypothesis, a tetraphenylmethane unit was appended to the N-terminus of the peptide substrate via a click reaction. Since FAM in itself is an unnatural component of this peptide, its possible role was tested by synthesizing two versions of the protected substrate: one in which the lysine conjugated FAM was on the N-terminal side (peptide **7**), and one in which it was on the C-terminus (peptide **8**). Since the peptide substrate has an overall charge of only +1, the addition of a large hydrophobic aryl cap was expected to cause solubility problems. To circumvent that, ornithines were incorporated at the N- and C-terminus of the peptide substrate, separated from it by a glycine residue (Figure 17).

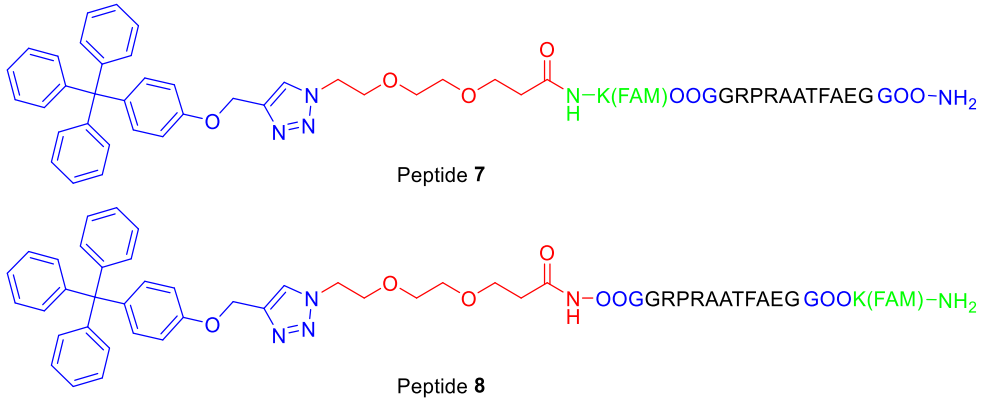

*Figure 17. Peptides **7** and **8**.*

5.1.Synthesis

The tetraphenylmethane stopper (aka the aryl cap) was synthesized in one step from commercially available 4-tritylphenol by treatment with propargyl bromide and K_2CO_3 (Scheme 1) and characterized by ^{1}H NMR. Attempts were made to synthesize a sulfonated protectide as well, in hope of getting greater protection due to charge repulsion, but attempts at sulfonation of the aryl cap led to inseparable product mixtures, the analysis of which (via ^{1}H NMR and LC-MS) was always inconclusive. This approach was therefore abandoned. The azido-PEG_2-acid linker was synthesized from cheap, commercially available diethylene glycol, starting with a high-yielding desymmetrization using ^{t}Bu-acrylate and sodium metal. The alcohol was then converted into an azide using DPPA and DBU, and the ^{t}Bu-ester was deprotected in 1:1 TFA:DCM to reveal the carboxylic acid, which was then characterized by ^{1}H NMR and ESI-MS (Scheme 1).

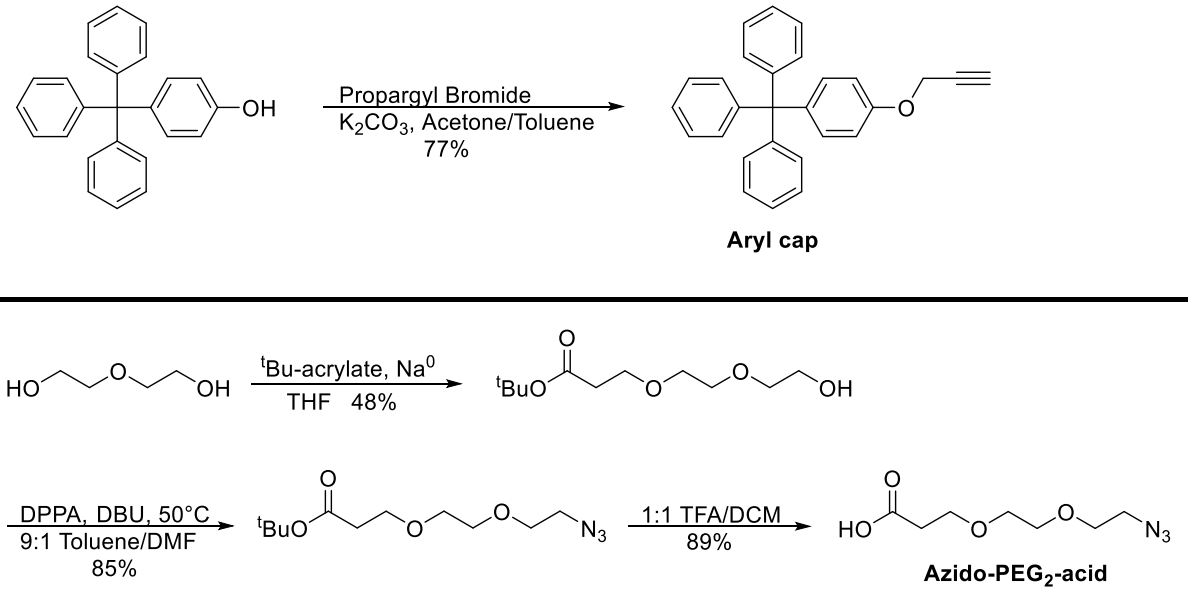

Scheme 1. Synthesis of aryl cap and azido-PEG_2-acid linker.

Synthesis of peptides **7** and **8** was carried out entirely on resin, using standard solid phase peptide synthesis up until the final step, in which the aryl cap was attached via an overnight solid phase click reaction, followed by cleavage and purification by standard methods.

5.2.Determination of proteolytic stability

The proteolytic stability of peptides **7** and **8** was tested in HeLa cell lysates, and the results were analyzed using analytical RP-HPLC (Figure 18). Surprisingly, peptides **7** and **8** both displayed half-lives shorter than that of the control peptide **1**, with $t_{1/2}$ of ~7 minutes and ~5 mins. For peptide **7** and peptide **8**, respectively. This most likely reflects a more active batch of cell lysates, as peptide **1** was not run in parallel with this particular batch The placement of FAM did not appear to make a difference in their half-lives, though it is worth noting that peptide **8** was completely degraded after 45 minutes, while trace amounts of peptide **7** were still seen after an hour.

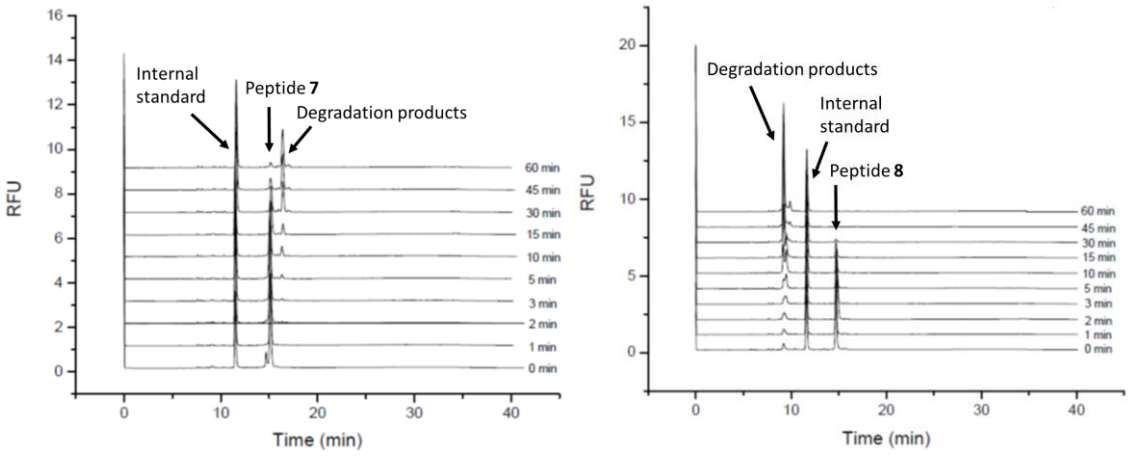

*Figure 18. RP-HPLC traces following the degradation of peptides **7** & **8** in HeLa cytosolic lysates.*

New versions of the protected substrate were synthesized (in the same way as above) with a few changes in hopes of increasing resistance: FAM was incorporated on both the N and C terminus (peptide **9**), the ornithines on the ends were replaced with three glutamic acids on each side to induce electrostatic repulsion (peptide **10**), or both (peptide **11**). In all three cases, a linker that is 2 PEG units long was used (Figure 19). With all three, however, trouble was encountered when trying to characterize the product. None of the products collected ionized by ESI-MS or

MALDI, and when run on the LC-MS, the only peaks seen were eluted off the column very quickly.

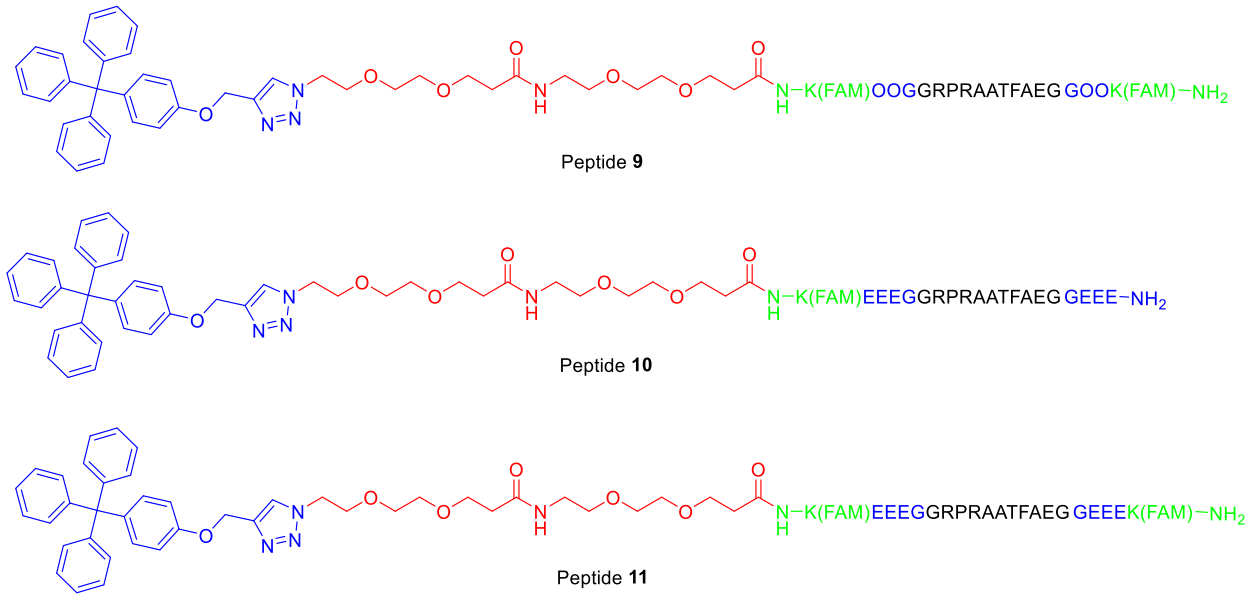

*Figure 19. Peptides **9**-**11**.*

6. Dendrimers as "Protectides"

As an extension of the steric blocking approach described above with the tetraphenylmethane group, the use of dendrimers as a capping motif was investigated as a protecting method. Dendrimers can be synthesized quite easily, making them practical to use. Their size can be systematically increased, with every generation synthesized, until a sufficient size is reached to effectively protect the peptides. Furthermore, their synthesis allows for the incorporation of multiple negative charges at the periphery, which may further help with protection due to the charge repulsion between them and the proteolytic cleft.[49,54,55] This can also provide sites for the conjugation of cell-penetrable ligands when applied intracellularly. To that end, benzyl hydroxy-dendrimers were synthesized, beginning from commercially available methyl 4-methylbromobenzoate and 3,5-dihydroxybenzyl alcohol, following a standard literature protocol.[96] Before final hydrolysis of the methyl esters on the periphery (once the desired

generation is reached), the benzylic alcohol at the focal point was converted to an azide to enable conjugation to the peptide via a click reaction (Scheme 2). The synthesis was high yielding for all the generations synthesized.

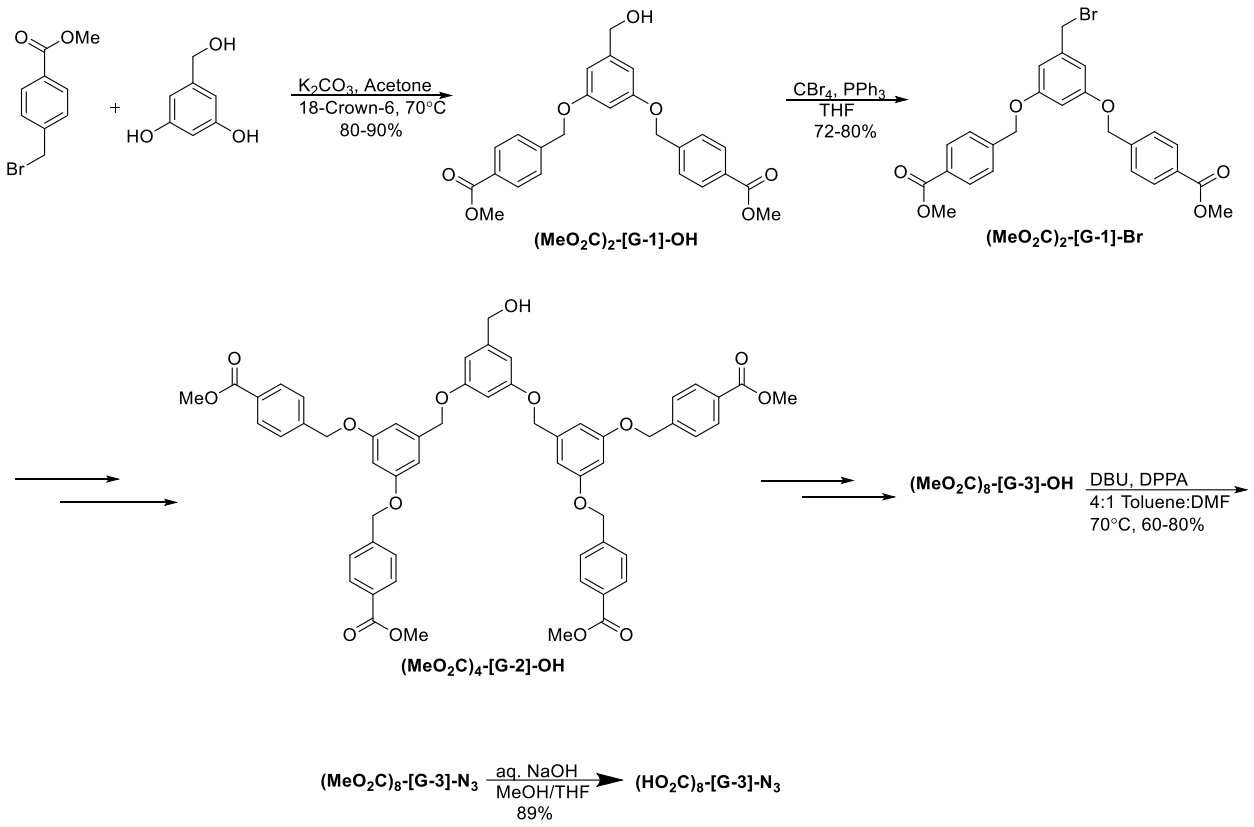

Scheme 2. Synthesis of azido-dendrimers.

Modeling suggested that the second generation ([G2]), third generation ([G3]), and fourth generation ([G4]) dendrimers would be in the size range necessary to restrict access into the clefts of cytosolic proteases (based on the crystal structure data available to date).[49,52–55,97] Dendrimers $(HO_2C)_4$-[G2]-N_3 and $(HO_2C)_8$-[G3]-N_3 (see Scheme 2 for naming) were synthesized. $(HO_2C)_4$-[G2]-N_3 and $(HO_2C)_8$-[G3]-N_3 were then clicked onto a purified propargyl glycine that was incorporated at the N-terminus of the substrate peptide to give the protected

peptides **12** and **13**, respectively. The reaction was done in 10 mM phosphate buffer (pH 8) using a synthesized tris-tri(methylazolyl)amine ligand (Scheme 3).

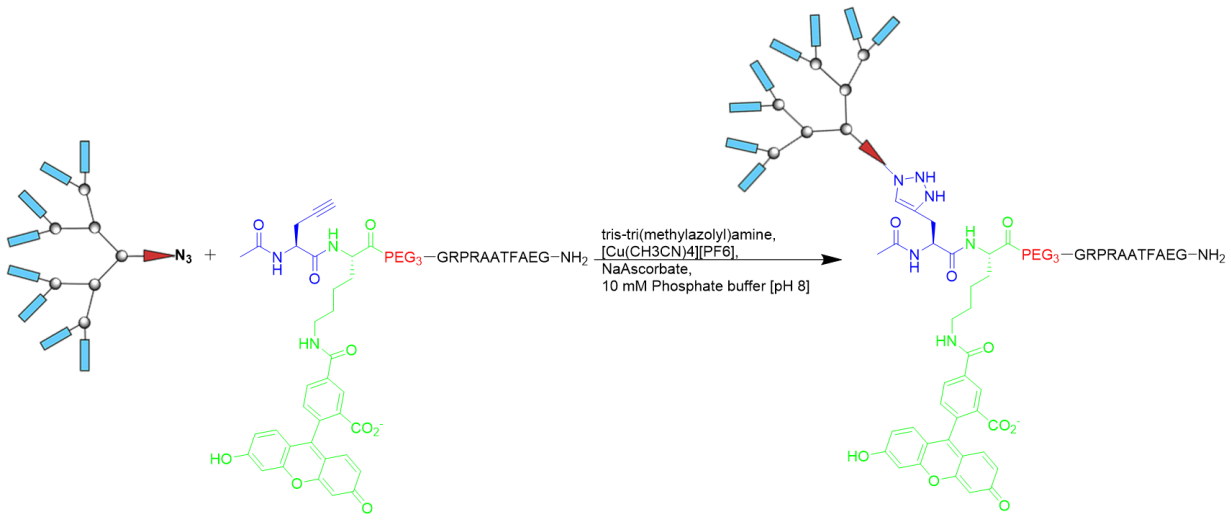

Scheme 3. Synthesis of dendrimer protected peptides via click reaction.

When tested for protease stability, peptide **12** showed a half-life of 35±7 minutes, an improvement over the unprotected peptide **1**. It was expected that peptide **13** would show an even greater increase in half-life as the size of the dendrimer increases. However, attempts at analyzing the results of the degradation assay using both analytical RP-HPLC and CE-LIF proved unsuccessful, as almost no signal was seen. This quench in fluorescence is most likely due to the high local concentration of acid present in the periphery of the later generation dendrimers. Later generation dendrimers were thus not pursued as protectides.

7. Dimerization as the Protection Strategy

All of the approaches taken thus far relied on adding bulk to the N-terminus of a peptide in order to block its entrance to the catalytic cleft of cytosolic peptidases. We decided to take a step back and focus merely on masking the N-terminus to hinder recognition without relying on sterics. In considering straight-forward synthetic approaches to masking the N-terminus, we

hypothesized that N-terminal dimerization of a peptide could mask its N-terminus in the same way that cyclization would, but without the synthetic challenges or added conformational constraints that can often decrease substrate efficacy. Unlike N-terminal bulk, it will not add un-necessary cargo that could bring about unforeseen changes in the peptide's properties and activity. The idea of peptide dimers was brought about by recent work reported by Kier and Andersen. In a comprehensive study on the effect of various capping motifs on the folding properties of β-hairpins, Kier et al. introduced dicarboxylate capping motifs, among others, leading to the capping of two β-hairpins with one shared cap, thereby forming dimeric adducts. This was synthetically very simple, requiring just 1 equivalent of a dicarboxylic acid coupled during solid-phase peptide synthesis like any other amino acid.[90] We adapted this method to create a dimer of the PKB substrate using succinic acid as the linker (peptide **14**). This followed the same general structure of all other protected peptides, with the addition of a glycine spacer between K(FAM) and the dicarboxylate linker (Figure 20).

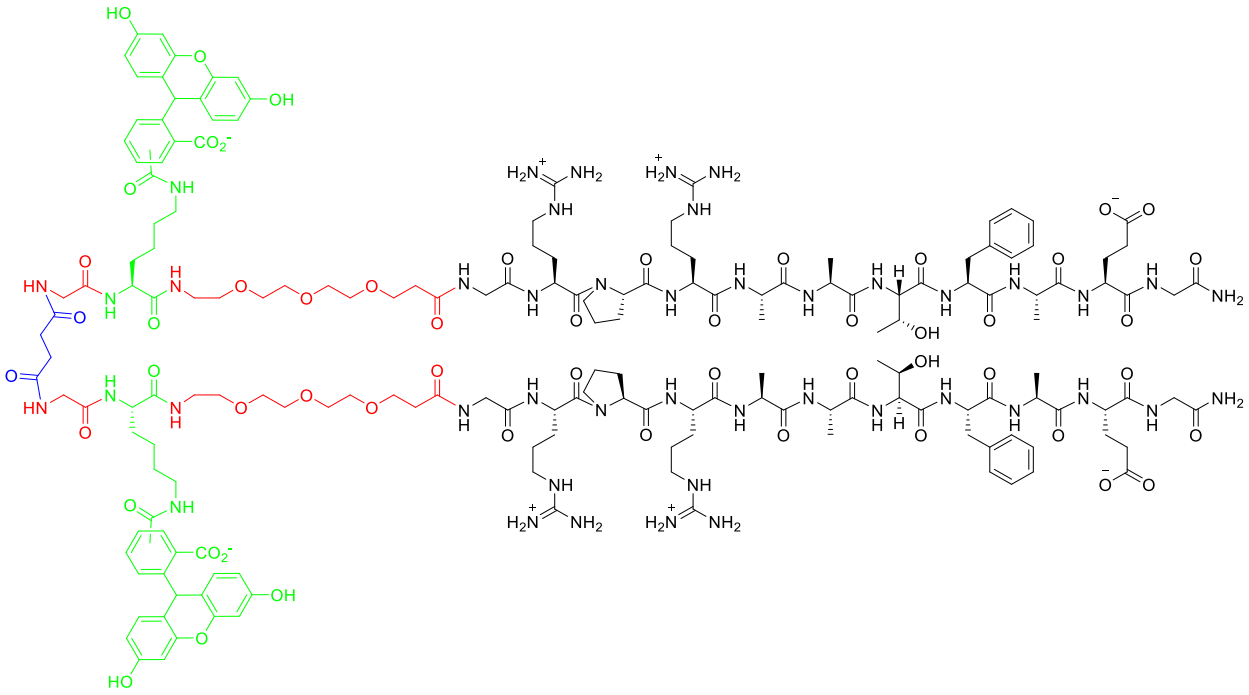

*Figure 20. Peptide **14**.*

The synthesis of the peptide dimer was successful on the automated synthesizer, on the microwave synthesizer, and by hand. Optimal results were achieved when the substrate sequence was synthesized on the automated synthesizer and all proceeding steps were done by hand. Dimerization proceeded efficiently, and the dimer was the major product of the reaction, according to LC/MS peak integration. Some succinic acid coupled to only one peptide was seen as well, and no peptide was seen that remained uncoupled. Despite the reported purity of the purchased carboxy-PEG_3-amine (reported to be 99.5% pure), significant amounts of dimers with differing (longer) lengths of PEG chains were observed by ESI-MS, even after multiple rounds of purification by RP-HPLC. We hypothesized that a longer PEG chain may make dimerization more favorable, but since the PEG_3 dimer remained the major product and the 1-2 unit change in the length of the PEG chain was not expected to have a significant effect on stability, we continued with the mixture for preliminary investigations. CE-LIF analysis of time points from a

degradation assay revealed a half-life of 420±24 minutes, a 28-fold increase over peptide **1**. Such an improvement in stability has not been seen before outside the realm of cyclized peptides. To confirm that these results do not reflect co-elution of the parent peptide and fragments, CE-MS was used to analyze the samples (done by Mac Gilliland; Ramsey lab). Based on integration of the peaks relative to an added internal standard, the half-life of peptide **1** was 5 minutes, while the half-life of peptide **14** was 2 hours (Figure 21), representing the same fold increase seen by CE-LIF.

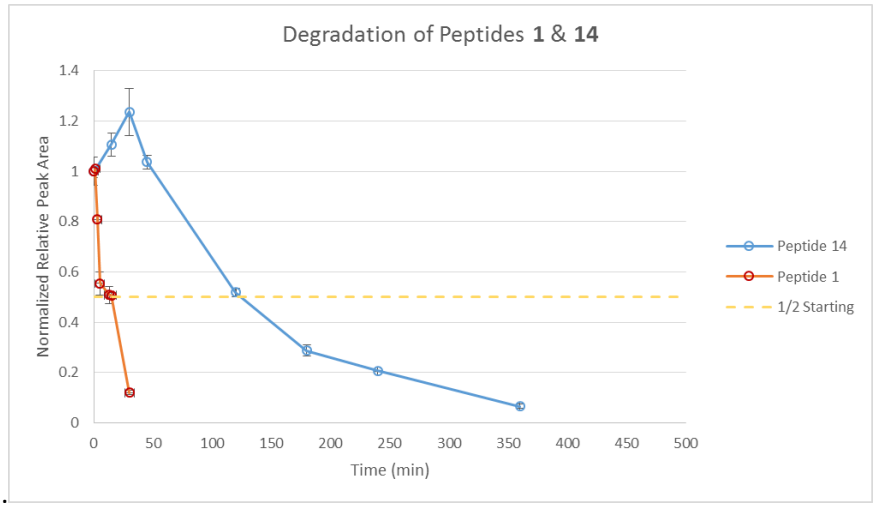

*Figure 21. Degradation of peptides **1** & **14** as analyzed by CE-MS. *analysis done by Mac Gilliland in the Ramsey lab. Error bars represent the standard deviation of three runs.*

7.1.Extension

7.1.1. Linker effect

To test the role of the linker, two additional versions of peptide **14** were synthesized, one using isophthalic acid (peptide **15**) and one using terephthalic acid (peptide **16**) as the linker (Figure 22). We were particularly interested to see if the rigidity of the linker will have any effect on the stability of the peptide dimer. When tested against peptide **14**, however, peptides **15** & **16** appeared to have half-lives within error of peptide **14** (Figure 23), indicating the linker used does

not affect the degradation resistance. This can be seen as advantageous, potentially allowing for the incorporation of dyes or conjugation sites in the linker, for example.

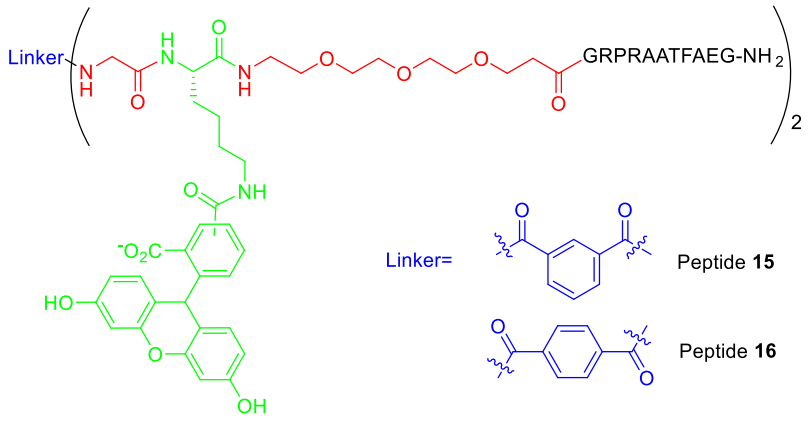

*Figure 22. Peptides **15** & **16**.*

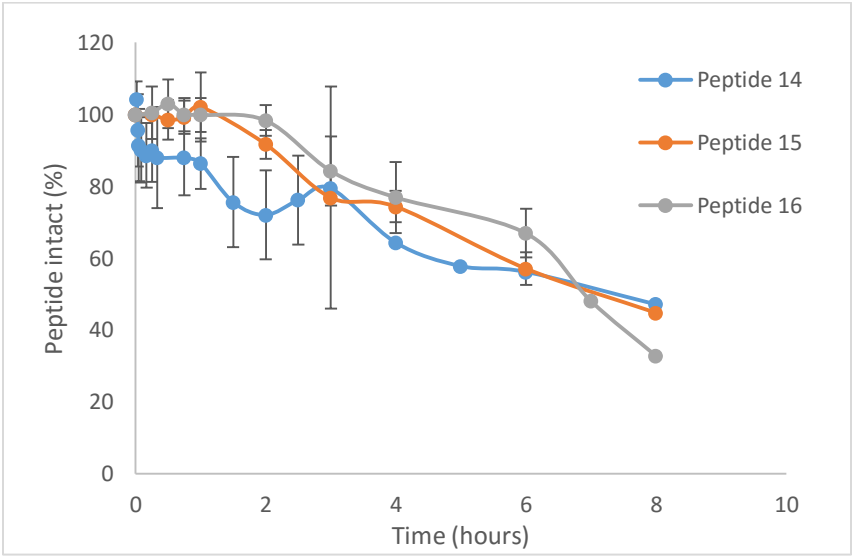

*Figure 23. Degradation of peptides **14**-**16** in HeLa cytosolic lysates. Error bars represent standard deviation of three runs.*

7.1.2. Substrate scope

To evaluate the generality of this approach, we applied it to other kinase substrates. Dimers of a known PKC substrate (QKRPSQRSKYL-NH_2)[98] and Abl substrate (EAIYAAPFAKKK-NH_2)[99] were synthesized, using succinic acid as the linker. The Abl dimer (peptide **19**) was synthesized with a PEG_4 linker. As we predicted, no dimers other than the desired one were

observed. The PKC dimer (peptide **20**) was already synthesized with PEG_3, so the mixture was used. A standard for comparison in which the N-terminus of the substrate sequence was simply capped with FAM was also synthesized for each substrate (Peptides **17** & **18**, Figure 24).

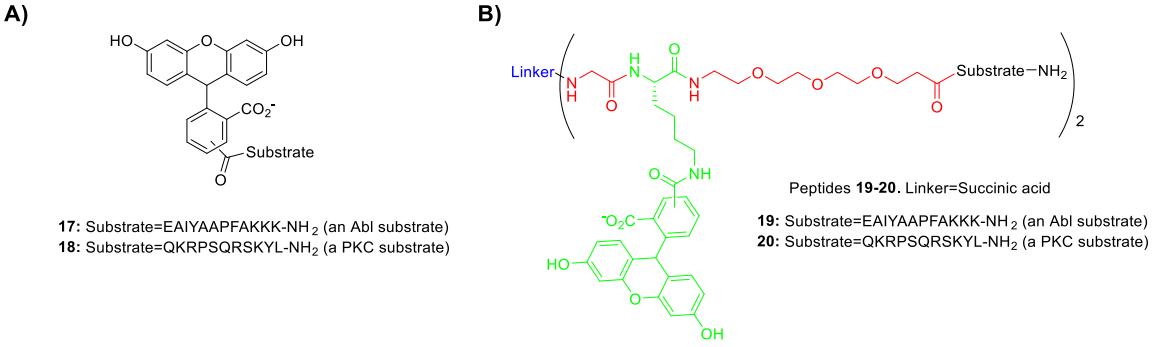

*Figure 24. (A) Peptide standards **17**-**18**. (B) Peptide dimers **19**-**20**. *Peptide **19** was synthesized with a PEG_4 linker.*

Analysis of peptide degradation showed an improvement with all peptides upon dimerization, with a 24-fold and 7.5-fold increase for the Abl and PKC substrates, respectively (Figure 25 & Table 2).

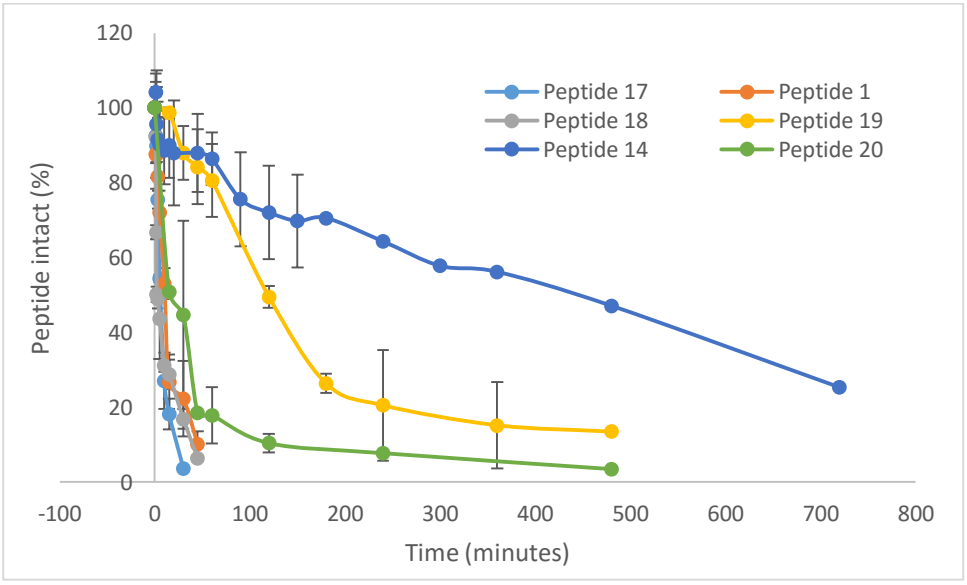

*Figure 25. Degradation of control peptides **1**, **17**, & **18** and dimerized peptides **14**, **19**, & **20** in HeLa cytosolic lysate. Error bars represent the standard deviation of three runs.*

Table 2. Half-lives of peptides in HeLa cell lysates.[a]

Peptide Standards	***$t_{1/2}$ (mins)***	***Peptide Dimer***	***$t_{1/2}$ (mins)***	***Fold Increase***
Peptide **1**	15±1	Peptide **14**	420±24	28
Peptide **17**	5±1	Peptide **19**	120±5	24
Peptide **18**	2±0.2	Peptide **20**	15±3	7.5

[a] Errors are from the standard deviation of three runs.

7.2.Substrate Efficacy

7.2.1. In vitro Phosphorylation

To assess the ability of the dimerized peptides to act as substrates for their respective enzymes, all peptides were synthesized using only one isomer of FAM ((5)-FAM) and a PEG_4 chain (herein indicated with ***** by the peptide number) in order to simplify analysis, since dimers with differing lengths of PEG chains (and even the 5- and 6- isomers of FAM) can be separated by CE, complicating the analysis. The peptides were incubated with purified kinase at 30 °C and phosphorylation was monitored over time using CE-LIF (Figure 26A&B). The identification of phosphorylated peaks was confirmed by HR ESI-MS. All dimer peptides were phosphorylated by their respective kinase, on one or both of the phosphorylation sites, indicating that the dimerization did not hinder the peptide's ability to act as a substrate. Dimers were phosphorylated to a similar extent as their un-dimerized counterpart, suggesting the rate of phosphorylation was not significantly perturbed (Table 3). Separation could not be achieved with peptide **20***, so phosphorylation could not be quantified. However, new peaks were clearly seen growing in (compared to the negative control) (Figure 26C&D) and HR ESI-MS confirms phosphorylation was taking place.

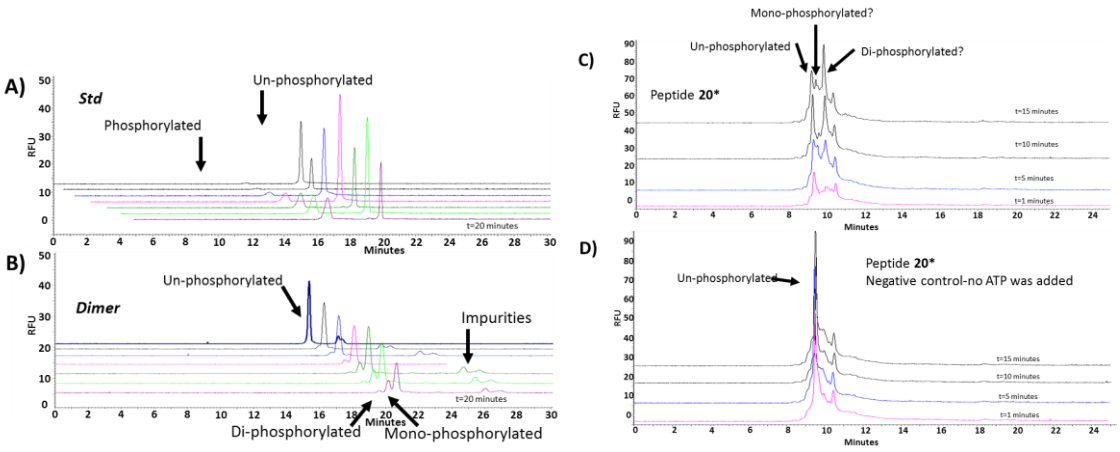

*Figure 26. Electropherograms following the in vitro phosphorylation of peptides **17*** (A) and **19*** (B). Time points were taken at t=0, 1, 3, 5, 10, 15, & 20 minutes. (C) & (D) are Electropherograms following the in vitro phosphorylation of peptide **20***. Complete separation was never achieved.*

*Table 3. Extent of in vitro phosphorylation of peptides **1***, **14***, & **17*-20*** after 20 minutes. † Full separation could not be achieved, and phosphorylation was not quantified.[a]*

Peptide Standard	***% Phosphorylated***	***Peptide Dimer***	***% Phosphorylated***
Peptide **1***	27±2	Peptide **14***	30±2
Peptide **17***	17±2	Peptide **19***	16±1
Peptide **18***	42±6	Peptide **20***	------

[a] Error represents the standard deviation of three runs

7.2.2. Phosphorylation in Cell Lysates

Since previous work in our lab has been done on increasing the lifetime of peptide **17**, we chose to move forward with peptides **17*** & **19*** for comparison. The phosphorylation of peptide **19*** in a cytosolic lysate was tested. Peptides **17*** & **19*** were incubated at 30°C in Baf/BCR-Abl cytosolic lysate containing ATP and a cocktail of phosphatase and protease inhibitors, and phosphorylation was monitored using CE-LIF (Figure 27). Both peptides **17*** & **19*** were phosphorylated over time at comparable rates: peptide **17*** was 87±2% phosphorylated after 2 hours, and peptide **19*** was 86±0.1% phosphorylated relative to non-degraded peptide (due to the overlay, peaks for peptide **19*** were de-convoluted as described previously[44] using Origin 9.0. The error reported for the calculated peak area was 3-9%).

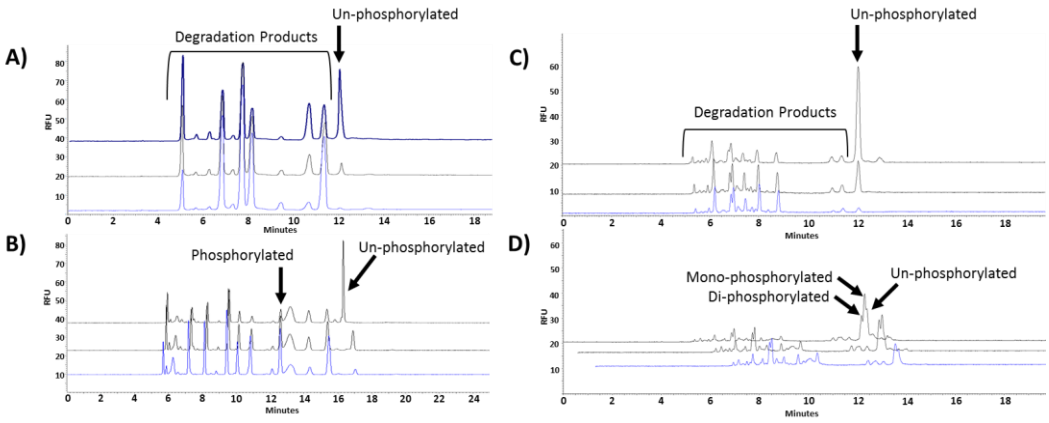

*Figure 27. Electropherograms monitoring the phosphorylation of peptides **17*** (A & B) and peptide **19*** (C & D) in Baf/BCR-Abl cytosolic lysates. Time points were taken at (top to bottom) t=1, 1.5, & 2 hours. (A) & (C) are the negative controls in which no ATP was added.*

7.2.3. Phosphorylation in Living Cells

The performance of peptide **19*** intracellularly was then assessed. Peptide **17*** or **19*** were pinocytosed, along with sodium pervanadate as phosphatase inhibitor, into live Baf/BCR-Abl cells and incubated at 37°C for 25 minutes. It is worth noting that pinocytosis puts a significant amount of stress on cells, making it an even more hostile environment for peptides. The cells were then lysed and the cellular contents analyzed by CE-LIF (Figure 28). Peptide **17*** seemed to have completely degraded, as no intact phosphorylated or un-phosphorylated peptide was seen. Peptide **19***, however, did not exhibit complete degradation, and both un-phosphorylated and di-phosphorylated peptide were seen. The peptide dimer was 54±8% phosphorylated relative to intact peptide remaining, and together, those constituted 19±2% of all species present. Interestingly, unlike with the *in vitro* assays, no mono-phosphorylated peptide was detected. This could be due to the more crowded environment within a cell, making a second phosphorylation event on the same peptide more favorable than the mono-phosphorylation of another substrate due to proximity.

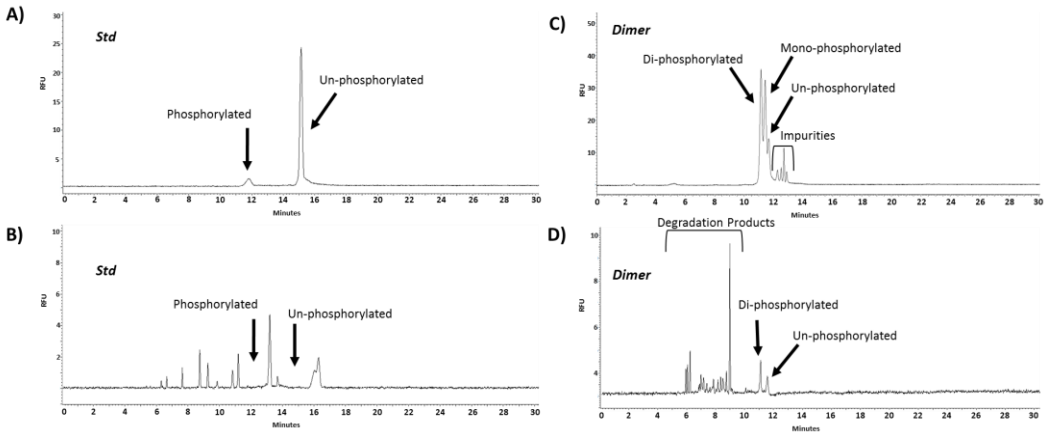

*Figure 28. Electropherograms measuring the amount of peptide **17*** (B) and **19*** (D) phosphorylated in Baf/BCR-Abl cells after 25 minutes of incubation. (A) and (C) show time points from in in vitro assays of peptide **17*** and **19***, respectively, for comparison of migration times.*

8. Conclusions

A variety of N-terminal capping motifs were tested for their ability to impart protease resistance on a PKB substrate peptide (results summarized in Table 4). Like most approaches that increase steric bulk, the ones examined here appeared to have only a minor influence, suggesting that steric hindrance alone is not effective. With all of the attempted steric caps, it is important to remember that the inhibition of digestion by cytosolic proteases could be the result of disruption of binding necessary for catalysis within the cleft, and not due to an inability to enter it. In that case, it stands to reason that endopeptidases would not be affected by the N-terminal steric cap protection approach, which could explain why only a limited increase in half-lives was seen.

Table 4. Half-lives of peptides in HeLa cytosolic lysates.[a]

	Peptide	**$t_{1/2}$ (minutes)**
PKB Substrate Std	Peptide **1**	15±1
Beta-hairpins	Peptide **2**	26±3
	Peptide **3**	30±5
	Peptide **4**	45±7
	Peptide **5**	25±2
Supramolecular	Peptide **6**	5±0.4
	Peptide **6**+CB[7]	20±1

Aryl Cap	Peptide **7**	~7
	Peptide **8**	~5
Dendritic	Peptide **12**	35±7

[a] Error was determined based on the standard deviation from three runs.

Of all the methods tested, the most successful was one that entirely neglected the idea of adding bulk for steric hindrance. Skewing proteases' ability to recognize the N-terminus of peptides via their dimerization effectively increased the half-life of peptides by up to 28-fold, leading to half-lives on the hour time scale in HeLa cytosolic lysates. This method is synthetically far simpler than peptide cyclization, the only method previously shown to impart this level of resistance, and did not affect their efficacy as substrates for their respective kinases. The use of this protection strategy in intracellular assays was demonstrated using peptide **19*** in Baf/Bcr-Abl cells, in which phosphorylation of the peptide was observed and successfully quantified via CE-LIF. This strategy is expected to further promote the use of peptide reporters for the study of intra-cellular enzymatic activity, in both healthy and diseased cells, generating further knowledge of their correlation to various disease states, potential therapeutics, and even monitoring disease progression and effectiveness of various therapies in patients.

9. Experimental

Synthesis of Peptide Substrates

Peptides were synthesized using manual or automated standard solid phase peptide synthesis (Thuramed Peptide Synthesizer, CEM Liberty 1 Microwave Peptide Synthesizer) using Fmoc protected amino acids on 0.057-0.25 mmol of RINK Amide resin. Four equivalents of standard amino acids were used for each peptide coupling while 2 equivalents of orthogonally protected lysine (for attachment of FAM) and PEG derivatives and 1 equivalent of dicarboxylic acid dimerization linkers were used. The sidechains of orthogonally protected lysine were protected with 1-(4,4-dimethyl-2,6- dioxocyclohex-1-ylidene-3-methylbutyl (N-ivDde) or

allyloxycarbonyl (N-alloc). Specific deprotection protocols are outlined below. (5)-FAM or (5,6)-FAM was coupled to the ε-NH of lysine or the N-terminal using 4 equivalents of FAM, 5 equivalents of PyBOP/HOBt and 8 equivalents of DIPEA in DMF and allowed to bubble with N_2 overnight. Coupling of FAM to a peptide was always the last step done on resin.

Peptides were cleaved from the resin in 9.5:2.5:2.5 trifluoroacetic acid (TFA), TIPS and water respectively for 3-4 hours. The TFA was evaporated and the cleaved peptides were precipitated using cold ethyl ether and extracted with water. Extracted peptides were lyophilized and then purified using semi-preparative RP-HPLC on a Vydac C18 semipreparative column with a gradient from '0 to 100% B' in 45-120 minutes. Solvent A was 95% H_2O, 5% CH_3CN and 0.1% TFA and Solvent B was made of 95% CH_3CN, 5% H_2O and 0.1% TFA. Second and third round of purification of peptide dimers was done with the column heated to 45°C. For purification of dendrimer conjugated peptides, a buffered mobile phase was used where solvent A was 10mM NH_4OAc in H_2O and solvent B was 10 mM NH_4OAc in 10% H_2O, 90% CH_3CN. Purified peptides were lyophilized and their purity confirmed by Analytical LC/MS on an Agilent Rapid Resolution LC-MSD system, equipped with an online degasser, binary pump, autosampler, heated column compartment, and diode array detector. Dendrimer conjugated peptides were dissolved in 10-11% NH_4OH/H_2O and characterized using HR ESI-MS.

Synthesis of Peptide Dimers

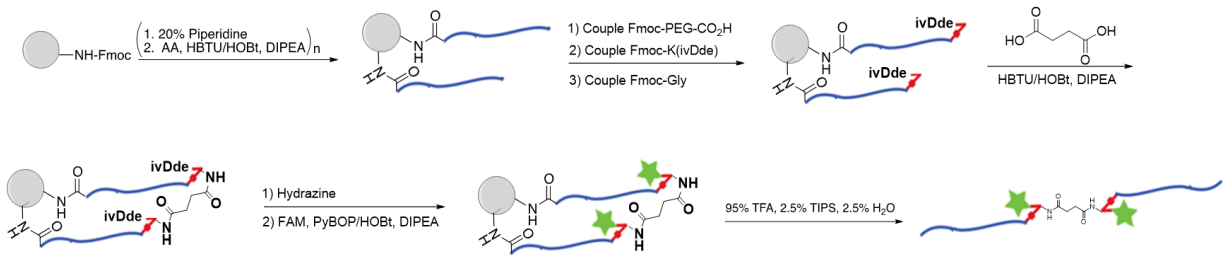

Substrate peptides were synthesized on 0.25 mmol RINK amide resin using standard Fmoc coupling. All proceeding couplings were done using the same conditions (unless otherwise noted) with differing equivalents of acid. Fmoc-protected PEG amino acid was then coupled using 2 equivalents for 4 hours, followed by Fmoc-Lys-ivDde using 2 equivalents for 4 hours, and then Fmoc-Gly using standard coupling conditions. After deprotection, succinic acid was coupled using 1 equivalent overnight for dimerization. Finally, the ivDde group was removed using 2% hydrazine-monohydrate in DMF (3 x 5 minutes), and FAM was coupled on using 4 equivalents of FAM, 5 equivalents of PyBOP/HOBt and 8 equivalents of DIPEA in DMF overnight.

On-Resin Click

$Cu(II)SO_4 \bullet 5H_2O$ (3.5 eq.) and Na-Ascorbate (3.5 eq.) were mixed in DMF and let stir for 30 minutes. The alkyne moiety (3.5 eq.) was then added to the mixture and let stir for an additional 30 minutes. The mixture was then added to the resin, followed by the addition of DIPEA (1µL/µmol resin loading). The reaction was agitated over-night, washed with DMF and DCM, and followed by the deprotection of a lysine as outlined below.

Alloc Deprotection

Alloc deprotections were carried out in 1:2 DCM:ACN in the presence of $Pd(OAc)_2$ (0.3 eq.), PPh_3 (1.5 eq.), NMM (10 eq.), and $PhSiH_3$ (10 eq.). Care was taken to ensure the $PhSiH_3$ was the last reagent added. The reaction was agitated over-night. After draining the solution, the resin was washed with THF (1 x 5mL x 5mins.), DMF (2 x 5 mL x 2 mins.), sodium diethyldithiocarbamate trihydrate solution (25 mg/ 1 mL DMF) (4-5 x 5 mL x 10 mins.), DMF (2 x 5 mL x 2 mins.), and DCM (2 x 5 mL x 5 mins.). *This series of washes was used following any reaction that used palladium.

ivDde Deprotection

The removal of ivDde from the sidechain of lysine was accomplished by treating the peptide resin 3 x 2 mins with 20 mL of 2% hydrazine monohydrate in DMF bubbling with N_2 followed by washing with DMF and DCM.

Synthesis of **aryl cap**

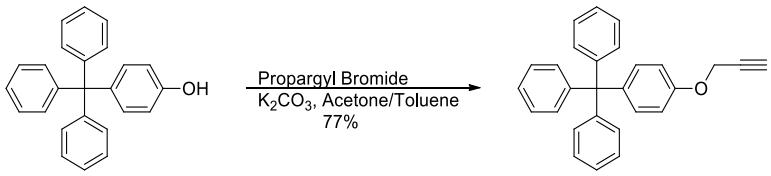

Synthesized as previously reported in literature.[100]

Synthesized as previously reported in literature.[101]

Synthesis of benzyl hydroxy-dendrimers

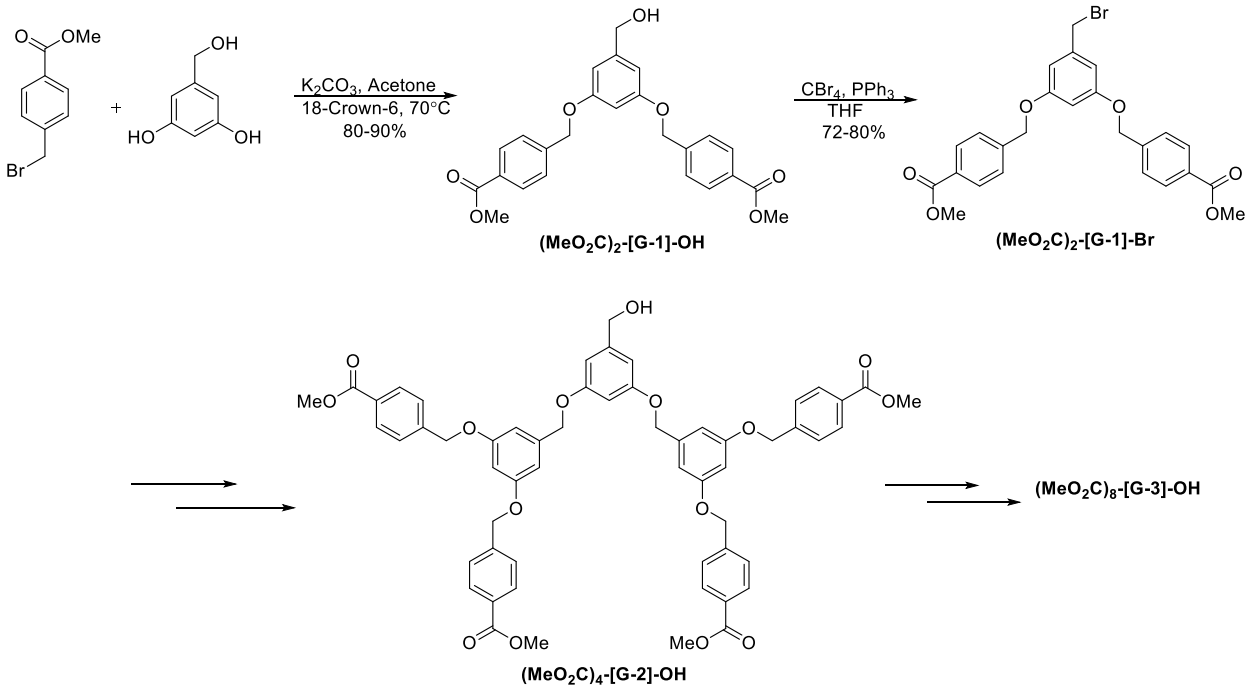

Synthesized as previously reported in literature.[96]

Synthesis of azido-dendrimers

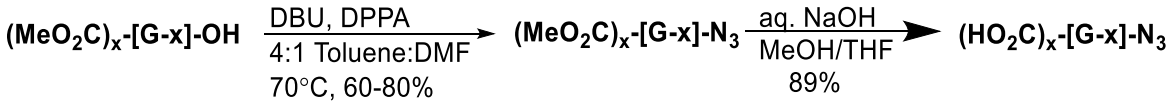

The benzyl hydroxyl-dendrimer (1.54 mmol) was dissolved in 4:1 toluene:DMF (25 mL). DPPA (3.94 mmol) and DBU (3.68 mmol) were added and the solution was let stir at 70 °C over-night. The resulting mixture was concentrated *in vacuo*, taken up in EtOAc, and washed with water. The solution was then dried over $MgSO_4$, and concentrated *in vacuo* to yield a dark brown sludge. The product was purified by column chromatography in 0% → 10% ether/DCM gradient to yield the product as a white solid.

$(MeO_2C)_4$-[G2]-N_3 (1.5449 g, 92.0% yield): ^{1}H NMR ($CDCl_3$) δ 8.06 (d, 8H), 7.49 (d,8H), 6.68 (s, 4H), 6.56 (s, 2H), 6.53 (s, 3H), 5.12 (s, 8H), 4.99 (s, 4H), 4.27 (s, 2H), 3.94 (s, 12H).

$(MeO_2C)_8$-[G3]-N_3 (0.7338 g, 73.1% yield): ^{1}H NMR ($CDCl_3$) δ 8.04 (d, 16H), 7.47 (d,16H), 6.67 (s, 8H), 6.65 (s, 4H), 6.55 (m, 9H), 5.08 (s, 16H), 4.97 (s, 12H), 4.25 (s, 2H), 3.92 (s, 24H).

Final hydrolysis of the esters was carried out as previously reported in literature.[96]

$(HO_2C)_4$-[G2]-N_3 (0.9883 g, 89.8% yield): ^{1}H NMR (MeOD) δ 8.00 (d, 8H), 7.98 (d,8H), 6.65 (s, 4H), 6.57 (s, 2H), 6.51 (s, 2H), 6.47 (s, 1H) 5.08 (s, 8H), 4.98 (s, 4H), 4.22 (s, 2H).

$(HO_2C)_8$-[G3]-N_3 (0.6943 g, 83.7% yield): ^{1}H NMR (MeOD) δ 7.86 (d, 16H), 7.25 (d,16H), 6.46 (s, 8H), 6.41 (s, 4H), 6.36 (s, 4H), 6.30 (s, 2H), 6.27 (s, 2H), 6.21 (s, 1H), 4.70 (s, 16H), 4.56 (s, 12H), 2.68 (s, 2H).

Synthesis of Tris-tri(methylazolyl)amine Ligand

Synthesized as previously reported in literature[92]

Solution Phase Click Reaction of Dendrimers

Excess of azide (8.13 µmol) was added to a 1 mM solution of propargyl peptide (0.193 µmol) in 10 mM phosphate buffer (pH 8). A pre-mixed solution of tris-tri(methylazolyl)amine (6.0 µmol) and $[Cu(CH_3CN)_4][PF_6]$ (4.0 µmol) in CH_3CN (200 µL) (previously stirred for one hour) was added, followed by sodium ascorbate (5.0 µmol) in minimal amount of buffer. The solution was stirred over-night in the dark. The reaction was quenched by addition of 0.1% TFA in 95% H_2O, 5% CH_3CN and lyophilized down to a solid. Products were then purified by RP-HPLC as described above.

Cell Culture

HeLa and Baf/Bcr-Abl cells were obtained from the American Type Culture Collection and cultured in DMEM medium supplemented with 10% FBS, penicillin (100 units/mL) and

streptomycin (100 µg/mL). All cells were maintained in a humidified atmosphere of 37 °C in 5% CO_2.

Degradation Assays

A HeLa cell pellet was washed with and resuspended in phosphate buffered saline (PBS; 137 mM NaCl, 10 mM Na_2HPO_4, 27 mM KCl, 1.75 mM KH_2PO_4, pH 7.4). The cells were submerged in liquid nitrogen for 1 min and rapidly thawed at 37 °C for a total of three cycles. The mixture was centrifuged at 14,000 x g for 15 min at 4 °C. The supernatant was transferred to a clean centrifuge tube and maintained on ice until use in the assay. Total protein in the lysate was determined by Bradford assay.

Assessment of peptide degradation was performed by incubating peptide (10 µM) with the HeLa cell lysate (3 mg/mL total cell protein) at 37 °C. Aliquots were removed over time and quenched by addition of HCl to a final concentration of 100 mM. Samples were diluted 20-50x in electrophoretic buffer prior to analysis by CE-LIF (see below for methods and conditions), or analyzed by analytical RP-HPLC without any prior dilution with a gradient from '0 to 100% B' in 25 minutes. Solvent A was 95% H_2O, 5% CH_3CN and 0.1% TFA and Solvent B was made of 95% CH_3CN, 5% H_2O and 0.1% TFA.

PKB Kinase Assay

PKB Kinase assays were performed by incubating peptide (0.75 µM peptide **1*** or 0.375 µM peptide **14***) with PKB-α (ThermoFisher Scientific; Waltham, MA) (0.125 ng/µL) in assay buffer [8 mM MOPS (pH 7.5), 0.2 mM EDTA, 4 mM $MgCl_2$, and 1 mM ATP] at 30 °C. Aliquots were removed over time and quenched by heating to 95°C for 4 minutes. Samples were diluted 20-50x in electrophoretic buffer prior to analysis by CE-LIF.

Abl Kinase Assay

Abl Kinase assays were performed as described above using 2.5 µM peptide **17*** or 1.25 µM peptide **19*** and 0.75 ng/µ Abl-1 (ThermoFisher Scientific; Waltham, MA) in assay buffer [50 mM Tris (pH 7.5), 1 mM $MnCl_2$, 5 mM $MgCl_2$, 2 mM DTT, and 1 mM ATP].

PKC Kinase Assay

PKC Kinase assays were performed as described above using 2.5 µM peptide **18*** or1.25 µM peptide **20*** and 5 ng/µL PKC-α (ThermoFisher Scientific; Waltham, MA) in assay buffer [20 mM MOPS (pH 7.2), 1 mM DTT, 1 mM $CaCl_2$, 10 mM $MgCl_2$, lipid activator, and 1 mM ATP].

Lysate Phosphorylation Assays

A Baf/BCR-Abl pellet was washed 2x with PBS buffer. The pellet was resuspended with Mammalian Protein Extraction Reagent (M-PER) with 1 mM sodium pervanadate and 1X Complete EDTA-Free Mini-TAB protease inhibitor cocktail (Roche) and vortexed for 10 minutes. The mixture was then centrifuged at 14,000 x g at 4 °C for 15 minutes, and the supernatant was reserved and kept on ice until use. Total protein concentration was determined by Bradford Assay.

Assessment of peptide phosphorylation was performed by mixing peptide (5 µM for peptide **17***, 2.5 µM for peptide **19***) with Baf/BCR-Abl cell lysate (3 mg/mL total cell protein) in assay buffer [50 mM Tris (pH 7.5), 1 mM $MnCl_2$, 5 mM $MgCl_2$, 2 mM DTT, and 1 mM ATP]. And incubating at 30 °C. Aliquots were removed and quenched by addition of HCl to a final concentration of 100 mM. Samples were diluted 20-100x in electrophoretic buffer prior to analysis by CE-LIF.

Intracellular Phosphorylation Assays

Approximately 5 million cells were isolated in a 1.5 mL tube and loaded with peptide **17*** or peptide **19*** by pinocytosis. The cells were incubated for 10 minutes at 37 °C with hypertonic loading solution (Influx, Life Technologies) containing 24 µM peptide and 1 mM sodium pervanadate, followed by pinosome lysis in hypotonic media to release the peptide into the cytosol and initiate the phosphorylation assay. The time at which the hypotonic media was applied was used at t=0 minutes. The cells were then pelleted and resuspended and incubated in full serum media containing 1 mM sodium pervanadate for 10 minutes at 37 °C. After the 10 minutes, the cells were pelleted and washed twice and then resuspended with PBS buffer. The cells were lysed and intracellular activity terminated by heat treatment at 95 °C for 5 minutes. The resulting lysate was centrifuged at 14000 rcf for 10 minutes at 4°C, and the supernatant was collected and analyzed via CE-LIF without any further dilution.

Capillary Electrophoresis

CE-LIF (488 nm) was performed using a Proteome-Lab PA 800 (Beckman Coulter, Fullerton, CA) equipped with 30 cm fused silica capillaries of 30 µM inner diameter, 360 µM outer diameter (Polymicro Technologies, Phoenix, Az). All methods were run at 8kV for 20-40 minutes. Electrophoretic buffer for all degradation assays was 100 mM borate, 100 mM sodium dodecyl sulfate (SDS), pH 7.7. Electrophoretic buffers for *in vitro* phosphorylation assays for peptides **1***, **17***, and **19*** was 100 mM tris-tricine, 5 mM SDS, pH 8.1; for peptide **18*** was 400 mM borate, pH 9.5; for peptide **14*** was 100 mM borate, 15 mM SDS, pH 11.3; for peptide **6*** was 500 mM borate, pH 9.6. For all lysate and intracellular assays, the electrophoretic buffer was 100 mM tris-tricine, 5 mM SDS, pH 8.1. In the case of phosphorylation of peptide **19*** in cell

lysates, the peaks were de-convoluted by using a Lorentzian fit in Origin 9.0 (OriginLab Corporation, Northampton, MA) as described previously.[44]

Chapter III. Current Methods for Characterizing and Sensing Histone Posttranslational Modifications

1. Packaging of DNA

The DNA found within eukaryotic nuclei carries most of the genetic instructions used in the growth, development, and functioning of organisms. In humans, this DNA is composed of 23 base-pairs of chromosomes, each comprising millions of base pairs of DNA, approximately 6 billion in total. When stretched linearly, this amounts to roughly two meters of DNA, all stored in the nucleus that is only 10 µm in diameter.[102] This requires a great deal of compaction, which is achieved through the wrapping of DNA into fundamental units called nucleosomes, which condense into chromatin, and can then coil tightly to form chromosomes (Figure 29).

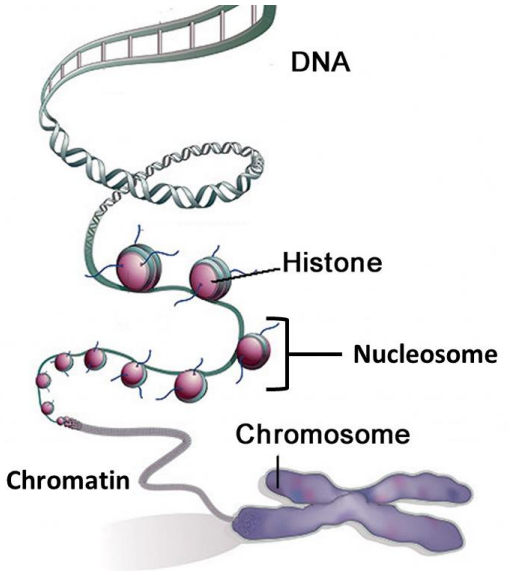

Figure 29. Representation of DNA packaging.

Each nucleosome consists of an octamer of four core histone proteins, H2A, H2B, H3, and H4, around which 147 DNA base pairs wrap. The nucleosomes are then connected by a linker region, composed of 20-30 base pairs.[103] They can be in one of two states: one in which the DNA is wrapped around the histone tightly, and is inaccessible for transcription (heterochromatin), or one in which it is loosely associated, resulting in gene activation (euchromatin) (Figure 30).

Which state it is in at any given time is determined by the various posttranslational modifications (PTMs) present on the histone proteins.

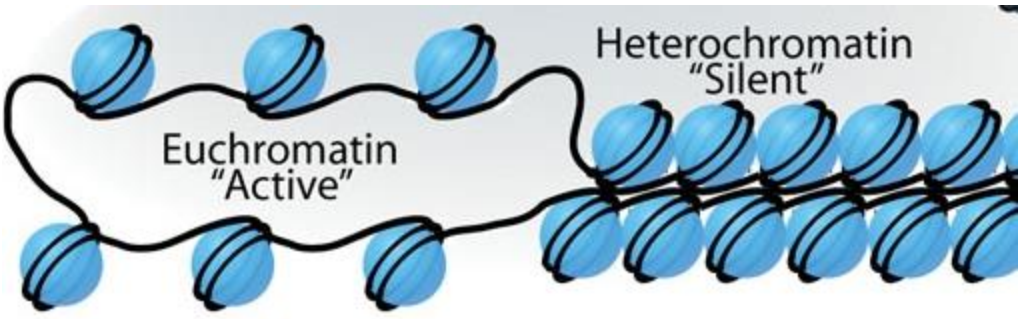

Figure 30. Representation of heterochromatin and euchromatin. (Adapted from Sha, K. and Boyer, L. A. The chromatin signature of pluripotent cells (May 31, 2009), StemBook, ed. The Stem Cell Research Community, StemBook, doi/10.3824/stembook.1.45.1,http://www.stembook.org.)

2. Posttranslational Modifications

The amino acid residues of histone proteins, especially of the unstructured tail domain, are subject to a large number of PTMs. These include the more common modifications, such as serine and threonine phosphorylation, arginine (mono- and di-) methylation, lysine (mono-, di-, and tri-) methylation, and lysine acetylation, as well as the less abundant modifications, such as proline isomerization, arginine deimination, ubiquitination, ADP ribosylation, and sumoylation (Figure 31). These PTMs can act individually or in concert to dictate DNA packaging and distinct downstream events, either by recruiting non-histone proteins and enzyme complexes to chromatin, which subsequently manipulate DNA, or by interrupting nucleosomal contacts and consequently affecting the high-order structure of chromatin.[2,104,105] As a result,

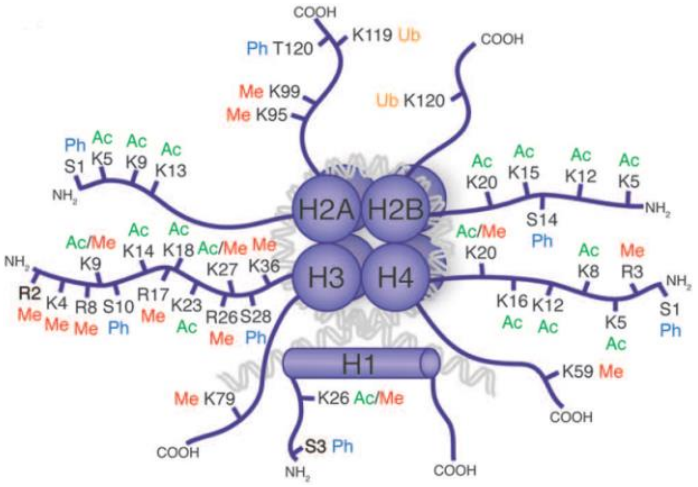

Figure 31. PTMs found at different sites on histone tails. (Adapted from [167])

histone PTMs are implicated in a wide range of biological processes, including gene transcription, DNA replication and repair, mitosis, and meiosis.[1] Consequently, dysregulation of histone PTMs is linked to various diseases, including cancer, asthma, and diabetes, among others, and can thus serve as valuable diagnostic indicators of disease progression.[1,2]

3. Current Tools for Studying Histone PTMs

Due to the biological ramifications of histone PTMs, there is great interest in mapping where, when, why, and how PTMs are installed and their subsequent downstream effects. The primary methods currently used to characterize PTMs require the use of antibodies as affinity reagents, which bring considerable limitations. They often suffer from a measurable amount of cross-reactivity, making it difficult to distinguish between distinct PTMs, such as different methylation states of lysine for example.[106,107] This is a critical shortcoming, as each distinct methylation state leads to different downstream events. Furthermore, antibodies are time-consuming, difficult, and expensive to produce, and quality, and thus efficacy, often varies from lot to lot.[7,107] Finally, the sequence specificity of antibodies renders them futile for the discovery of new PTMs, and even binding to a known target site can be disrupted by PTMs at proximal residues. Several biomolecule-based designs, such as affibodies and aptamers, have shown potential as antibody surrogates.[108,109] However, these systems are limited by sensitivity to pH and temperature, and like antibodies, binding is often not sequence independent.

The use of mass spectrometry (MS) proteomics has emerged as a powerful platform for mapping histone PTMs. Since every PTM leads to a change in the element composition of a residue, each is associated with a defined mass shift (change in its molecular weight), and can

thus be identified by MS regardless of neighboring residues.[110] The most common approach to MS-based proteomics is the bottom-up approach. After isolation from cells or tissue, proteins are proteolytically digested, usually by trypsin, and the peptide fragments are analyzed by HPLC/MS/MS. The efficient detection of PTMs, however, is then highly dependent on the abundance of the PTM in a sample. In the proteolytic digest, the modified peptides are in very low abundance, thus requiring an enrichment step prior to analysis (Figure 32).[111,112] Several enrichment methods are outlined below.

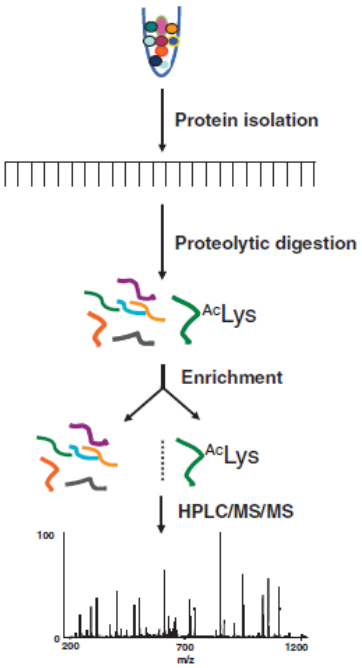

*Figure 32. Work-flow of proteomic analysis of PTMs. Reproduced with permission from Wiley: Proteomics **2009**, 9 (20), 4632.*

3.1. Enrichment of Modified Fragments

Many approaches for PTM enrichment have been established, and often vary based on the PTM of interest (Figure 33). The most effective PTM enrichment is that of phospho-peptides using immobilized metal affinity chromatography (IMAC) or metal oxide affinity chromatography (MOAC) (Figure 33). These methods take advantage of the unique chemical characteristics of the phosphate group-its negative charge and ability to interact with ion exchange beads and to participate in coordinate covalent bonding with metal ions. IMAC using Fe^{3+} was used to enrich phospho-peptides in some of the first successful phospho-proteomics studies,[113,114] and has since been continually improved, with now an array of metal ions (i.e. Ga^{3+}, Zr^{3+}, Al^{3+}) now available for use.[110] MOAC has also been widely used, and currently represents an improvement over IMAC. A titanium oxide-based solid matrix has proven to be easier to implement and more robust for the analysis of complex protein samples,[115] and its utility has been demonstrated in several proteomic studies.[116–118] Both IMAC and MOAC have

been applied to efficient proteomic studies, leading to the identification of tens of thousands of phospho-peptides.[110] While extremely efficient, this method is specific to enriching phosphorylated peptides, and cannot be extended to other PTMs.

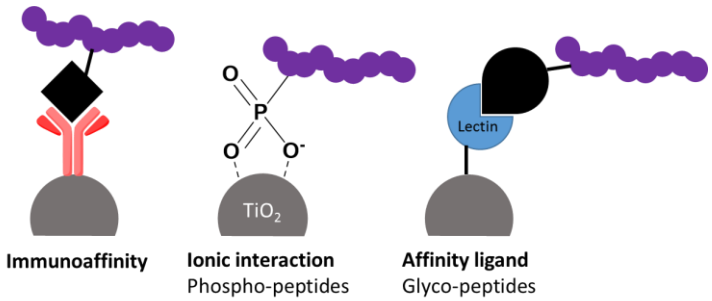

Figure 33. Examples of PTM enrichment methods for subsequent MS analysis.

Another approach often seen in the literature is one based on chemical-derivatization. One way this is done is via metabolic labeling. Azides are the most popular chemical handle for this purpose due to their small size and bioorthogonality. The chemically modified PTM proteins can then be conjugated to an affinity linker, such as biotin, for subsequent enrichment. This method has been successfully used towards enrichment of farnesylated,[119] palmitoylated,[120] and myristoylated[121] proteins. Analogues of SAM have also been developed that allow the transfer of alkynes,[122,123] and azides[124] to lysine and arginine[125] in place of a methyl group, in some cases requiring protein engineering to accommodate the unnatural SAM analogue.[126,127] Alternatively, a PTM can be derivatized *in vitro* via chemical modification, converting it into a site for affinity labeling. For example, Wells et al. described the tagging of sites modified by O-linked β-N-acetylglucosamine (O-GlcNAc) via mild β-elimination followed by Michael addition with biotin pentylamine for subsequent

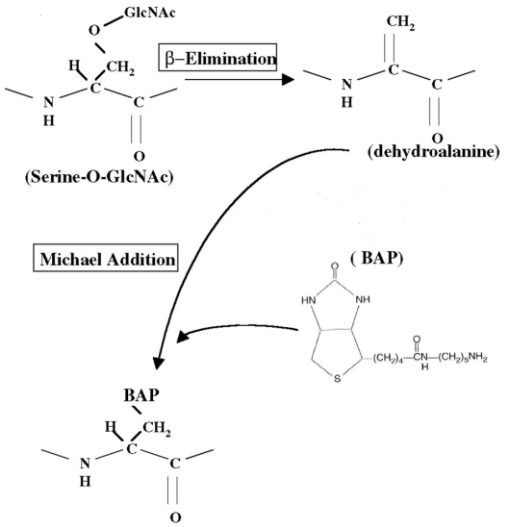

Figure 34. β-elimination of O-GlcNAc and replacement with BAP via Michael addition.

enrichment (Figure 34).[128] The oxidation and conjugation of glycopeptides to hydrazide resin is another example of a commonly used derivatization method. Non-glycoproteins can be washed away, and the glycoproteins are subsequently released via enzymatic cleavage by peptide-N-glycosidase F (PNGase F) (Figure 35).[129,130] Recently, Lewallen et al. described a derivatization strategy to label citrullinated proteins. They developed a biotin-conjugated phenylglyoxal probe which, under acidic conditions, reacts selectively with citrulline. They went on to demonstrate the use of this probe as an antibody surrogate for western blotting and as a chemical handle to enrich citrullinated peptides for MS.[131] The derivatization approach has been mostly applied to sugars and lipid-modified residues thus far. The development of selective reactions for less reactive modifications can be extremely challenging, and is lagging behind.[110,112] Furthermore, although useful, chemical derivatization does have its drawbacks. Even the most efficient reactions suffer from some sample loss, and often produce unwanted side products that can further complicate analysis down the road.

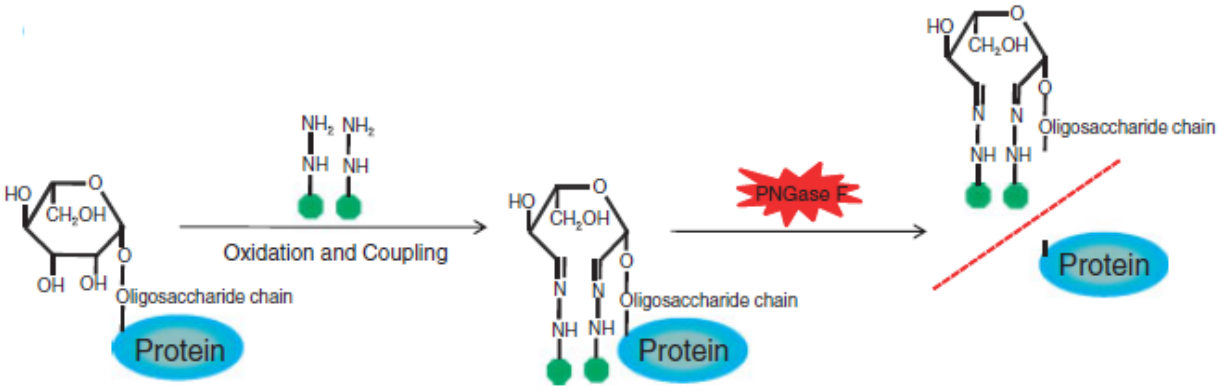

*Figure 35. Chemical derivatization and subsequent enzymatic cleavage for enrichment of glycoproteins or peptides. Reproduced with permission from Wiley: Proteomics **2009**, 9 (20), 4632.*

As an alternative to the derivatization approach, affinity based enrichment can be used. The most common example of that is antibody-based enrichment, perhaps the most widely used of all the approaches described thus far. The antibody corresponding to the PTM of interest can be

linked to a solid support and peptides from tryptic digest bearing that PTM can be isolated by immunoaffinity purification (Figure 33). Pan-PTM antibodies have been developed and used to study lysine acetylation,[132–134] arginine methylation,[135] and tyrosine nitration,[136] among others. While antibodies have the advantage of being very specific, therefore alleviating the concern of inefficient separation, their specificity can also be problematic. Although "pan-antibodies" are commercially available, there are still cases in which the antibodies are affected by nearby residues.[137,138] Their high cost and batch to batch variability can also be seen as a disadvantage, and is especially prominent when it comes to small PTMs, such as acetyl lysine or methyl lysine, since generating quality antibodies against them is difficult due to their similarity to their non-modified counterparts.[112] Furthermore, because of the generally tight binding of antibodies, release of the enriched peptides can often result in contamination of the sample with antibody fragments.

Aside from antibodies, immobilized domains that can specifically recognize PTMs have gained traction. Lectins, for example, have the ability to specifically bind carbohydrates, and have been used for the isolation of glycoproteins or peptides (Figure 33).[139–143] Triple malignant brain tumor domains of L3MBTL1, which sequence-independently recognizes mono- and di-methylated lysine, was used to enrich mono- and di-methylated lysine containing peptides, with minimal sequence specificity compared to antibodies.[144] This approach has also been taken with tandem-repeat ubiquitin-binding entities (TUBEs)[145] and Macro domain[146] to enrich ubiquitinated lysine and ADP-ribosylated proteins, respectively. More recently, interest has arisen in using small synthetic receptors as alternative affinity reagents.[147,148] Various synthetic receptors able to recognize certain PTMs in a sequence independent manner have been and are continuing to be developed, including sulfonatocalix[n]arenes,[149–151] mercaptophanes,[3,152–154] and

cucurbit[7]uril (CB7),[155] all of which have shown the ability to selectively bind methylated lysine and/or arginine, a class of PTMs that is particularly difficult to identify due to its small size. With their low cost, reproducibility, and stability to a range of conditions, synthetic receptors can serve as great tools for studying histone PTMs.

4. Purpose of This Work

In this work, one of the Waters' group mercaptophanes, A_2B,[3] selective for trimethyllysine (KMe_3), was used as an affinity reagent and applied towards affinity chromatography. Modification of one of the monomers, or the receptor as a whole, was done to anchor various linkers for immobilization on different resins. The effect of linkers and various buffers on the binding properties of A_2B to various methylation states of lysine on a short histone peptide was analyzed, and finally, a column packed with resin bound A_2B was used to successfully separate two peptides with the same sequence, differing only in the methylation of the lysine, demonstrating the feasibility of this approach.

Chapter IV. The Use of Small Molecule Receptors for Affinity Chromatography

1. Waters Group Mercaptophanes

As described in the previous chapter, improved methods for enriching protein samples in methylated Lys and Arg are greatly needed to move the field forward. The need to rely on antibodies, whether for directly studying the PTMs, or for enriching them for MS studies, is costing not only in money, but progress as well. The need for alternative methods is becoming more and more evident with the efforts to map the protein methylome. Protein methylation plays an integral role in cellular signaling, and yet it is poorly understood due to the lack of efficient tools to study it. This chapter describes the work done to apply a synthetic receptor towards the separation of peptides containing methylated lysine via affinity chromatography (Figure 36).

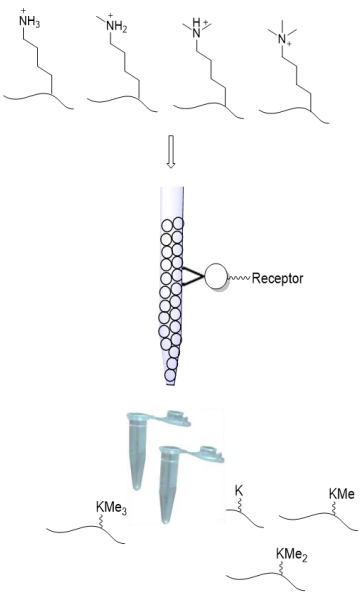

Figure 36. Affinity chromatography using a synthetic receptor for the separation of KMe_3.

1.1.Dynamic Combinatorial Chemistry (DCC)

The design and synthesis of organic receptors, such as cucurbiturils,[93,95,155] calixarenes,[149–151] and cyclophanes,[156,157] can be quite challenging. The de novo design requires an exact knowledge of how the desired target binds to its native host, and even then is never a guarantee of a successful receptor for that target. Futhermore, macrocyclization is often very low yielding.[156] Subsequent systematic changes to the structure are yet another challenge, with selective functionalization being yet again difficult and time consuming. Since many synthetic receptors contain multiple identical subunits in the macrocycle. To circumvent the need for de novo design and ease the re-design process, dynamic combinatorial chemistry (DCC) (Figure 37) has gained popularity in recent years as a high throughput method for synthesizing and identifying receptors. It uses thermodynamic control to produce a large library of potential receptors via reversible covalent bond formation. By mixing several monomers together, a large library of macrocycles forms under equilibrium. When an analyte is added, equilibrium shifts according to Le Chatelier's principle, amplifying the most thermodynamically stable receptor.[158–160] Thus the best host is discovered by competitive selection. This initial hit can then be used to further study the guest-host interactions by changing various aspects of the structure in an individual manner, one monomer at a time. This high throughput method allows for iterative redesign using simple and straightforward syntheses.

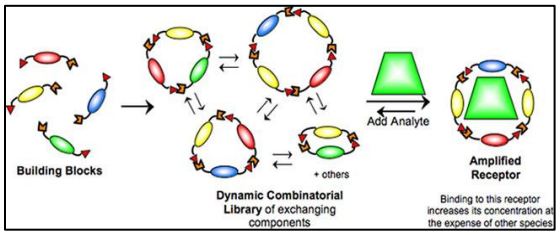

Figure 37. Cartoon representation of dynamic combinatorial chemistry (DCC).

1.2.Macrocyclic Receptor for Trimethyllysine

Over the past several years, the Waters' group has used DCC to study synthetic receptors for methylated lysine. Using disulfide exchange as their reversible reaction, and a short histone sequence as the guest, they developed a macrocyclic receptor, **A_2B** (composed of monomers **A** &

B), that selectively binds K(Me_3) over the lower methylation states of lysine (Figure 38 and Table 5). This receptor was found to have an affinity comparable to that of the HP1 chromodomain, which is quite impressive, considering the size disparity between the two, and the added dependence of the chromodomain on the surrounding sequence.[3] Several other such receptors (with selectivity towards KMe_3) were reported by the Waters' lab, such as $\mathbf{A_2N}$[152] and $\mathbf{A_2D}$,[153] as well as by others, such as Sulfonatocalix[4]arene (**CX4**).[150] While the use of these receptors was briefly attempted, the majority of the work outlined below was done using $\mathbf{A_2B}$, as it is the most straightforward to synthetically modify, and thus was used as a proof of concept.

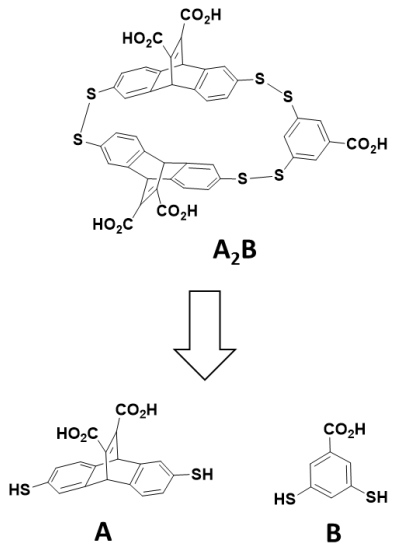

*Figure 38. Structure of **A_2B** and monomers **A** & **B**.*

*Table 5. Dissociation constants for the binding of **A_2B** to Ac-WGGG-QTARK$_n$STG-NH$_2$ (H3K9Me$_n$; n=0-3) as reported in the literature.[152] The peptide sequence represents residues 5-12 of Histone 3, 3 glycines as spacers, and a tryptophan for concentration determination. All peptides were acetal capped and amidated at the C-terminus.*

Peptide	K_d (µM)	Selectivity (relative to H3K9)
H3K9Me_3	2.6±0.1	8
H3K9Me_2	6.3±0.3	3.5
H3K9Me_1	13.9±0.1	1.6
H3K9	22±1	--

2. Modification of Receptors for Attachment to Resin

To begin this work, receptors had to be modified to create a point of attachment to a solid support. Looking at $\mathbf{A_2B}$, the easiest point to incorporate a linker was on the carboxylate of monomer **B**. The carboxylates were not thought to play a major role in the binding of KMe_3, and the functionalization of one out of the five was not expected to dramatically affect the solubility.

Monomer **B** was expected to be easy to functionalize and incorporate into DCC libraries to form the modified receptor **A_2B**. Monomers **A** and **B**, and the receptor **A_2B** were all synthesized as previously reported in the literature.[3,160] Several types of functionalization were explored as possible means for immobilization, as described below.

2.1.FLAGtag

The first linker appended onto monomer **B** was a FLAGtag peptide, with the intention of immobilizing the receptor on an anti-FLAG resin. The FLAGtag peptide was made on a microwave synthesizer, with 7 glycines added to the N-terminus to act as spacers. Monomer **B** was trityl protected to make **Trt-B** (Scheme 4), and an excess of the crude product was used to cap the peptide by hand using standard SPPS. After cleavage from resin and purification, the modified monomer, termed **B-FLAG** was put in a biased DCC library to form **A_2B-FLAG** (Scheme 5). The library was analyzed by LC/MS, and after two days, rac- and meso-**A_2B-FLAG** can be seen as the major product (Figure 39).

Scheme 4. Synthesis of Trt-B.

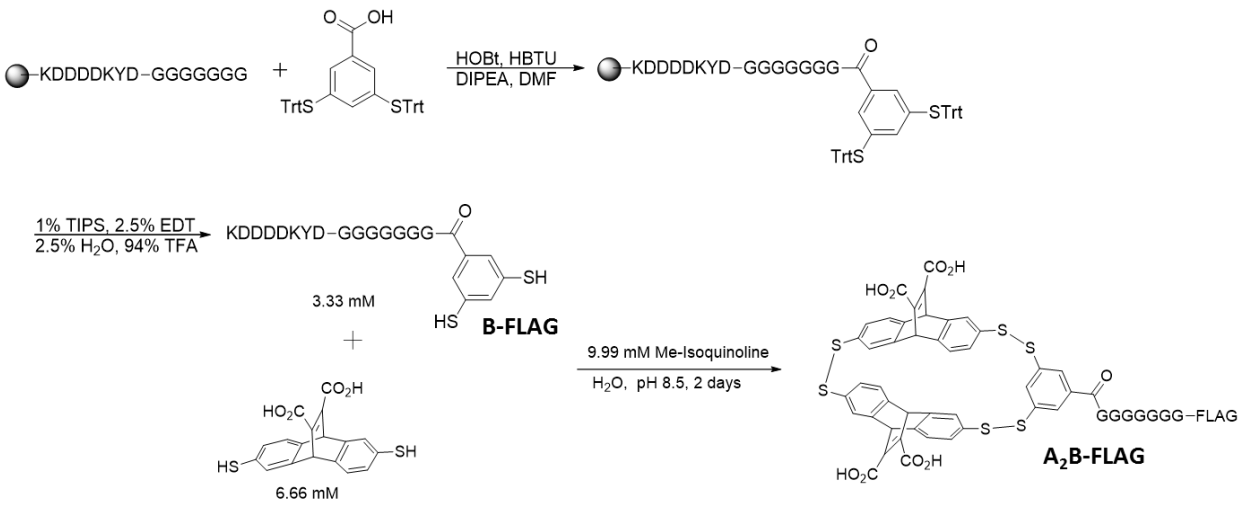

*Scheme 5. Synthesis of **A_2B-FLAG**.*

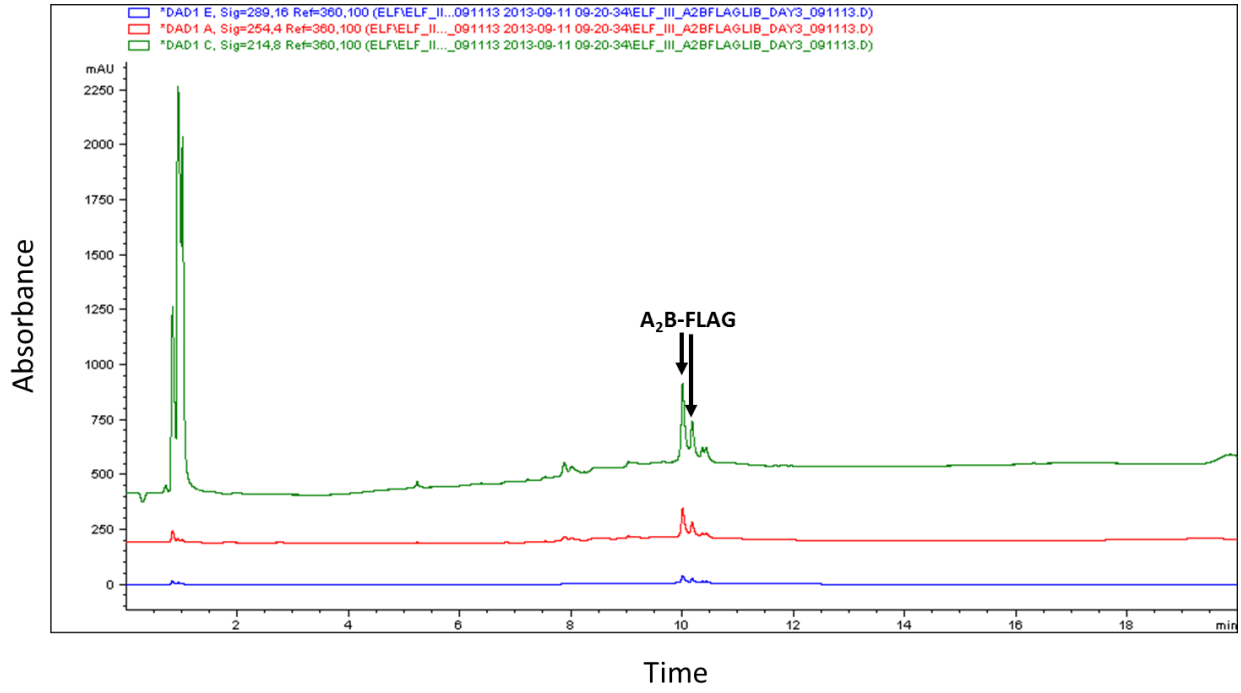

*Figure 39. LC/MS trace of a biased **A_2B-FLAG** DCC library at 2 days. Run in a gradient from 5 to 80% B; solvent A=0.2% FA/H_2O; Solvent B=0.2% FA/ACN.*

Upon purification, ITC was used to test the binding of **A_2B-FLAG** to H3K9Me_n peptide guests (the same peptides used with **A_2B**). The loss of the carboxylate on monomer **B** weakened the binding of the receptor to all peptides, but the selectivity remained comparable (Table 6), altogether confirming the minor role of the carboxylate in binding. For these purposes, one can

argue the weakened binding is an advantage, as H3K9Me and H3K9 now don't bind at all, potentially improving separation.

*Table 6. Dissociation constants for the binding of **A_2B-FLAG** to Ac-WGGG-QTARK$_n$STG-NH$_2$ (H3K9Me$_n$; n=0-3) as measured by ITC.[a] The peptide sequence represents residues 5-12 of Histone 3, 3 glycines as spacers, and a tryptophan for concentration determination.*

Peptide	K_d (μM)	Selectivity (relative to H3K9)
H3K9Me$_3$	13.2±1.1	> 10 fold
H3K9Me$_2$	35.9±4.3	> 4-fold
H3K9Me	>150	--
H3K9	>150	--

[a] Conditions: 26 °C in 10 mM borate buffer, pH 8.5. Error is the standard deviation from 3 runs.

Once the binding ability of **A_2B-FLAG** was confirmed, experiments were undertaken to immobilize it on an anti-FLAG resin. This was done by first combining the **A_2B-FLAG** with the resin, then adding a reducing agent to release monomer **A**. Measurement of the released monomer indicated the amount of receptor that has been immobilized. The anti-FLAG resin (100 uL slurry) (obtained from the Chen lab; purchased from Sigma-Aldrich) was incubated with **A_2B-FLAG** (300 uL of 230 uM solution in in 1X PBS buffer (pH 7.4)) for 5 hours at 2-8°C (per instructions from the resin manufacturers). The resin was then washed several times with 1X PBS buffer and agitated in excess 0.1M glycine•HCl buffer (pH 3.45) for elution of the receptor (per manufacturers' instructions). The rapid drop in pH is expected to disrupt the binding interactions, allowing for the release of the **A_2B-FLAG** from the resin. This was done twice, ensuring the most stringent elution conditions. It is worth noting that at this point, the resin had lost most of its color, suggesting the elution conditions were doing more than just eluting the receptor off the resin. The remaining resin was then washed with 1X PBS buffer and incubated with TCEP in 1X PBS buffer for 2.5 hours. The three supernatant solutions (the two rounds of acid elution, and the TCEP elution) were then concentrated and analyzed by analytical HPLC. As can be seen from the HPLC traces, no **A_2B-FLAG** nor monomer **A** could be seen (Figure 40),

suggesting **A_2B-FLAG** never successfully bound to the resin in which case it is unclear if the problem was with the receptor, or the resin itself. One possibility is that the glycine spacer incorporated into the receptor was not long enough, and disrupted the recognition of the FLAG-epitope by the anti-FLAG antibody. In addition, the problems with antibodies discussed above still apply in this case, and it cannot be entirely ruled out that this was simply a bad batch. Alternatively, it is possible the amounts recovered were too small to detect by the methods available to us. Tests run prior to these experiments determined the limit of detection of the analytical HPLC used was rather close to the expected concentration of receptor if fully eluted off the resin; so incomplete binding or elution would have been undetectable. Unfortunately, not enough resin was available at the time to work with increased concentrations. Several other immobilization options were pursued as described below, and this approach was not investigated further

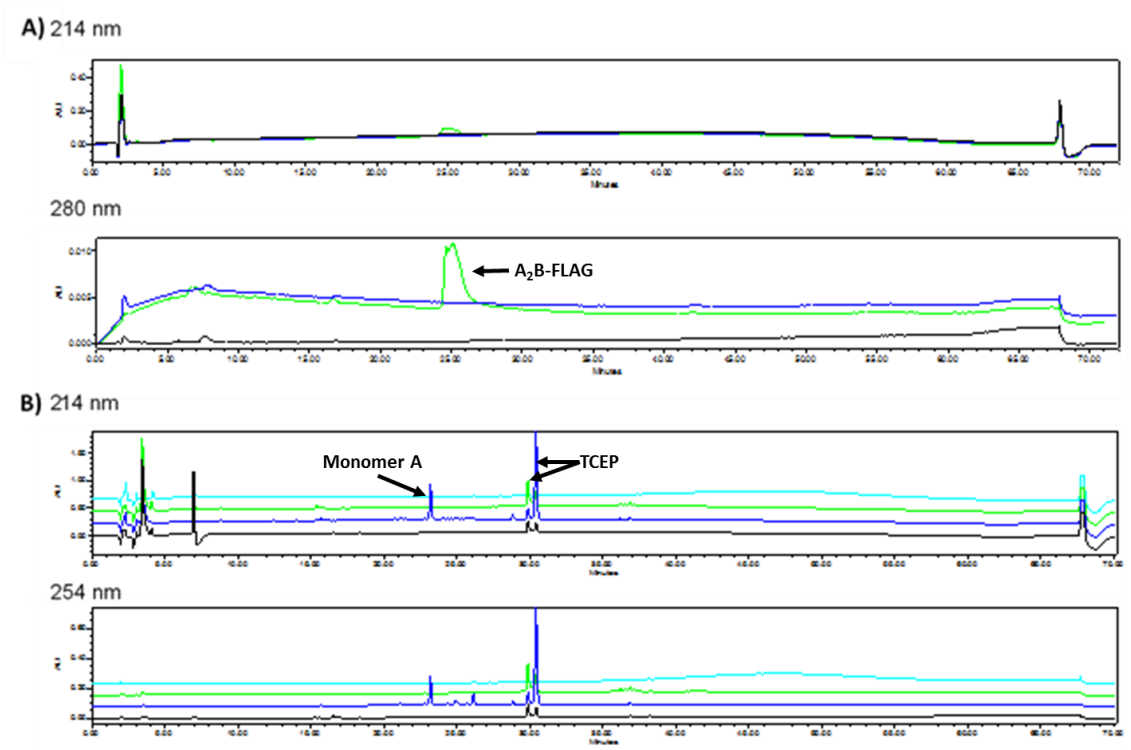

*Figure 40. HPLC traces of **(A)** Glycine•HCl buffer elutions (blue and black) and solution of **A_2B-FLAG** in glycine•HCl buffer (green); **(B)** PBS buffer blank (light blue), TCEP in PBS buffer (green), and TCEP+monomer **A** in PBS buffer (dark blue), TCEP elution (black). All traces were run at 0→100% B in 60 mins; A=0.1%TFA/H_2O, B=0.1%TFA/ACN.*

2.2.Amine Linker

To avoid the use of antibodies, the direct attachment of receptor to resin was investigated. An amine functionality was chosen, for conjugation onto NHS-activated agarose resin (purchased from Bio-Rad). Due to the sterics at the carboxylates of **A**, they have been found to be quite unreactive,[161] so cross-linking of receptors was not expected to be a problem. **Trt-B** was activated for coupling by forming the NHS ester (**Trt-B-NHS**). N-Boc-1,4-butanediamine was then coupled on, followed by a TFA global deprotection to yield the monomer termed **B-NH_2** (Scheme 6). Upon use of this monomer in a DCC library biased towards **A_2B-NH_2**, however, nothing but the free monomers was seen (Figure 41). The same issue has been observed by another group member when amino groups were incorporated into the monomers.[162]

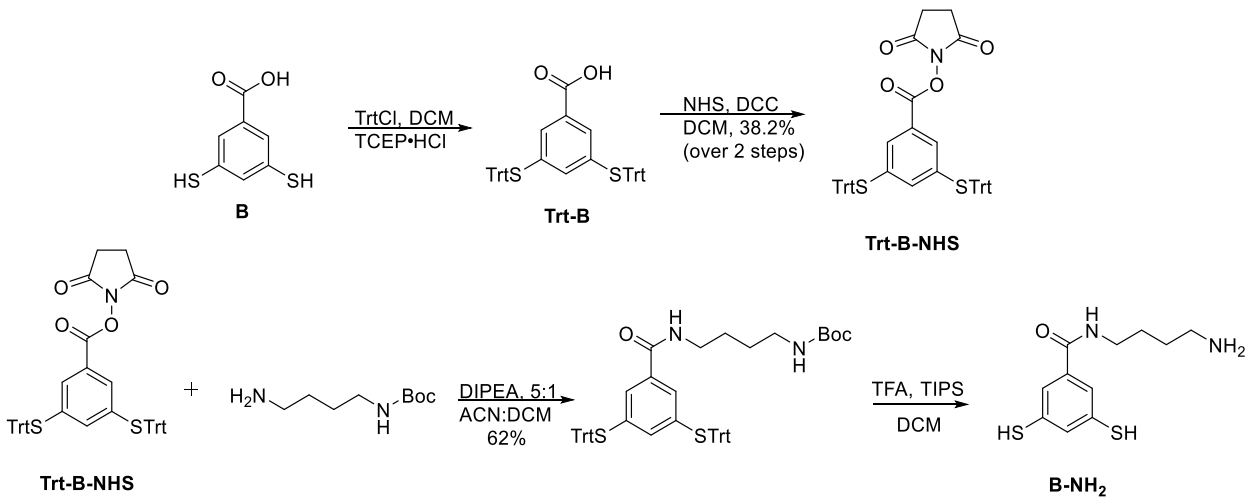

*Scheme 6. Synthesis of **B-NH$_2$**.*

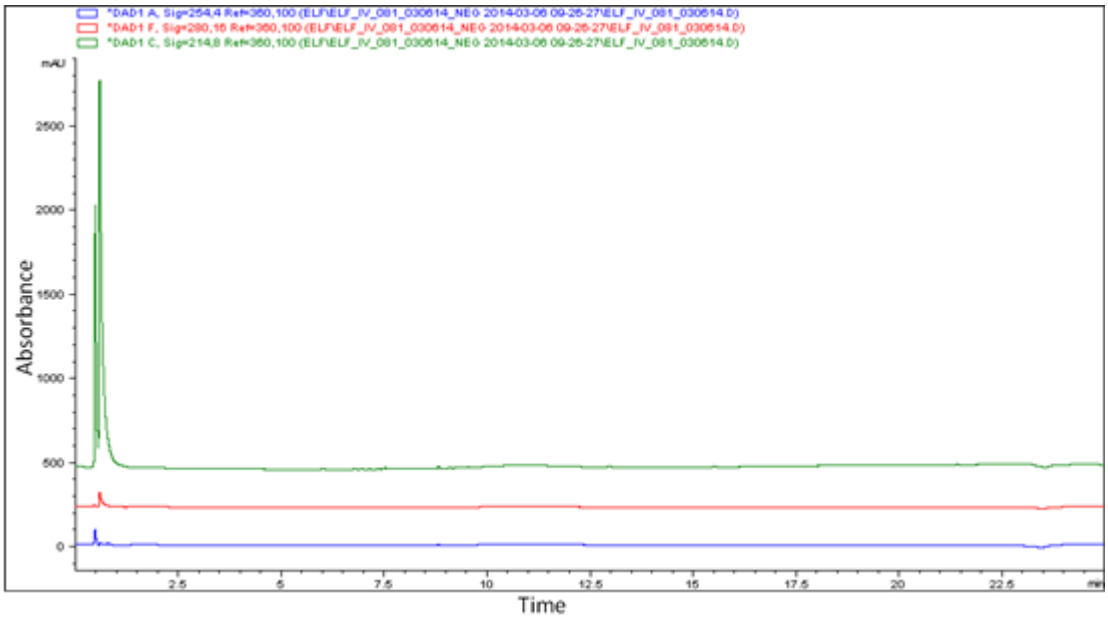

*Figure 41. LC/MS trace of a biased **A$_2$B-NH$_2$** library. Run in 10→90%B in 25 mins; A/B=NH$_4$OAc in H$_2$O/ACN.*

Since this problem was not previously seen with **A$_2$B** or **A$_2$B-FLAG**, it was assumed this was specifically due to the presence of the amine. To try to circumvent this issue, an Fmoc protected version of the monomer, **B-NH$_2$-Fmoc**, was synthesized (Scheme 7). The fully protected intermediate, was unable to be purified by standard column chromatography, as the slightly acidic silica removes the trityl groups, while treatment of the silica with base prior to usage causes the removal of the Fmoc group. As such, the final deprotection was carried out on

the crude product, and the final **B-NH$_2$-Fmoc** monomer was purified by HPLC in NH_4OAc buffer. Oddly enough, while the ^1H NMR of the purified product appeared clean, there were no peaks for the aromatic ring, leaving a spectra that looks much like that of the N-Fmoc-1,4-butanediamine alone. However, the mass of N-Fmoc-1,4-butanediamine did not appear by ESI-MS, and the late retention time of the product on the HPLC (24 mins) is highly un-characteristic of a free amine. TLC comparison was unhelpful, as both stuck to the baseline, but ESI-MS confirmed that the major mass seen is that of monomer **B-NH$_2$-Fmoc**.

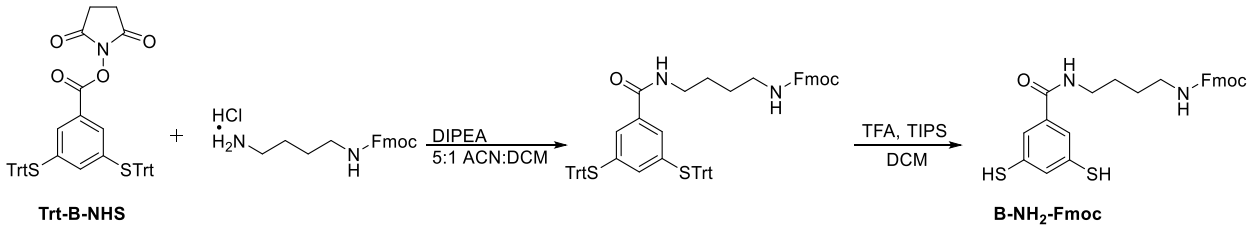

*Scheme 7. Synthesis of **B-NH$_2$-Fmoc**.*

B-NH$_2$-Fmoc was then put into a DCC library templated by Me-Isoquinoline. For this library, 5:3 THF:DMSO was used instead of water, due to the insolubility of any **B-NH$_2$-Fmoc** macrocycles that may form. The library was analyzed by LC/MS as before, and the same trace was seen on day 5, 7, and 13 (Figure 42). Many species appeared to be present, but the only identifiable mass was that of monomer **A**. Oddly enough, it eluted around 8 mins, while free **A** is known to elute within the first minute or two, so its identity remained in question, despite the mass seen. It appeared that despite the protection of the amine functionality, the synthesis of the receptor bearing the amine functionality was simply un-favorable, and further optimization was not attempted. Instead, direct attachment was envisioned via activation of un-modified receptor and conjugation onto an amino-sepharose resin (see section 4.1 below).

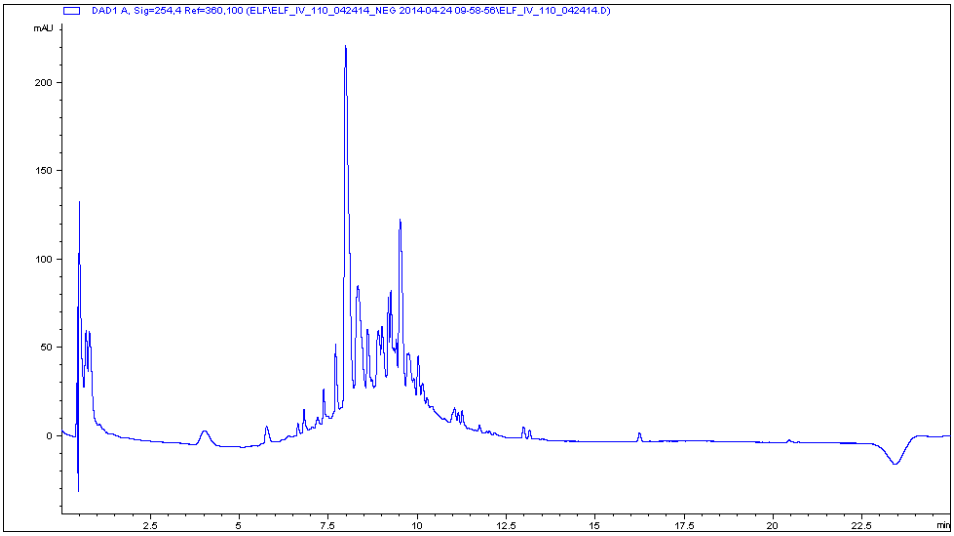

*Figure 42. LC/MS trace of biased **A_2B-NH_2-Fmoc** library (3.3 mM **B-NH_2-Fmoc**, 6.6 mM **A**, and 10.4 mM Me-Isoquinoline in 5.5 mL 5:3 THF:DMSO) after 7 days. Run in a gradient of 10-90%B in which A=0.2% FA/H_2O and B=0.2% FA/ACN.*

2.3.Biotinylated Receptors

Biotin is one of the most commonly used recognition motifs due to its picomolar affinity to avidin and streptavidin. Various resins are commercially available for the immobilization of biotinylated molecules, and this represented another feasible approach for our system. Instead of modifying monomer **B** as before, biotinylation was carried out directly on **A_2B**. The biotinylated derivative was synthesized using a short polyethylene glycol (PEG) diamine linker (Biotin-PEG_3-NH_2), as reported in the literature (Scheme 8).[161]

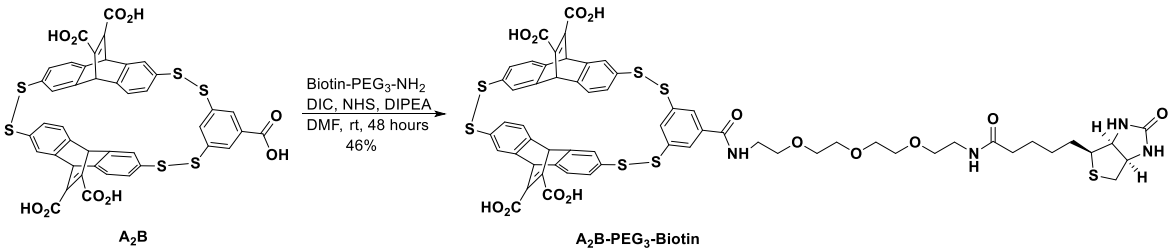

*Scheme 8. Synthesis of **A_2B-PEG_3-Biotin**.*

To immobilize the biotinylated receptor, **A_2B-PEG_3-Biotin** was incubated with NeutrAvidin agarose resin (purchased from Thermo Scientific) for one hour in 1X PBS buffer (pH 7.4) at 2-8°C (per instructions from the resin manufacturers). The resin was then washed several times

with 1X PBS buffer and agitated in 8 M guanidine•HCl buffer (pH 1.5) for elution of any unbound receptor. The remaining resin was then washed with 1X PBS buffer, followed by TCEP in 1X PBS buffer. The incubation solution, washes, and eluted solutions were all analyzed by HPLC (Figure 43). No **A** or **A_2B-PEG_3-Biotin** were seen in any of the solutions, including the incubation solution, which is known to have contained a large excess of **A_2B-PEG_3-Biotin**.

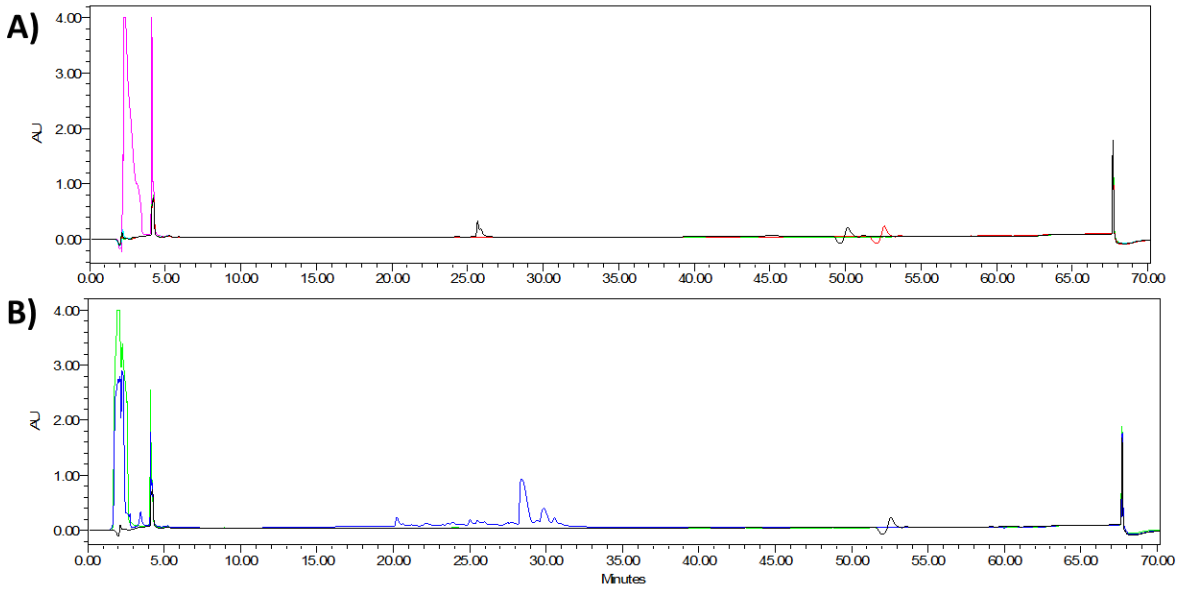

*Figure 43. HPLC traces of (A) 1X PBS buffer (red), **A_2B-PEG_3-Biotin**/PBS buffer (black), incubation solution (green), post-incubation washes (light blue), and acid elutions (pink); (B) 1X PBS buffer (black), monomer **A**+TCEP in PBS buffer (blue), TCEP elution (green).*

In light of these results, a sample of **A_2B-PEG_3-Biotin** was given to the Strahl lab to confirm its ability to bind to avidin. Dot-blot confirmed that the biotin tag can still be recognized (Figure 44), and this approach was deemed feasible.

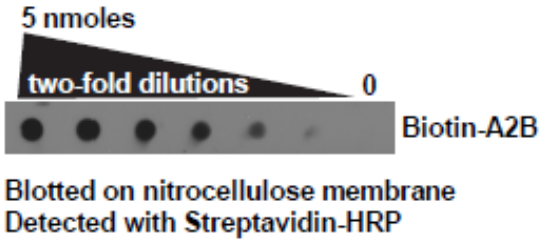

Figure 44. Dot-blot assay with A_2B-PEG_3-Biotin.

3. Additional Binding Studies

Before proceeding with the use of the receptors for affinity chromatography, further studies were done to determine the effect of the synthetic modifications and buffer conditions on the binding of the receptors to peptides. Since we envisioned beginning with the separation of only H3K9 and H3K9Me$_3$, the binding only to those two peptides were tested. Initial attempts to measure the binding of **A_2B-PEG$_3$-Biotin** were done using fluorescence polarization, as reported in the literature for **A_2B**, using FAM-QTARKMe$_n$STG-NH_2 .[3] As a control, the binding of the peptide to un-modified **A_2B** was tested as well, and surprisingly no binding was seen to the KMe$_3$, which in the literature was reported to bind this peptide with a K_d of 25±3 μM. ITC was then used, and **A_2B** was found to bind to the peptide with a K_d of 14.8±0.6 μM, which is higher than that previously seen when using ITC to measure binding to Ac-WGGG-QTARKMe$_3$STG-NH_2 (H3KMe$_3$).[152] When H3KMe$_3$ was tested, a comparable K_d was observed, suggesting the FAM-cap was weakening the binding, or possibly the lack of a spacer between it and the H3 5-12 sequence. Due to this discovery, all binding studies from this point forward were done using ITC. Using this method, **A_2B-PEG$_3$-Biotin** showed no substantial binding to H3K9Me$_3$ (K_d>150 μM). To test whether this was due to the proximity of the biotin to the binding site, **A_2B-PEG$_{11}$-Biotin** was synthesized. It did not, however, restore binding. It was hypothesized that perhaps the biotin is somehow occupying the binding pocket, since not all modifications seem to have this effect (see **A_2B-FLAG**). If that was indeed the case, that problem should be alleviated once the receptor is displaced by avidine (as in our intended system), since it is doubtful this **A_2B**:biotin interaction is stronger than that of biotin with avidine. Since applying this to affinity chromatography will undoubtly require screening buffers, it was decided it would be advantageous to first carry out a comprehensive salt study on the receptors prior to any modification.

3.1.Salt Study

A salt study was done on both **A_2B** and **A_2D**[153] (Figure 45), a receptor previously reported by our lab to bind asymmetric dimethyl arginine (aR(Me_2)) with high selectivity over un-modified arginine. The binding affinity of each receptor to a peptide that is either un-modified, or contains the modification relevant to that receptor, was measure by ITC in buffers containing differing amounts of NaCl (Table 7). For both receptors, increased concentrations of salt weakened the binding of both peptides, but had a greater effect on the binding of the un-modified peptide than that of the modified one, suggesting electrostatics played a much bigger role in the binding of the un-modified peptides. This can be advantageous to affinity chromatography; at certain salt concentrations, the un-modified peptide no longer binds to the receptor, while the modified one still does so with reasonable affinity that allows for release from the resin without the need for harsh conditions.

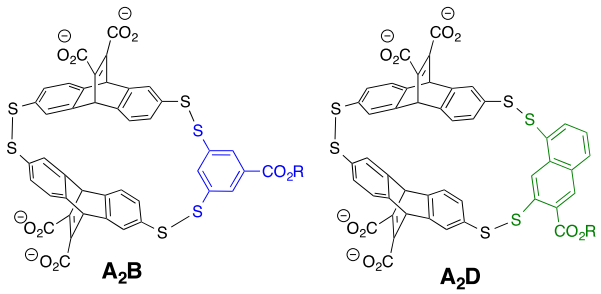

*Figure 45. **A_2B** and **A_2D**.*

*Table 7. Dissociation constants for the binding of **A_2B** and **A_2D** to Ac-WGGG-QTARKnSTG-NH_2 (n=0 or 3) or Ac-YGGG-QTAXKSTG-NH2 (X=R or aR(Me_2)) as measured by ITC.[a] The peptide sequences represent residues 5-12 of Histone 3, 3 glycines as spacers, and a tryptophan or tyrosine for concentration determination.*

Entry	Guest	Receptor	NaCl Concentration (mM)	K_{dissoc} (μM)[a]
1[b]	Ac-WGGG-QTARKSTG-NH_2	**A_2B**	0	22±1
2			30	≥85
3			90	≥180
4			120	≥280
5			150	≥280
6[b]	Ac-WGGG-QTARK(Me_3)STG-NH_2		0	2.6±0.1
7			30	12.6±0.9
8			60	12.8±0.02
9			90	23.9±0.7
10			120	26.4±0.7
11			150	≥45
12[c]	Ac-YGG-QTARKSTG-NH_2	**A_2D**	0	≥60
13			30	≥115
14			60	≥140
15			90	≥205
16			120	≥270
17			150	≥365
18[c]	Ac-YGG-QTA-aR(Me_2)-KSTG-NH_2		0	5.1±0.1
19			30	11.4±0.3
20			60	18.1±1.8
21			90	29.9±2.9
22			120	34.9±3.6
23			150	≥55

[a]Determined by ITC at 26°C in 10 mM borate buffer, pH 8.5, with varying concentrations of NaCl. Errors are the standard deviation of two runs. [b]Data reported by Pinkin and Waters.[1] [c]Data reported by James et. al..[2]

4. Affinity chromatography

4.1. Direct Attachment

The first method attempted to immobilize receptors was via direct attachment. Since the synthesis of an amine functionalized **A_2B** was unsuccessful, we looked to attach un-functionalized **A_2B** to an amino-sepharose resin (purchased from GE Healthcare). **CX4**, another well studied receptor that is known to selectively bind KMe_3, was attached as well, via NHS activation (to form **CX4-NHS**), followed by addition of the resin to the crude reaction mixture.

A_2B was attached using standard amide coupling procedure (Scheme 9). The efficiency of the coupling was determined by Kaiser test.

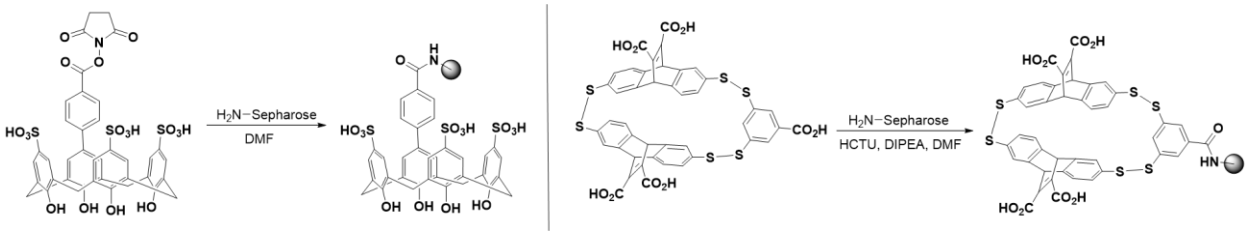

*Scheme 9. Attachment of **CX4** and **A_2B** to amino-sepharose resin.*

In both cases, the resin appeared to shrink upon attachment of the receptors. This is problematic for affinity chromatography, as the peptides run through such a column would not be able to properly interact with the receptors. None-the-less, columns were packed with **CX4**-Sepharose resin and **A_2B**-Sepharose resin and a 1:1 mixture of H3K9 and $H3K9Me_3$ (50 uL peptide solution, 5 uM of each/0.3 mL column) were run through them in 3 different solvents: 10 mM borate buffer (pH 8.5), 10 mM phosphate buffer (pH 7.4), and unbuffered mQ water. Three column volumes were collected from each column and given to the Chen lab for MS analysis. Each columns was washed with acetonitrile at the end and that sample was dried down and given for analysis as well. For both receptors, under all conditions tried, both peptides were barely, if at all, detectable. With the sensitivity of the instrument used being orders of magnitude lower than the concentrations used here, these peptides should be detectable even with the dilution incurred from running through the column. This suggested that the peptides were sticking to the resin, and this immobilization strategy was incompatible with the goals envisioned.

4.2.Attachment via Biotin

With confirmation that **A_2B-biotin** binds NeutrAvidin in a dot-blot, along with the fact that the NeutrAvidin resin remained swelled after incubation with **A_2B-biotin**, we moved forward with the use of the immobilized **A_2B-biotin** on NeutrAvidin agarose resin, as it seemed to have the most promise. In designing an effective technique, the two requirements were to maximize selectivity, and to develop conditions for separation that were in line with the standard procedures for MS analysis. We envisioned using a protocol described by Lin and Garcia, in which histone proteins are taken through a propionylation step prior to trypsin digestion, and again after, before enrichment and subsequent MS analysis (Scheme 10).[163] The first propionylation step caps any un-methylated lysines, thereby lessening the number of cleavage sites and preventing the formation of exceedingly small, hydrophilic fragments that would be difficult to detect. Based on previous studies of our receptors,[3] as well as the results of the salt studies above, we postulated that such capping of the un-modified lysines would enhance the selectivity of our receptors by reducing non-specific electrostatic interactions, and decreasing the binding affinity of the un-methylated (now propionylated) fragments to **A_2B**. The second propionylation step would cap the N-terminus of the newly formed fragments, thereby serving the same purposes. Our goal is to then take the propionylated and digested sample and run it

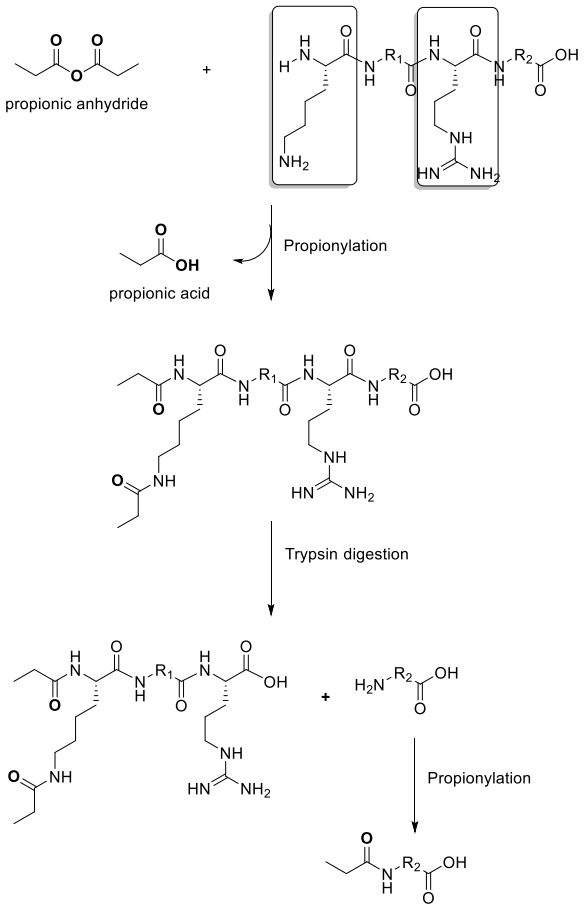

Scheme 10. Envisioned work-flow for derivatization and digestion of proteins prior to MS analysis.[163] R_1 and R_2 represent any amino acids other than lysine and arginine.

through the receptor-bound columns to achieve enrichment of fragments containing methylated lysines. For initial experiments, model peptides were chosen that would represent a typical fragment formed by this propionylation and digestion of Histone 3. Residues 3-8 of Histone 3 (H3 3-8) would be one of the fragments formed under such conditions, since trypsin would cleave at the carboxyl side of only arginines in this scenario. Two versions of this peptide were synthesized-one in which lysine 4 is propionylated (prop-H3K4prop) and one in which it is trimethylated (prop-H3K4Me$_3$). Both peptides contained 3 glycines as spacers and a tryptophan for concentration determination at the N-terminus, and the N-terminus of both was capped with a propionyl group (Figure 46). Measurement of the binding affinity of **A_2B** to these peptides showed the predicted results: prop-H3K4Me$_3$ bound to **A_2B** with a K_d of 8.8±0.05 µM, while prop-H3K4prop showed no binding (Table 8).

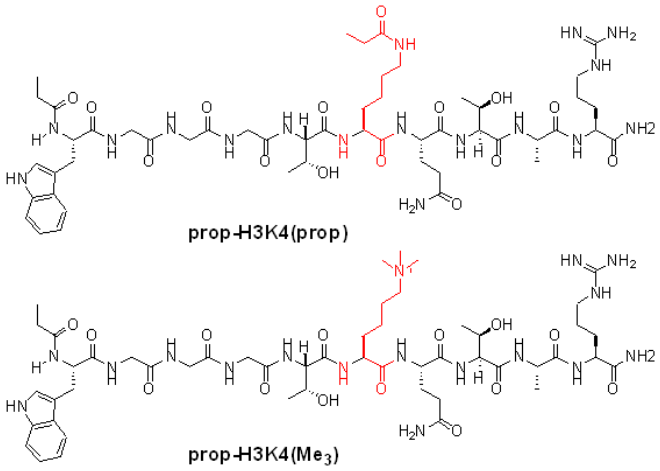

Figure 46. Model peptides prop-H3K4prop and H3K4Me$_3$. K4 is highlighted in red.

*Table 8. Dissociation constants for the binding of prop-H3 3-8 peptides to **A_2B** as measured by ITC.[a]*

Peptide	**K_d (μM)**
Prop-H3K4prop	>200
Prop-H3K4Me_3	8.8±0.05

[a]Conditions: 26 °C in 10 mM borate buffer, pH 8.5. Error is the standard deviation from 2 runs.

4.3. Initial Results

Since synthesis of the acetylated versions of the propionylated model peptides (where all propionyl groups were replaced with acetyl groups; from here on referred to as H3K4Me_n) were higher yielding, and the acetyl capping was expected to have the same effect as the propionylation, all following experiments were performed with the acetylated peptides. An initial set of three buffers were chosen to test on the **A_2B**-NeutrAvidin columns: 1 mM and 10 mM phosphate buffers (pH 7.4), since phosphate buffers at neutral pH are quite common for handling biological samples, and 10 mM borate buffer (pH 8.5), since this buffer was used in all previous binding studies of receptors, and would thus best reflect the expected behavior. For quantification by MS, standard solutions of varying ratios of H3K4Ac and H3K4Me_3 were made and analyzed by LC-MS/MS (all LC-MS/MS was done by Ling Xie, Chen lab) to construct a calibration curve; one for each of the initial buffers to be used (Figure 47).

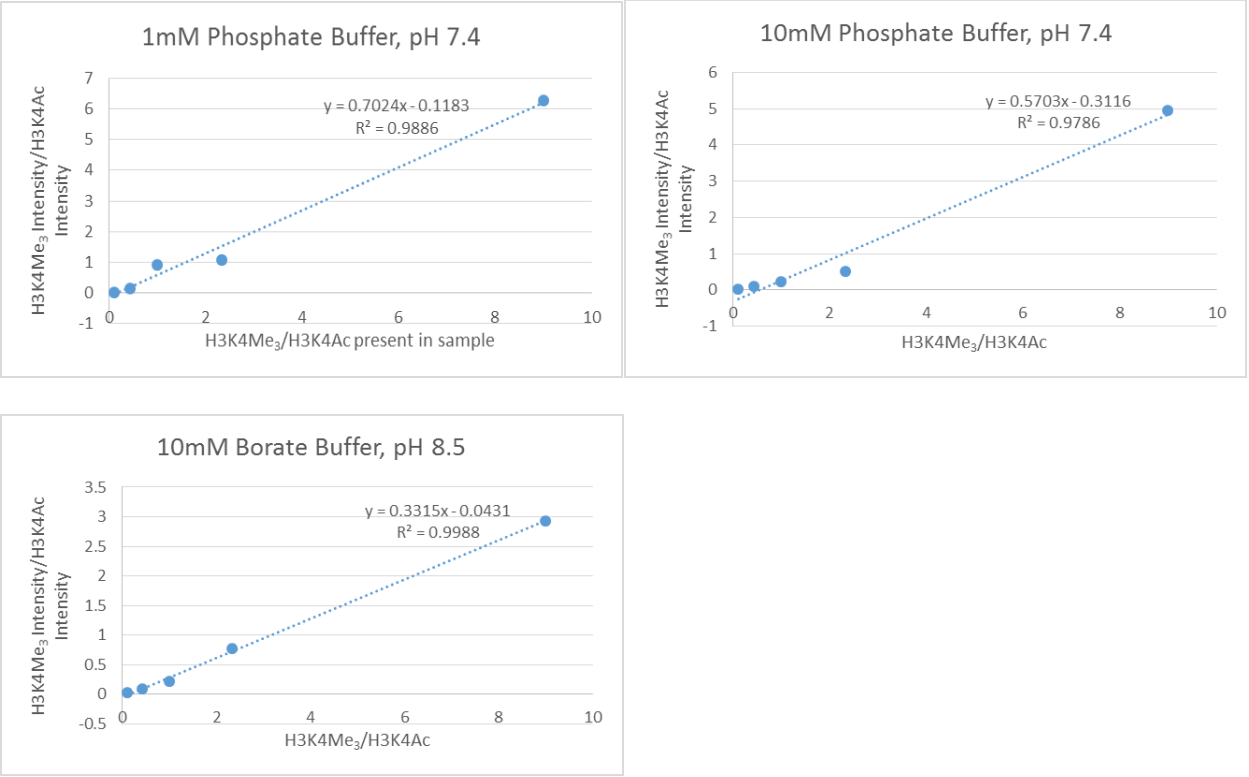

Figure 47. Calibration curves for 1 mM phosphate buffer (pH 7.4), 10 mM phosphate buffer (pH 7.4), and 10 mM borate buffer (pH 8.5).

Three columns packed with **A_2B**-NeutrAvidin resin were loaded with a 1:1 mixture of $H3K4Me_3$ and H3K4Ac in the elution buffer and run in parallel. Five fractions (1 column volume each) were collected from each, and analyzed by LC-MS/MS. In both phosphate buffers, the peptides peaked in different fractions, with $H3K4Me_3$ being the later eluting of the two, suggesting some separation was taking place as expected. While H3K4Ac eluted entirely in the first 2 fractions, $H3K4Me_3$ peaked in fraction 2, with ratios of 2:1 and 6:1 ($H3K4Me_3$:H3K4Ac) in 1 mM and 10 mM phosphate buffer, respectively. In the borate buffer, however, H3K4Ac was seen peaking at the second fraction (much like $H3K4Me_3$ did in the phosphate buffers), while $H3K4Me_3$ did not appear to elute off the column at all within the 5 fractions collected, suggesting it remained bound on the immobilized receptor (Figure 48).

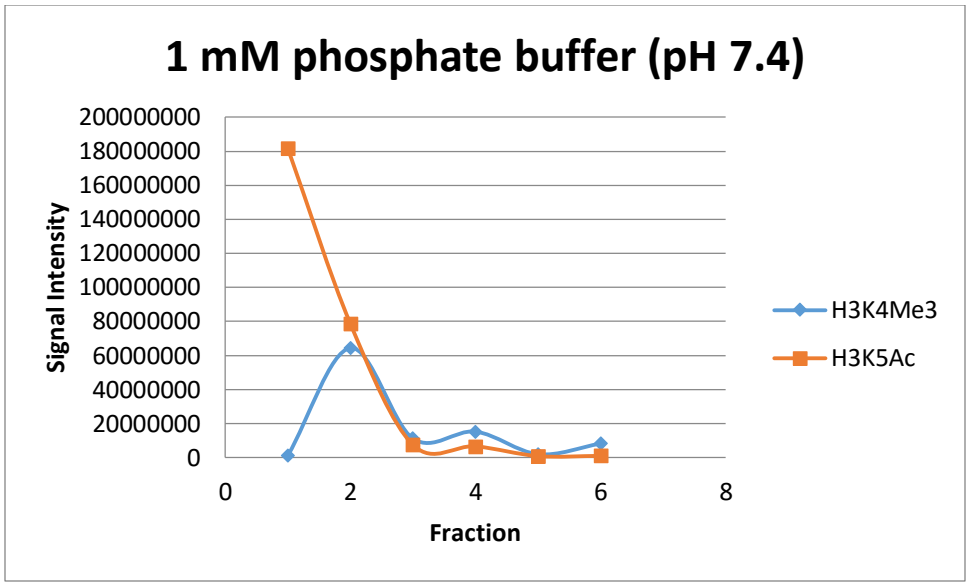
1 mM phosphate buffer (pH 7.4)
Signal Intensity
200000000
180000000
160000000
140000000
120000000
100000000
80000000
60000000
40000000
20000000
0
0
2
4
6
8
Fraction
H3K4Me3
H3K5Ac

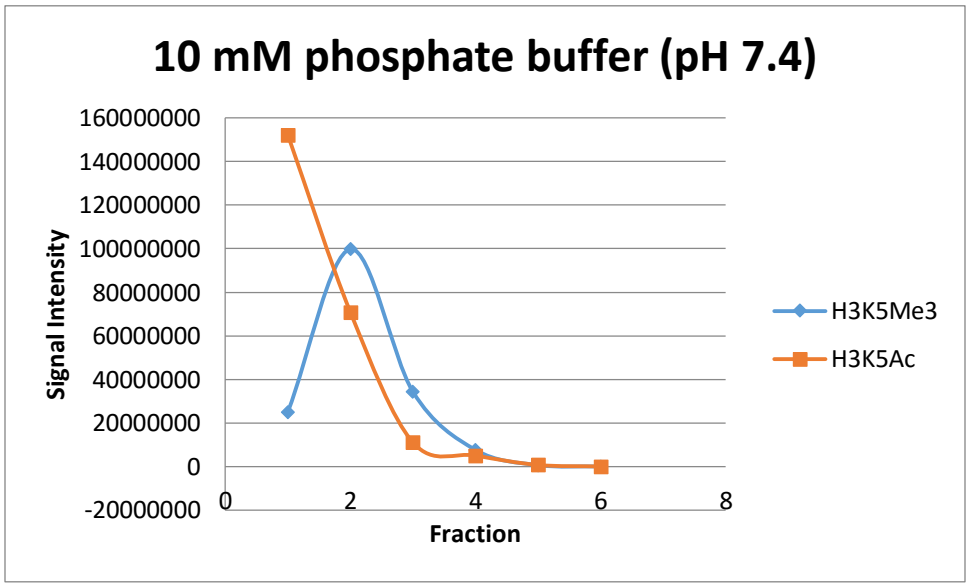
10 mM phosphate buffer (pH 7.4)
Signal Intensity
160000000
140000000
120000000
100000000
80000000
60000000
40000000
20000000
0
-20000000
0
2
4
6
8
Fraction
H3K5Me3
H3K5Ac

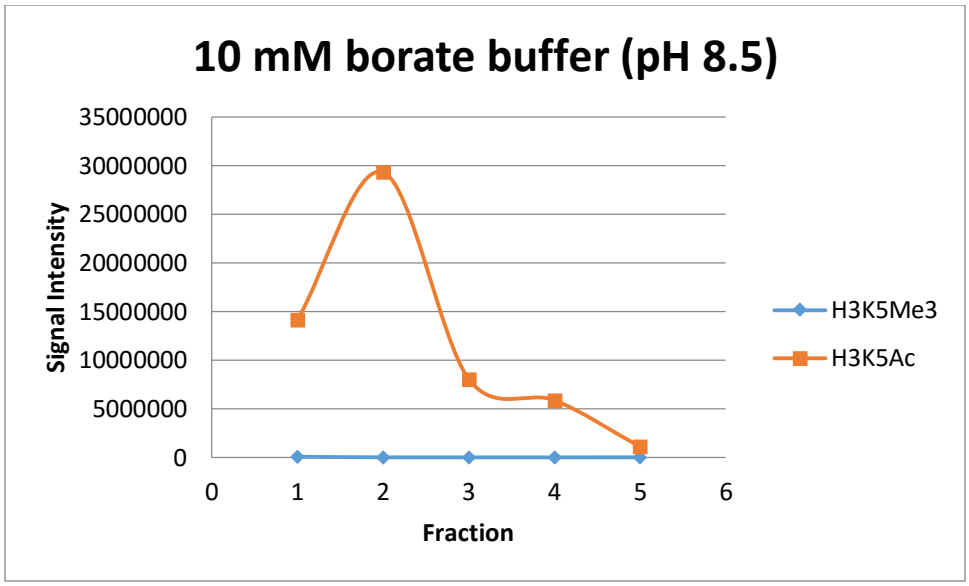

Figure 48. Elution patterns of H3K4Me$_3$ and H3K4Ac in different buffers analyzed by LC-MS/MS.

Based on the results of the salt study conducted on **A_2B**, following the elution of H3K4Ac with a high salt buffer should weaken the binding of H3K4Me$_3$ to **A_2B** and release it from the resin. When 10 mM borate+120 mM NaCl buffer (pH 8.5) was added after the initial elution, H3K4Me$_3$ then eluted from the column and peaked at fraction 6, the first fraction collected after switching to the high salt buffer. It continued to elute from the column thereafter, reaching up to 50:1 H3K4Me$_3$:H3K4Ac. No such enrichment was seen when a column devoid of **A_2B** was used (Figure 49).

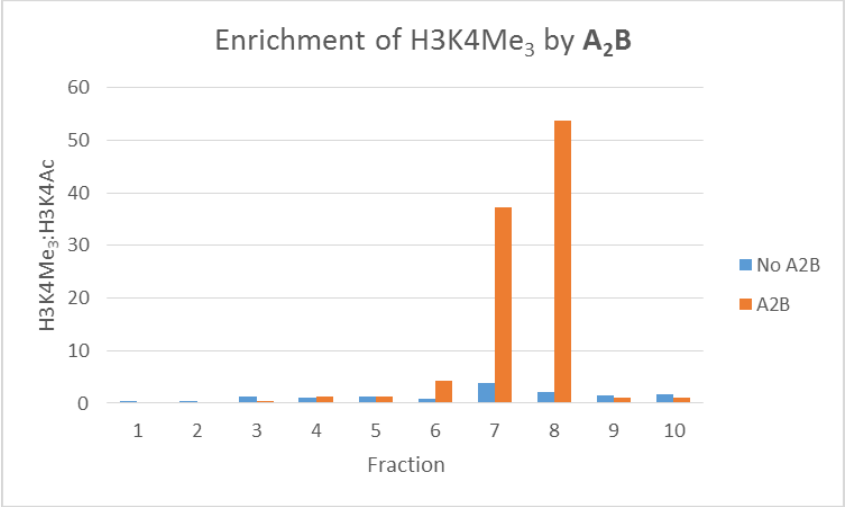

*Figure 49. Enrichment of H3K4Me$_3$ with and without **A$_2$B**.*

5. Conclusions and Ongoing Work

The separation of a trimethyllysine containing peptide from its acetylated counterpart using a synthetic receptor was demonstrated. In light of these promising results, work is currently being done to apply this technique to more complex peptide mixtures; ones that more closely mimic digested proteins. A mixture of model peptides based on residues 27-45 of Histone 3 (from the Strahl lab) (Figure 50. H3 27-45 peptides. Lysine 36 is highlighted in red.) were taken through the propionylation-digestion-propionylation procedure described by Lin and Garcia,[163] followed by desalting, and column separation. If enrichment of the fragment containing trimethyllysine is seen here, this can potentially be taken on to digested proteins. This separation approach represents an advantage over currently used antibody-based approaches, as it requires much milder conditions for release, is reproducible, and far cheaper. The ability to detect PTMs is highly dependent on their separation from more abundant, un-modified residues, and a simple procedure such as the one developed here can greatly facilitate the mapping of PTMs in the human proteome, further narrowing the current gap in knowledge.

H3K35: KSAPSTGGVKKPHRYKPGT-GG-K(Biotin)-NH_2

H3K35Me_3: KSAPSTGGVK(Me_3)KPHRYKPGT-G-K(Biotin)-NH_2

Figure 50. H3 27-45 peptides. Lysine 36 is highlighted in red.

6. Experimental

Peptide Synthesis and Purification

Peptides were synthesized using manual or automated standard solid phase peptide synthesis (Thuramed Peptide Synthesizer, or CEM Liberty 1 Microwave Peptide Synthesizer) using Fmoc protected amino acids on 0.057 mmol of RINK Amide resin or CLEAR-Amide resin. Four equivalents of standard amino acids, or 2 eq. of specially modified amino acids (Fmoc-KAc-CO_2H, Fmoc-K(Alloc)-CO_2H), were used for each peptide coupling. The amino acid residues were activated for coupling with HBTU and HOBt in the presence of DIPEA in DMF. The N-terminus was acetyl capped, propionyl capped, or capped with (5,6)-FAM. Peptides were acetylated at the N-terminus by treating the resin with 5% acetic anhydride and 6% 2,6-lutidine in 5 mL of DMF bubbling with N_2 for 40 minutes. Propionic acid was coupled to the N-terminus as a specially modified amino acid (see above). (5,6)-FAM was coupled to the N-terminus using 4 equivalents of (5,6)-FAM, 5 equivalents of PyBOP/HOBt and 8 equivalents of DIPEA in DMF and allowed to bubble with N_2 overnight.

Propionylation of lysine was done by coupling an Alloc protected lysine as a specially modified amino acid (see above). After capping of the N-terminus, an Alloc deprotection was carried out in 1:2 DCM:ACN in the presence of $Pd(OAc)_2$ (0.3 eq.), PPh_3 (1.5 eq.), NMM (10 eq.), and $PhSiH_3$ (10 eq.). Care was taken to ensure the $PhSiH_3$ was the last reagent added. The reaction

was agitated over-night. After draining the solution, the resin was washed with THF (1 x 5mL x 5mins.), DMF (2 x 5 mL x 2 mins.), sodium diethyldithiocarbamate trihydrate solution (25 mg/ 1 mL DMF) (4-5 x 5 mL x 10 mins.), DMF (2 x 5 mL x 2 mins.), and DCM (2 x 5 mL x 5 mins.). Finally, propionic acid was coupled to the ε-NH of lysine using standard coupling conditions.

Peptides were cleaved from the resin in 9.5:2.5:2.5 trifluoroacetic acid (TFA), TIPS and water respectively for 3-4 hours. The TFA was evaporated and the cleaved peptides were precipitated using cold ethyl ether and extracted with water. Extracted peptides were lyophilized and then purified using semi-preparative RP-HPLC on a Vydac C18 semipreparative column with a gradient from '0 to 100% B' in 45-120 minutes. Solvent A was 95% H_2O, 5% CH_3CN and 0.1% TFA and Solvent B was made of 95% CH_3CN, 5% H_2O and 0.1% TFA. Purified peptides were lyophilized and their purity confirmed by Analytical LC/MS on an Agilent Rapid Resolution LC-MSD system, equipped with an online degasser, binary pump, autosampler, heated column compartment, and diode array detector.

Synthesis of monomers **A**, **B**, and **D**

Synthesized as previously reported in literature.[3,152–154,160]

Synthesis of **Trt-B**

B **Trt-B**

To a mixture of monomer **B** (0.6103 g, 3.28 mmol), TrtCl (1.8270 g, 6.55 mmol), and TCEP·HCl (unmeasured-tip of a spatula) was added dry DCM to form a cloudy suspension. The

reaction was let stir under nitrogen for 30 minutes at room temperature, at which point it was a clear yellow solution. The solution was washed with water, dried over $MgSO_4$, and concentrated *in vacuo* to yield the product as a white solid. The crude product was carried on as is to proceeding reactions.

Synthesis of **Trt-B-NHS**

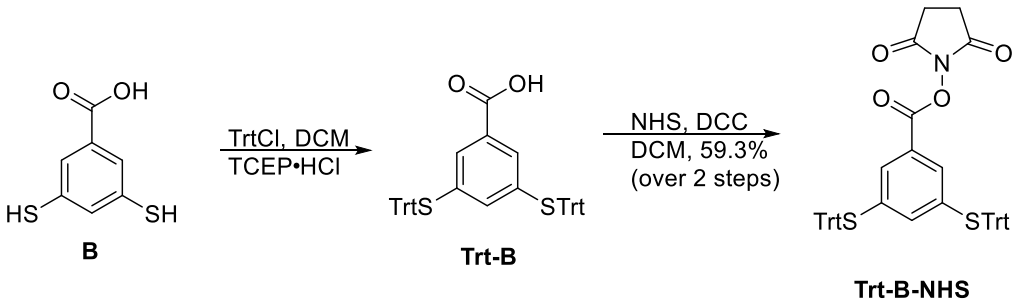

Trt-B was synthesized as described above.

Crude **Trt-B** (0.894 g), NHS (0.0193 g, 0.17 mmol), and DCC (0.0336 g, 0.16 mmol) were dissolved in dry DCM and let stir under nitrogen for 1 hour at room temperature. The resulting precipitate was filtered and concentrated *in vacuo* to yield white solids. The product was purified by column chromatography in DCM to yield the product as a white solid (0.0391 g, 59.3% yield over 2 steps). ^{1}H NMR ($(CD_3)CO$) δ 7.21-7.51 (m, 33H), 2.84 (d,4H).

Synthesis of **B-FLAG**

Peptides were synthesized by automated solid phase peptide synthesis on an CEM Liberty1 Microwave Peptide Synthesizer using Fmoc protected amino acids on a Clear-Amide resin. The amino acid residues were activated for coupling with HBTU and HOBt in the presence of DIPEA in DMF. 2 x 15 minute cycles were used for each amino acid coupling step. Deprotections were carried out in 20% piperazine in DMF for approximately 2 x 5 minutes. The

N-terminus was capped with Trt-protected **B**, which was coupled the same way described above but for 5 hours. Cleavage of the peptide from the resin was performed in 95:5:2.5:2.5 TFA: EDTA: TIPS: water for 3-4 hours. TFA was evaporated and cleavage products were precipitated with cold ether. The peptide were extracted with water and lyophilized. The peptide was purified by reversed phase HPLC, using a Vydac C-18 semi preparative column and a gradient of 0 to 100% B in 45 minutes, where solvent A was 10mM NH_4OAc in water and solvent B was 10mM NH_4OAc in acetonitrile. Once purified, the peptide was lyophilized to powder and peptide identity was confirmed by MALDI-MS [M-H^+]: expected 1579.54, observed 1580.

Synthesis of **B-NH_2**

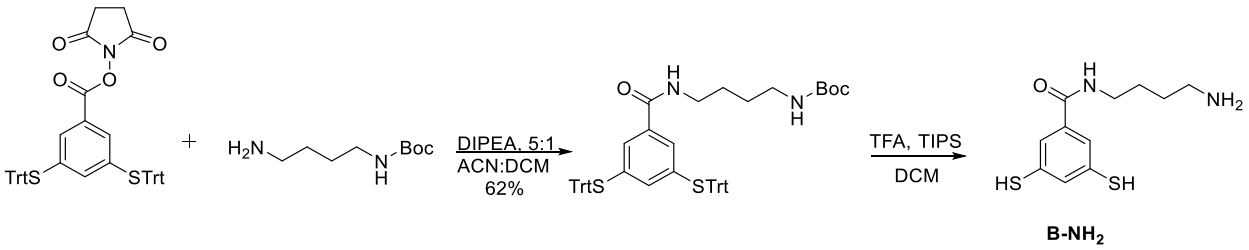

4-Boc-1,4-diaminobutane (0.02 mL, 0.10 mmol) was added to a solution of **Trt-B-NHS** (0.0596 g, 0.08 mmol) in 5:1 ACN:DCM. DIPEA (0.02 mL, 0.12 mmol) was added and the solution was let stir under nitrogen overnight. Ethyl acetate was added and the organic solution was transferred to a separatory funnel and washed with sat. aq. Na_2CO_3 (2x), H_2O (2x), and brine. The organic layer was dried over $MgSO_4$ and concentrated *in vacuo* to yield the product as white solids (0.0407 g, 62%). ^1H NMR ($(CD_3)CO$) δ 6.93-7.34 (m, 33H), 6.02 (bs, 1H), 3.26 (q, 2H), 3.12 (q, 2H), 1.53 (m, 4H), 1.49 (s, 9H).

The above product (0.0377 g, 0.045 mmol) was dissolved in DCM and purged with nitrogen. Excess TFA (1.4 mL, 18.3 mmol) was added dropwise, followed by the addition of excess TIPS

(0.27 mL, 1.318 mmol). The reaction was let stir at room temperature for one hour. The product was extracted with degassed NH_4OH (2% in water) and the solution was acidified with glacial acetic acid and lyophilized to give the product as a white solid. Product identity was confirmed by HR ESI-MS ([M+H$^+$]: expected 257.07, observed 257.09). Yield was not determined due to the presence of salts.

Synthesis of **B-NH_2-Fmoc**

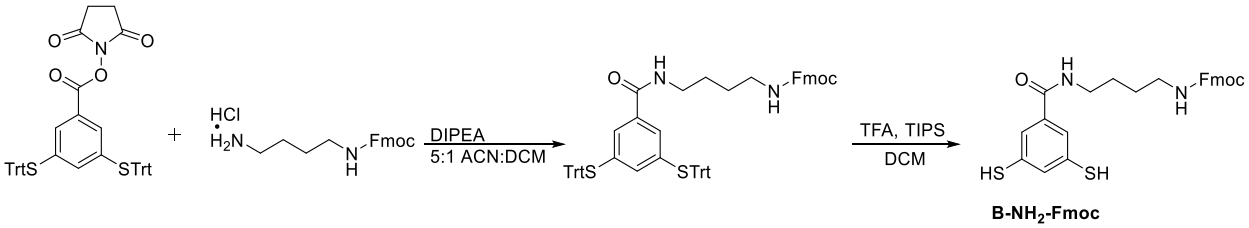

B-NH_2-Fmoc was synthesized in the same way as **B-NH_2** using 4-Fmoc-1,4-diaminobutane with the following exceptions: The crude fully protected intermediate was carried on without any purification. The final product was purified by reversed phase HPLC, using a Vydac C-18 semi preparative column and a gradient of 0 to 100% B in 45 minutes, where solvent A was 10mM NH_4OAc in water and solvent B was 10mM NH_4OAc in acetonitrile. Once purified, the product was lyophilized to powder and the identity of the compound was confirmed by HR ESI-MS. ([M-H$^+$] 477.19). Yield was not determined due to the presence of salts.

Synthesis and purification of **A_2B** and **A_2D**

Synthesized as previously reported in literature.[3,153,160]

A_2B and **A_2D** salt study (* all ITC experiments were run as described at the end of this section)

A_2B + H3K9

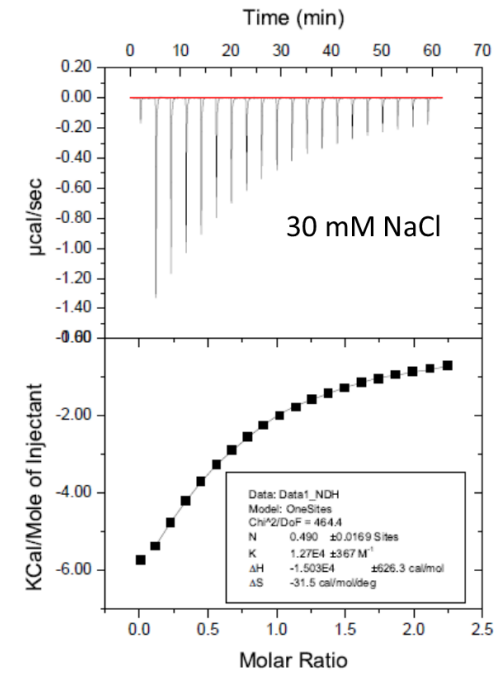

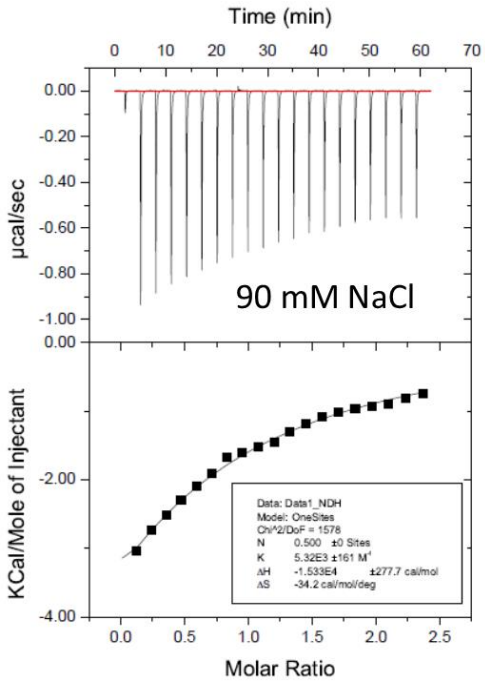

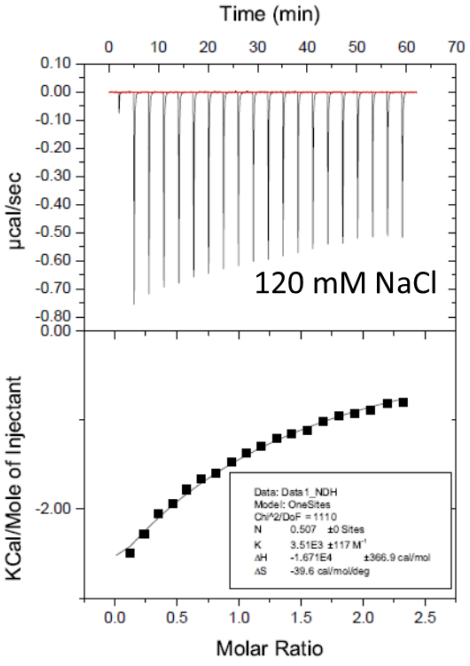

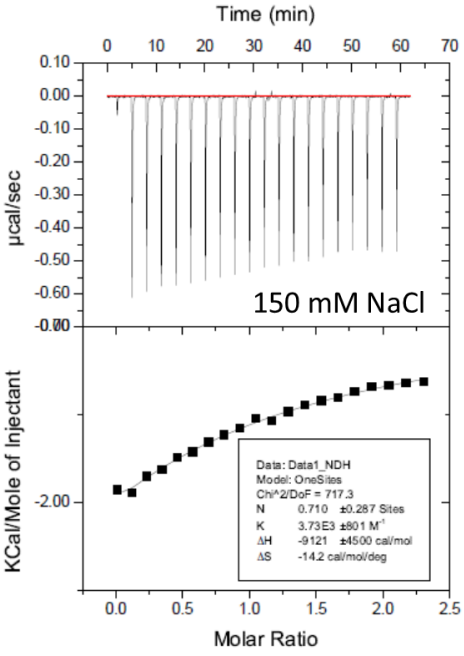

$\underline{A_2B}$ + $\underline{H3K9/Me_3}$

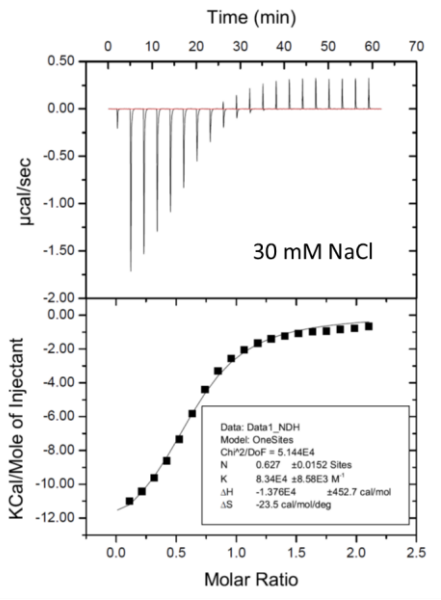
Time (min)
µcal/sec
30 mM NaCl
KCal/Mole of Injectant
Molar Ratio
Data: Data1_NDH
Model: OneSites
Chi^2/DoF = 5.144E4
N 0.627 ±0.0152 Sites
K 8.34E4 ±8.58E3 M-1
ΔH -1.376E4 ±452.7 cal/mol
ΔS -23.5 cal/mol/deg

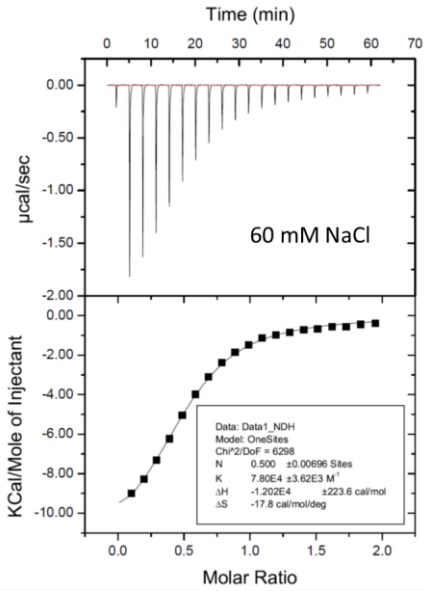
Time (min)
µcal/sec
60 mM NaCl
KCal/Mole of Injectant
Molar Ratio
Data: Data1_NDH
Model: OneSites
Chi^2/DoF = 6298
N 0.500 ±0.00696 Sites
K 7.80E4 ±3.62E3 M-1
ΔH -1.202E4 ±223.6 cal/mol
ΔS -17.8 cal/mol/deg

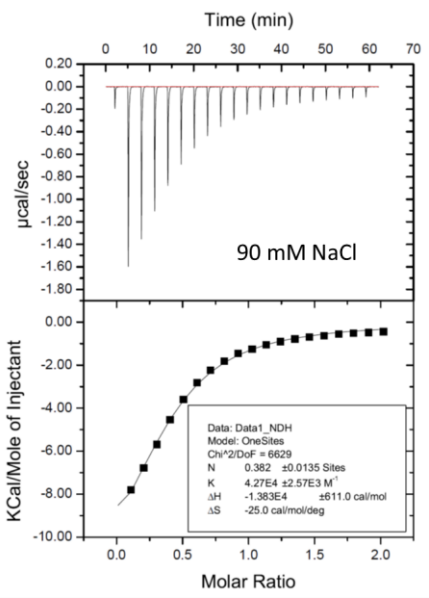
Time (min)
µcal/sec
90 mM NaCl
KCal/Mole of Injectant
Molar Ratio
Data: Data1_NDH
Model: OneSites
Chi^2/DoF = 6629
N 0.382 ±0.0135 Sites
K 4.27E4 ±2.57E3 M-1
ΔH -1.383E4 ±611.0 cal/mol
ΔS -25.0 cal/mol/deg

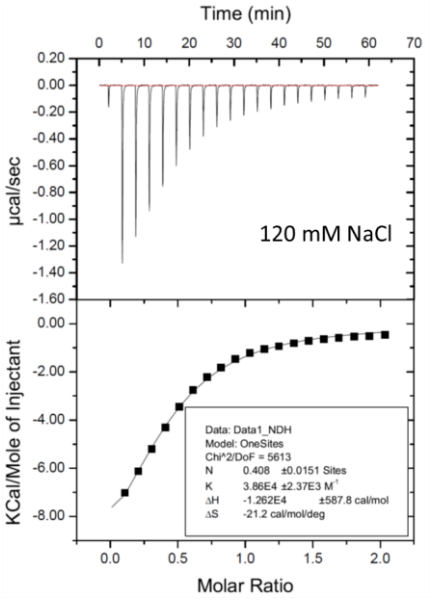
Time (min)
µcal/sec
120 mM NaCl
KCal/Mole of Injectant
Molar Ratio
Data: Data1_NDH
Model: OneSites
Chi^2/DoF = 5613
N 0.408 ±0.0151 Sites
K 3.86E4 ±2.37E3 M-1
ΔH -1.262E4 ±587.8 cal/mol
ΔS -21.2 cal/mol/deg

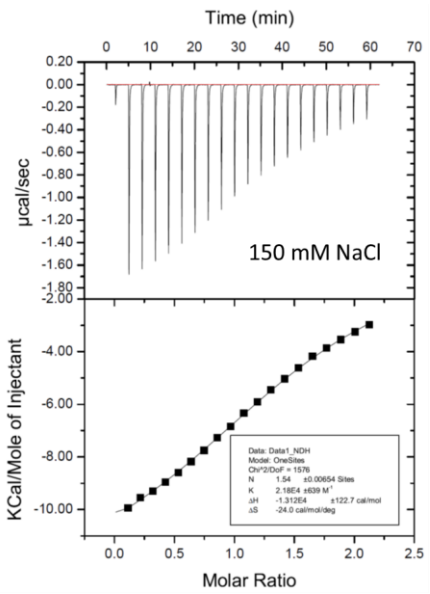

$\underline{A_2D}$ + $\underline{H3R8}$

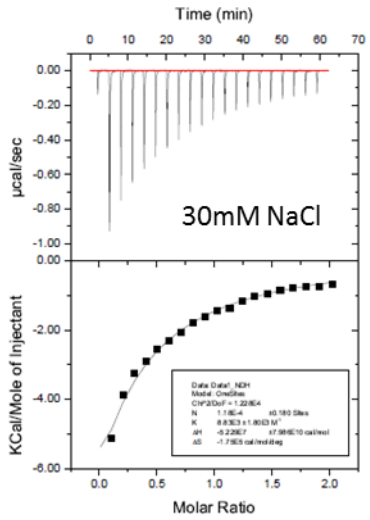

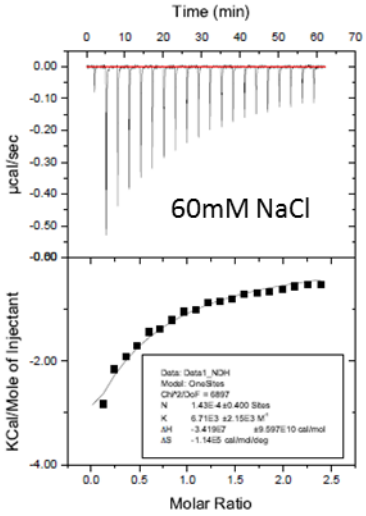

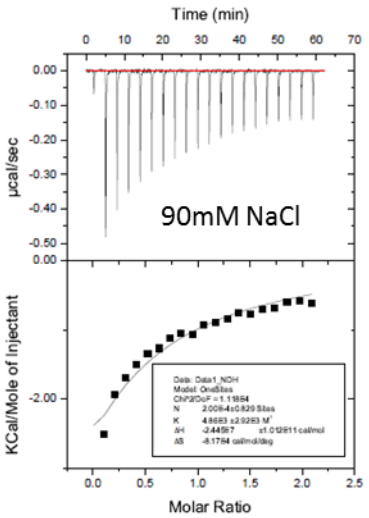

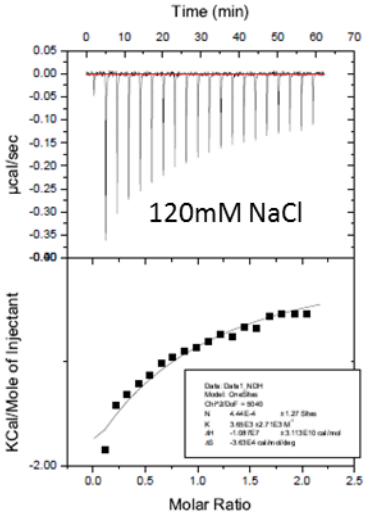

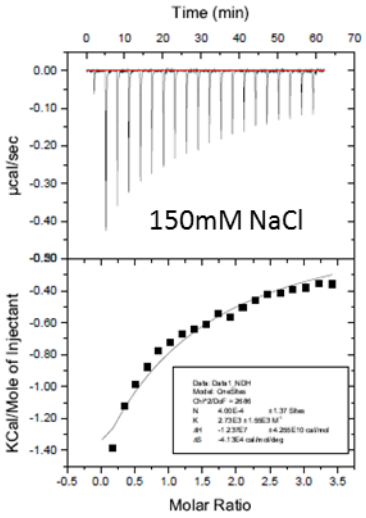

A_2D + H3aR8Me_2

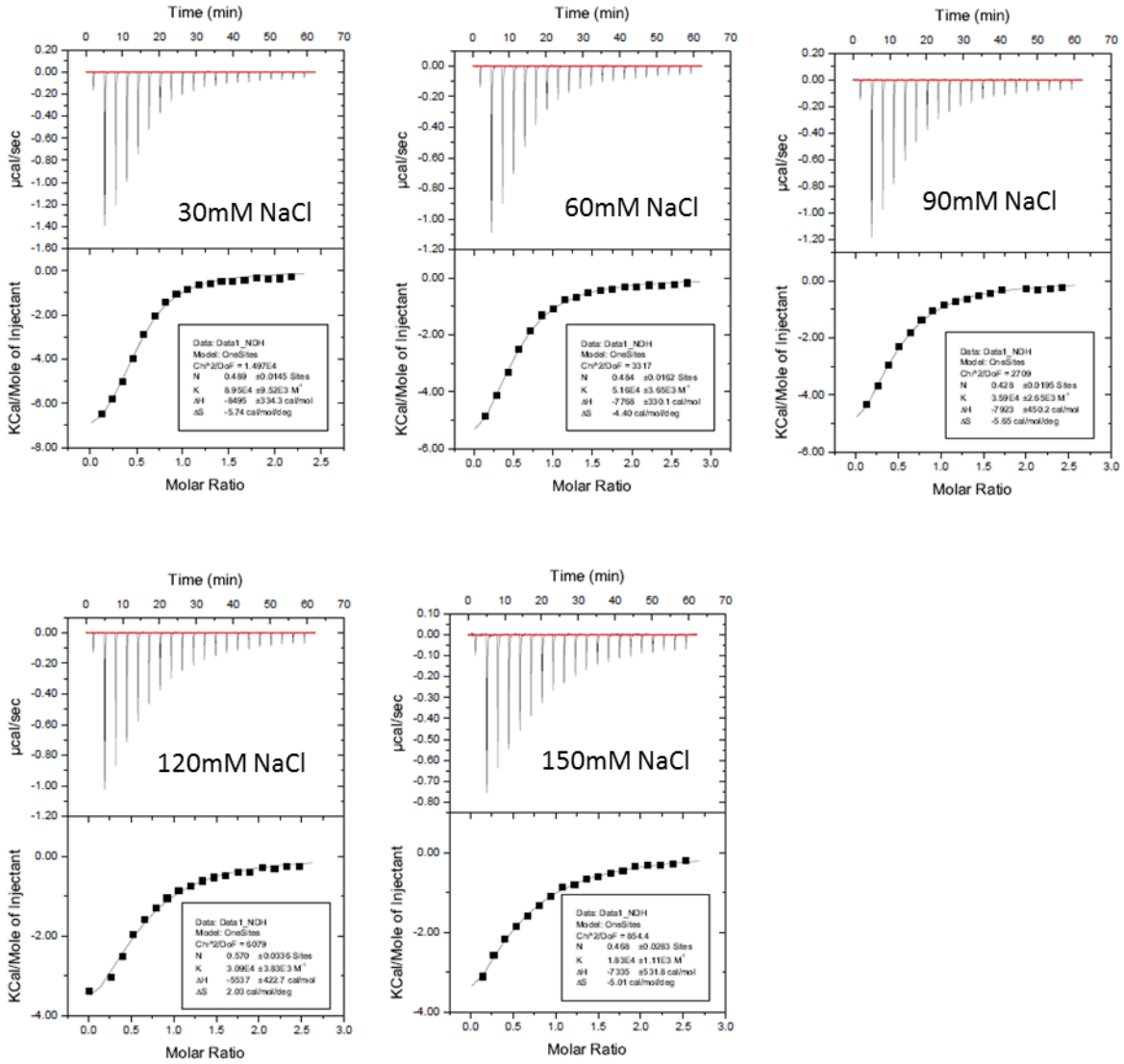

Synthesis and purification of **A_2B-FLAG**, **A_2B-PEG$_4$-N$_3$**, **A_2B-NH$_2$** and **A_2B-NH$_2$-Fmoc**

Synthesized as **A_2B** (see above), replacing monomer **B** with **B-FLAG**, **B-NH$_2$**, **B-NH$_2$-Fmoc**, or **B-PEG$_4$-N$_3$**. In the case of **A_2B-NH$_2$-Fmoc**, 5:3 THF:DMSO was used as the solvent instead of buffered water. **A_2B-FLAG** and **A_2B-PEG$_4$-N$_3$** were purified as described above for **A_2B**, and characterized by MALDI-MS.

A_2B-FLAG: [M-H$^+$] expected 2286.36, observed 2287.

A_2B-PEG_4-N_3: [M-H^+] expected 1136.12, observed 1135.

A_2B-FLAG binding studies

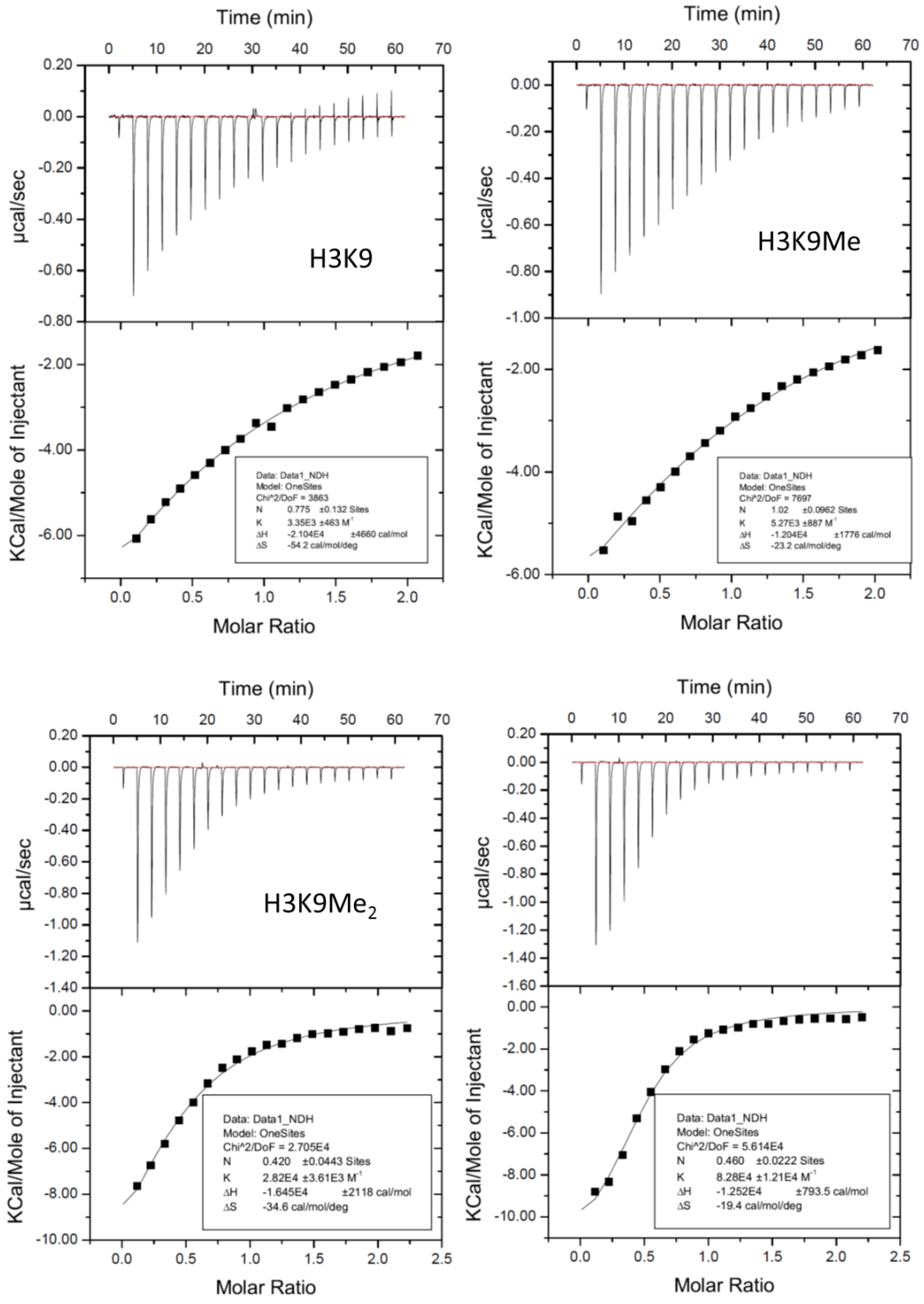

Synthesis of **A_2B-PEG_n-Biotin**

Synthesized as previously reported in literature,[161] with the exception that commercially available biotinylated PEG was used.

A_2B-PEG_n-Biotin binding studies to $H3K9Me_3$

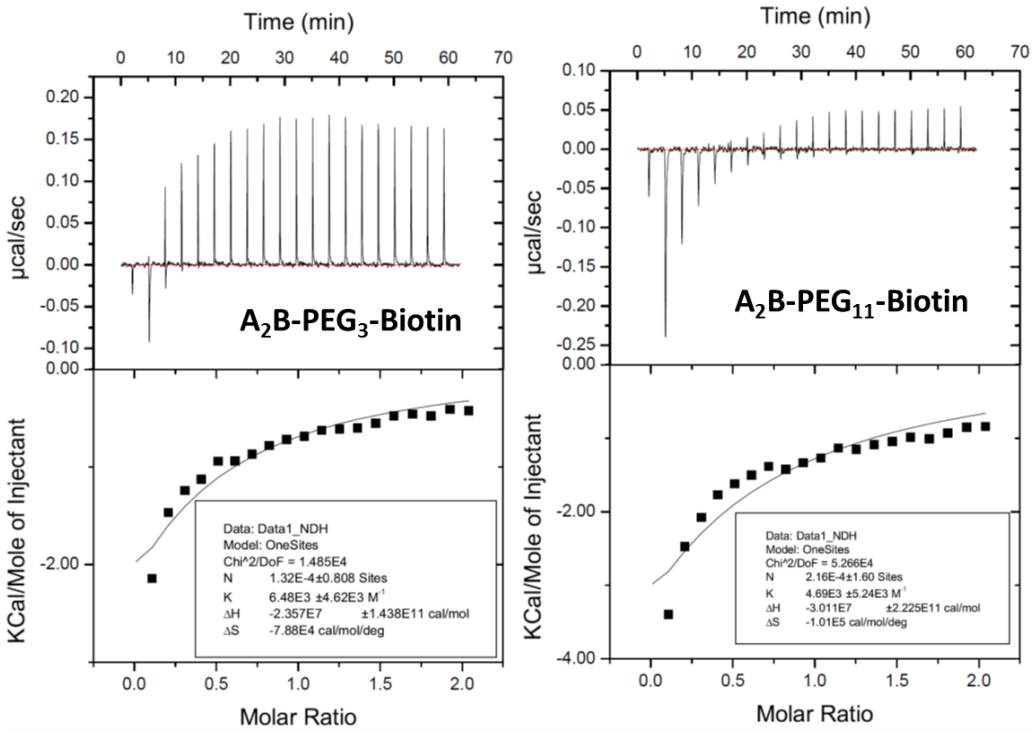

Synthesis of **CX4-NHS**

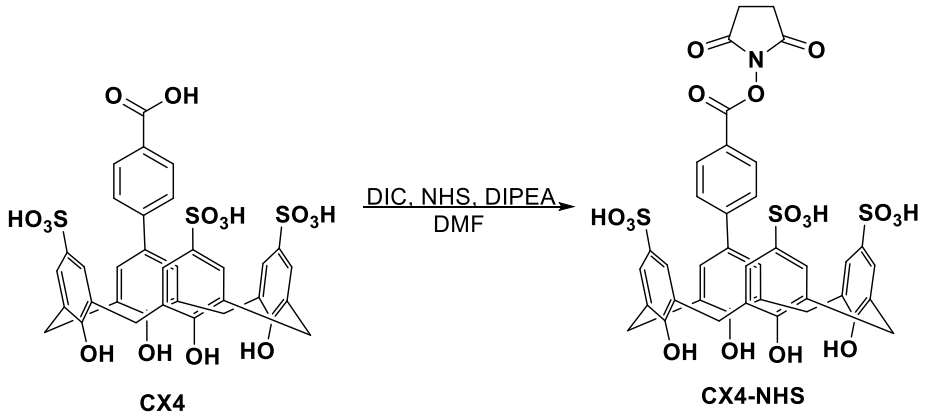

CX4 (made as previously described in the literature)[164] (0.00559 g, 7 µmol) and NHS (0.00097 g, 8 µmol) were dissolved in dry DMF (0.2 mL) and molecular sieves were added. DIPEA (1 µL, 6 µmol) was added, followed by DIC (1.5 µL, 9 µmol) and the solution was let stir for 2 hours. NHS (0.00097 g, 8 µmol) was again added, and the reaction was let stir for an additional 2 hours. The crude reaction mixture was then used to attach to resin as outlined below.

Attachment of **CX4** to Sepharose resin

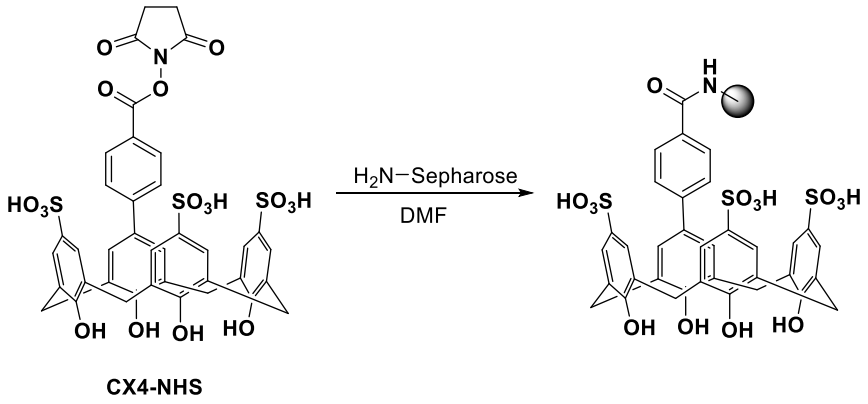

CX4-NHS

0.3 mL of H_2N-Sepharose resin was let incubate in the crude **CX4-NHS** reaction mixture over night. The incubation solution was decanted, and the resin washed with DMF, DCM, MeOH, H_2O, and the buffer to be used for elution.

Attachment of **A_2B** to Sepharose resin

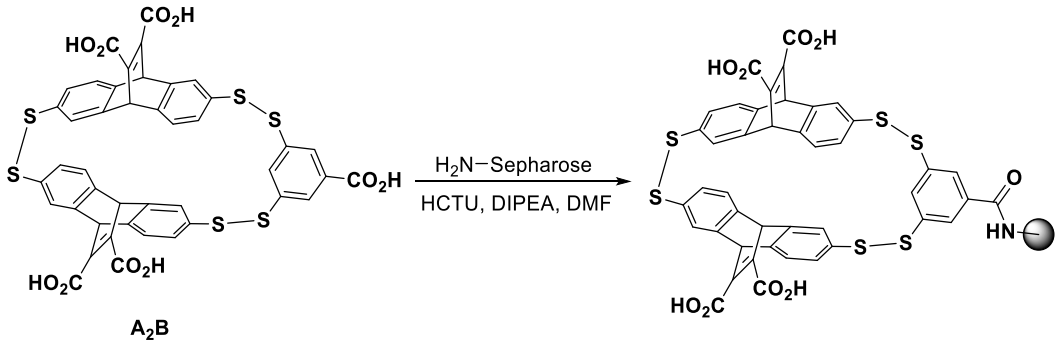

A_2B

0.3 mL of H_2N-Sepharose resin was let incubate in a solution of **A_2B** (0.005 g, 5.6 µmol), HCTU (0.0099 g, 23.9 µmol), and DIPEA (8.4 µL, 48.2 µmol), in DMF overnight. The incubation solution was decanted, and the resin washed with DMF, DCM, MeOH, H_2O, and the buffer to be used for elution.

Immobilization of **A_2B-PEG$_3$-Biotin** onto NeutrAvidin agarose resin

0.25 mL of resin slurry (Pierce Neutravidin Resin; Thermo Scientific, catalog # 29204) was centrifuged and the supernatant was decanted. The resin was washed with 1X PBS buffer (3 times), and 0.6 mL of 50 µM **A_2B-PEG$_3$-Biotin** in 1X PBS buffer was added and let incubate over night at 4 °C. The resin was then washed with 1X PBS buffer (3 times), followed by water (3 times).

Affinity Chromatography with **A_2B-PEG$_3$-Biotin** on NeutrAvidin Agarose Resin

A_2B-PEG$_3$-Biotin bound resin was prepared as outlined above, and 0.25 mL were packed into a 1 mL plastic column. The resin was washed with 3 column volumes of 10 mM borate buffer (pH 8.5), and 25 µL of 5 uM H3K5Me$_3$ and 5 uM H3K5prop in 10 mM borate buffer (pH 8.5) were loaded onto the column. 10 mM borate buffer (pH 8.5) (5X column volume), followed by 10 mM borate+120 mM NaCl buffer (pH 8.5) (5X column volume) were run through the column, and fractions were collected (1 column volume/fraction).

For the negative control, the column was packed with NeutrAvidin Agarose resin (not bound to a receptor).

All collected fractions were lyophilized and desalted (as described in literature[165]) prior to LC-MS/MS analysis.

ITC Binding Studies

All ITC titrations were performed using a MicroCal AutoiTC200 at 26 °C. Data analysis was performed using the built in Origin 7 software using a one site binding model. A 10 mM pH 8.5 sodium borate buffer was used for all experiments. All concentrations were determined using a NanoDrop2000 with a xenon flash lamp, 2048 element linear silicon CCD array detector, and 1 mm path length. ~1.1–2.4 mM solutions of peptide were titrated into ~100–180 μM solutions of receptor using 2 μL injections every 3 minutes. Heats of dilution of peptides were subtracted prior to analysis in Origin.

REFERENCES

(1) Wang, G. G.; Allis, C. D.; Chi, P. *Trends Mol. Med.* **2007**, *13* (9), 363.

(2) Bhaumik, S. R.; Smith, E.; Shilatifard, A. *Nat. Struct. Mol. Biol.* **2007**, *14* (11), 1008.

(3) Ingerman, L. A.; Cuellar, M. E.; Waters, M. L. *Chem. Commun. (Camb).* **2010**, *46* (11), 1839.

(4) Wu, D.; Sylvester, J.; Parker, L.; Zhou, G.; Kron, S. J. *Biopolymers* **2011**, *94* (4), 475.

(5) Yewdell, J. W.; Reits, E.; Neefjes, J. *Nat. Rev. Immunol.* **2003**, *3* (12), 952.

(6) Prével, C.; Pellerano, M.; Van, T. N. N.; Morris, M. C. *Biotechnol. J.* **2014**, *9* (2), 253.

(7) Blow, N. *Nature* **2007**, *447* (7145), 741.

(8) González-Vera, J. a. *Chem. Soc. Rev.* **2012**, *41* (5), 1652.

(9) Zhao, N.; He, Y.; Mao, X.; Sun, Y.; Zhang, X.; Li, C. zhong; Lin, Y.; Liu, G. *Electrochem. commun.* **2010**, *12* (3), 471.

(10) Adjemian, J.; Anne, A.; Cauet, G.; Demaille, C. *Langmuir* **2010**, *26* (12), 10347.

(11) Ohtsuka, K.; Maekawa, I.; Waki, M.; Takenaka, S. *Anal. Biochem.* **2009**, *385* (2), 293.

(12) Liu, G.; Wang, J.; Wunschel, D. S.; Lin, Y. *J. Am. Chem. Soc.* **2006**, *128* (38), 12382.

(13) Kerman, K.; Kraatz, H.-B. *Analyst* **2009**, *134* (12), 2400.

(14) Kerman, K.; Mahmoud, K. A.; Kraatz, H.-B. *Chem. Commun.* **2007**, *37*, 3829.

(15) Xiao, H.; Liu, L.; Meng, F.; Huang, J.; Li, G. *Anal. Chem.* **2008**, *80* (13), 5272.

(16) Mahmoud, K. A.; Hrapovic, S.; Luong, J. H. T. *ACS Nano* **2008**, *2* (5), 1051.

(17) Cheng, W.; Chen, Y.; Yan, F.; Ding, L.; Ding, S.; Ju, H.; Yin, Y. *Chem. Commun. (Camb).* **2011**, *47* (10), 2877.

(18) Yan, X.; Yang, L.; Wang, Q. *Angew. Chemie - Int. Ed.* **2011**, *50* (22), 5130.

(19) Liu, Q.; Wang, J.; Boyd, B. J. *Talanta*. 2015, pp 114–127.

(20) Pavan, S.; Berti, F. *Analytical and Bioanalytical Chemistry*. 2012, pp 3055–3070.

(21) González-Vera, J.; Morris, M. *Proteomes* **2015**, *3* (4), 369.

(22) Yeh, R.-H.; Yan, X.; Cammer, M.; Bresnick, A. R.; Lawrence, D. S. *Real time visualization of protein kinase activity in living cells.*; in Press, 2002; Vol. 277.

(23) Wang, Q.; Lawrence, D. S. *J. Am. Chem. Soc.* **2005**, *127* (21), 7684.

(24) Van, T. N. N.; Pellerano, M.; Lykaso, S.; Morris, M. C. *ChemBioChem* **2014**, No. 15, 2298.

(25) Ellard, J. M.; Zollitsch, T.; Cummins, W. J.; Hamilton, A. L.; Bradley, M. *Angew. Chemie - Int. Ed.* **2002**, *41* (17), 3233.

(26) Akers, W. J.; Xu, B.; Lee, H.; Sudlow, G. P.; Fields, G. B.; Achilefu, S.; Edwards, W. B. *Bioconjug. Chem.* **2012**, *23* (3), 656.

(27) Marme, N.; Knemeyer, J. P.; Sauer, M.; Wolfrum, J. *Bioconjug. Chem.* **2003**, *14* (6), 1133.

(28) Chen, H.; Ahsan, S. S.; Santiago-Berrios, M. B.; Abruna, H. D.; Webb, W. W. *J. Am. Chem. Soc.* **2010**, *132* (21), 7244.

(29) Sharma, V.; Agnes, R. S.; Lawrence, D. S. *J. Am. Chem. Soc.* **2007**, *129* (10), 2742.

(30) Agnes, R. S.; Jernigan, F.; Shell, J. R.; Sharma, V.; Lawrence, D. S. *J. Am. Chem. Soc.* **2010**, *132* (17), 6075.

(31) Oien, N. P.; Nguyen, L. T.; Jernigan, F. E.; Priestman, M. A.; Lawrence, D. S. *Angew. Chemie - Int. Ed.* **2014**, *53* (15), 3975.

(32) Mock, M.; Roques, B. P. *Proc. Natl. Acad. Sci. U. S. A.* **2002**, *99* (10), 6527.

(33) Fudala, R.; Ranjan, A. P.; Mukerjee, A.; Vishwanatha, J. K.; Gryczynski, Z.; Borejdo, J.; Sarkar, P.; Gryczynski, I. *Curr. Pharm. Biotechnol.* **2011**, *12* (5), 834.

(34) Hirata, J.; Chung, L. P.; Ariese, F.; Irth, H.; Gooijer, C. *J. Chromatogr. A* **2005**, *1081*, 140.

(35) Lowe, S. B.; Dick, J. A. G.; Cohen, B. E.; Stevens, M. M. *ACS Nano* **2012**, *6* (1), 851.

(36) Prasuhn, D. E.; Feltz, A.; Blanco-Canosa, J. B.; Susumu, K.; Stewart, M. H.; Mei, B. C.; Yakovlev, A. V; Loukov, C.; Mallet, J. M.; Oheim, M.; Dawson, P. E.; Medintz, I. L. *ACS Nano* **2010**, *4* (9), 5487.

(37) Sapsford, K. E.; Granek, J.; Deschamps, J. R.; Boeneman, K.; Blanco-Canosa, J. B.; Dawson, P. E.; Susumu, K.; Stewart, M. H.; Medintz, I. L. *ACS Nano* **2011**, *5* (4), 2687.

(38) Sapsford, K. E.; Farrell, D.; Sun, S.; Rasooly, A.; Mattoussi, H.; Medintz, I. L. *Sensors Actuators, B Chem.* **2009**, *139* (1), 13.

(39) Proctor, A.; Wang, Q.; Lawrence, D. S.; Allbritton, N. L. *Analyst* **2012**, *137* (13), 3028.

(40) Proctor, A.; Wang, Q.; Lawrence, D. S.; Allbritton, N. L. *Anal. Chem.* **2012**, *84* (16), 7195.

(41) Turner, A. H.; Lebhar, M. S.; Proctor, A.; Wang, Q.; Lawrence, D. S.; Allbritton, N. L. *ACS Chem. Biol.* **2015**, *11*, 355.

(42) Phillips, R. M.; Bair, E.; Lawrence, D. S.; Sims, C. E.; Allbritton, N. L. *Anal. Chem.* **2013**, *85* (12), 6136.

(43) Mainz, E. R.; Dobes, N. C.; Allbritton, N. L. *Anal. Chem.* **2015**, *87* (15), 7987.

(44) Zigoneanu, I. G.; Sims, C. E.; Allbritton, N. L. *Anal. Bioanal. Chem.* **2015**, *407* (30), 8999.

(45) Geier, E.; Pfeifer, G.; Wilm, M.; Lucchiari-Hartz, M.; Baumeister, W.; Eichmann, K.;

Niedermann, G. *Science* **1999**, *283* (February), 978.

(46) Tomkinson, B. *Trends Biochem. Sci.* **1999**, *24* (9), 355.

(47) Glas, R.; Preta, G.; De Klark, R.; Gavioli, R. *J. Oncol.* **2010**, *2010*, 1.

(48) Saric, T.; Beninga, J.; Graef, C. I.; Akopian, T. N.; Rock, K. L.; Goldberg, A. L. *J. Biol. Chem.* **2001**, *276* (39), 36474.

(49) Fulop, V.; Bocskei, Z.; Polgar, L. *Cell* **1998**, *94* (2), 161.

(50) Turzynski, A.; Mentlein, R. *Eur. J. Biochem.* **1990**, *190* (3), 509.

(51) Beninga, J.; Rock, K. L.; Goldberg, A. L. *J. Biol. Chem.* **1998**, *273* (30), 18734.

(52) Brandstetter, H.; Kim, J. S.; Groll, M.; Huber, R. *Nature* **2001**, *414* (6862), 466.

(53) Pal, A.; Kraetzner, R.; Gruene, T.; Grapp, M.; Schreiber, K.; Gronborg, M.; Urlaub, H.; Becker, S.; Asif, A. R.; Gartner, J.; Sheldrick, G. M.; Steinfeld, R. *J. Biol. Chem.* **2009**, *284* (6), 3976.

(54) Guhaniyogi, J.; Sohar, I.; Das, K.; Stock, A. M.; Lobel, P. *J. Biol. Chem.* **2009**, *284* (6), 3985.

(55) Ray, K.; Hines, C. S.; Coll-Rodriguez, J.; Rodgers, D. W. *J. Biol. Chem.* **2004**, *279* (19), 20480.

(56) Kaspar, A. A.; Reichert, J. M. *Drug Discovery Today*. 2013, pp 807–817.

(57) Weinstock, M. T.; Francis, J. N.; Redman, J. S.; Kay, M. S. *Biopolymers* **2012**, *98* (5), 431.

(58) Pollaro, L.; Heinis, C. *Medchemcomm* **2010**, *1* (5), 319.

(59) Dennis, M. S.; Zhang, M.; Gloria Meng, Y.; Kadkhodayan, M.; Kirchhofer, D.; Combs, D.; Damico, L. A. *J. Biol. Chem.* **2002**, *277* (38), 35035.

(60) Hopp, J.; Hornig, N.; Zettlitz, K. A.; Schwarz, A.; Fuß, N.; Müller, D.; Kontermann, R. E. *Protein Eng. Des. Sel.* **2010**, *23* (11), 827.

(61) Levy, O. E.; Jodka, C. M.; Ren, S. S.; Mamedova, L.; Sharma, A.; Samant, M.; D'Souza, L. J.; Soares, C. J.; Yuskin, D. R.; Jin, L. J.; Parkes, D. G.; Tatarkiewicz, K.; Ghosh, S. S. *PLoS One* **2014**, *9* (2), 1.

(62) Fosgerau, K.; Hoffmann, T. *Drug Discov. Today* **2015**, *20* (1), 122.

(63) Miller, S. M.; Simon, R. J.; Ng, S.; Zuckermann, R. N.; Kerr, J. M.; Moos, W. H. *Drug Dev. Res.* **1995**, *35* (1), 20.

(64) Hamamoto, K.; Kida, Y.; Zhang, Y.; Shimizu, T.; Kuwano, K. *Microbiol. Immunol.* **2002**, *46* (11), 741.

(65) Tugyi, R.; Uray, K.; Ivan, D.; Fellinger, E.; Perkins, A.; Hudecz, F. *Proc. Natl. Acad. Sci. U. S. A.* **2005**, *102* (2), 413.

(66) Houston, K. M. DEVELOPMENT OF PROTEASE-RESISTANT β-HAIRPIN PEPTIDES FOR THE DETECTION OF ENZYMATIC ACTIVITY IN CANCER CELLS, University of North Carolina at Chapel Hill, 2014.

(67) Hook, D. F.; Bindschadler, P.; Mahajan, Y. R.; Sebesta, R.; Kast, P.; Seebach, D. *Chem. Biodivers.* **2005**, *2* (5), 591.

(68) Frackenpohl, J.; Arvidsson, P. I.; Schreiber, J. V.; Seebach, D. *Chembiochem* **2001**, *2* (6), 445.

(69) Porter, E. A.; Weisblum, B.; Gellman, S. H. *J. Am. Chem. Soc.* **2002**, *124* (25), 7324.

(70) Hill, D. J.; Mio, M. J.; Prince, R. B.; Hughes, T. S.; Moore, J. S. *Chemical Reviews*. 2001, pp 3893–4011.

(71) Goodman, C. M.; Choi, S.; Shandler, S.; DeGrado, W. F. *Nat. Chem. Biol.* **2007**, *3* (5), 252.

(72) Patch, J. A.; Barron, A. E. *Curr. Opin. Chem. Biol.* **2002**, *6* (6), 872.

(73) Cline, L. L.; Waters, M. L. *Pept. Sci.* **2009**, *92* (6), 502.

(74) Yang, S.; Proctor, A.; Cline, L. L.; Houston, K. M.; Waters, M. L.; Allbritton, N. L. *Analyst* **2013**, *138* (15), 4305.

(75) Roxin, A.; Zheng, G. *Future Med. Chem.* **2012**, *4* (12), 1601.

(76) Tapeinou, A.; Matsoukas, M.-T.; Simal, C.; Tselios, T. *Biopolymers* **2015**, *104* (5), 453.

(77) Passioura, T.; Katoh, T.; Goto, Y.; Suga, H. *Ann. Rev. Biochem.* **2014**, *83*, 727.

(78) Joo, S. H. *Biomolecules and Therapeutics*. 2012, pp 19–26.

(79) Bockus, A. T.; McEwen, C. M.; Lokey, R. S. *Curr. Top. Med. Chem.* **2013**, *13*, 821.

(80) Byk, G.; Halle, D.; Zeltser, I.; Bitan, G.; Selinger, Z.; Gilon, C. *J. Med. Chem.* **1996**, *39* (16), 3174.

(81) Hess, S.; Ovadia, O.; Shalev, D. E.; Senderovich, H.; Qadri, B.; Yehezkel, T.; Salitra, Y.; Sheynis, T.; Jelinek, R.; Gilon, C.; Hoffman, A. *J. Med. Chem.* **2007**, *50* (24), 6201.

(82) Hess, S.; Linde, Y.; Ovadia, O.; Safrai, E.; Shalev, D. E.; Swed, A.; Halbfinger, E.; Lapidot, T.; Gilon, C.; Hoffman, A. *Obesity* **2008**, *51*, 1026.

(83) Tal-Gan, Y.; Hurevich, M.; Klein, S.; Ben-Shimon, A.; Rosenthal, D.; Hazan, C.; Shalev, D. E.; Niv, M. Y.; Levitzki, A.; Gilon, C. *J. Med. Chem.* **2011**, *54* (14), 5154.

(84) White, C. J.; Yudin, A. K. *Nat. Chem.* **2011**, *3* (7), 509.

(85) Shchemelinin, I.; Sefc, L.; Necas, E. *Folia Biologica*. 2006, pp 81–101.

(86) Fabbro, D.; Cowan-Jacob, S. W.; Moebitz, H. *British Journal of Pharmacology*. June 2015, pp 2675–2700.

(87) Zhang, J.; Yang, P. L.; Gray, N. S. *Nat. Rev. Cancer* **2009**, *9* (1), 28.

(88) Kunkel, M. T.; Ni, Q.; Tsien, R. Y.; Zhang, J.; Newton, A. C. *J. Biol. Chem.* **2005**, *280* (7), 5581.

(89) Li, H.; Sims, C. E.; Kaluzova, M.; Stanbridge, E. J.; Allbritton, N. L. *Biochemistry* **2004**, *43* (6), 1599.

(90) Kier, B. L.; Andersen, N. H. *J. Pept. Sci.* **2014**, *20* (9), 704.

(91) Kier, B. L.; Shu, I.; Eidenschink, L. a; Andersen, N. H. *Proc. Natl. Acad. Sci. U. S. A.* **2010**, *107* (23), 10466.

(92) Park, J. H.; Waters, M. L. *Org. Biomol. Chem* **2013**, *11*, 69.

(93) Logsdon, L. A.; Schardon, C. L.; Ramalingam, V.; Kwee, S. K.; Urbach, A. R. *J. Am. Chem. Soc.* **2011**, *133* (42), 17087.

(94) Logsdon, L. A.; Urbach, A. R. *J. Am. Chem. Soc.* **2013**, *135* (31), 11414.

(95) Ramalingam, V.; Urbach, A. R. *Org. Lett.* **2011**, *13* (18), 4898.

(96) Hawker, C. J.; Wooley, K. L.; Fréchet, J. M. J. *J. Chem. Soc. Perkin Trans. 1* **1993**, No. 12, 1287.

(97) Aertgeerts, K.; Tennant, M. G.; Kraus, M. L.; Rogers, J.; Sang, B.; Skene, R. J.; Webb, D. R.; Sridhar Prasad, G. *Protein Sci.* **2004**, *13* (2), 412.

(98) Yasuda, I.; Kishimoto, A.; Tanaka, S.-I.; Tominaga, M.; Sakurai, A.; Nishizuka, Y. *Biochem. Biophys. Res. Commun. Febr.* **1990**, *166* (14), 1220.

(99) Songyang, Z.; Carraway, K. L.; Eck, M. J.; Harrison, S. C.; Feldman, R. A.; Mohammadi, M.; Schlessinger, J.; Hubbard, S. R.; Smith, D. P.; Eng, C. *Nature*. 1995, pp 536–539.

(100) Skorobogatyi, M. V; Pchelintseva, A. A.; Petrunina, A. L.; Stepanova, I. A.; Andronova, V. L.; Galegov, G. A.; Malakhov, A. D.; Korshun, V. A. *Tetrahedron* **2006**, *62* (6), 1279.

(101) Schellinger, J. G.; Danan-Leon, L. M.; Hoch, J. A.; Kassa, A.; Srivastava, I.; Davis, D.; Gervay-Hague, J. *J. Am. Chem. Soc.* **2011**, *133* (10), 3230.

(102) Annuziato, A. T. *Nat. Educ.* **2008**, *1* (1), 26.

(103) McGinty, R. K.; Tan, S. *Chem. Rev.* **2015**, *115* (6), 2255.

(104) Kouzarides, T. *Cell* **2007**, *128*, 693.

(105) Bannister, A. J.; Kouzarides, T. *Cell Res.* **2011**, *21* (3), 381.

(106) Fuchs, S. M.; Krajewski, K.; Baker, R. W.; Miller, V. L.; Strahl, B. D. *Curr. Biol.* **2011**, *21* (1), 53.

(107) Kazanecki, C. C.; Kowalski, A. J.; Ding, T.; Rittling, S. R.; Denhardt, D. T. *J. Cell. Biochem.* **2007**, *102* (4), 925.

(108) Williams, B. A. R.; Lin, L.; Lindsay, S. M.; Chaput, J. C. *J. Am. Chem. Soc.* **2009**, *131* (18), 6330.

(109) Uhlen, M. *BioTechniques*. 2008, pp 649–654.

(110) Huang, H.; Lin, S.; Garcia, B. A.; Zhao, Y. *Chem. Rev.* **2015**, *115* (6), 2376.

(111) Aebersold, R.; Mann, M. *Nature* **2003**, *422* (6928), 198.

(112) Zhao, Y.; Jensen, O. N. *Proteomics* **2009**, *9* (20), 4632.

(113) Ficarro, S. B.; McCleland, M. L.; Stukenberg, P. T.; Burke, D. J.; Ross, M. M.; Shabanowitz, J.; Hunt, D. F.; White, F. M. *Nat. Biotechnol.* **2002**, *20* (3), 301.

(114) Nuhse, T. S.; Stensballe, A.; Jensen, O. N.; Peck, S. C. *Mol. Cell. Proteomics* **2003**, *2* (11), 1234.

(115) Jensen, S. S.; Larsen, M. R. *Rapid Commun. Mass Spectrom.* **2007**, *21* (22), 3635.

(116) Aryal, U. K.; Ross, A. R. *Rapid Commun Mass Spectrom* **2010**, *24* (2), 219.

(117) Thingholm, T. E.; Larsen, M. R.; Ingrell, C. R.; Kassem, M.; Jensen, O. N. *J. Proteome Res.* **2008**, *7* (8), 3304.

(118) Olsen, J. V; Blagoev, B.; Gnad, F.; Macek, B.; Kumar, C.; Mortensen, P.; Mann, M. *Cell* **2006**, *127* (3), 635.

(119) Kho, Y.; Kim, S. C.; Jiang, C.; Barma, D.; Kwon, S. W.; Cheng, J.; Jaunbergs, J.; Weinbaum, C.; Tamanoi, F.; Falck, J.; Zhao, Y. *Proc. Natl. Acad. Sci. U. S. A.* **2004**, *101* (34), 12479.

(120) Kostiuk, M. A.; Corvi, M. M.; Keller, B. O.; Plummer, G.; Prescher, J. A.; Hangauer, M. J.; Bertozzi, C. R.; Rajaiah, G.; Falck, J. R.; Berthiaume, L. G. *FASEB J.* **2008**, *22* (3), 721.

(121) Martin, D. D. O.; Vilas, G. L.; Prescher, J. A.; Rajaiah, G.; Falck, J. R.; Bertozzi, C. R.; Berthiaume, L. G. *FASEB J.* **2008**, *22* (3), 797.

(122) Binda, O.; Boyce, M.; Rush, J. S.; Palaniappan, K. K.; Bertozzi, C. R.; Gozani, O. *ChemBioChem* **2011**, *12* (2), 330.

(123) Islam, K.; Zheng, W.; Yu, H.; Deng, H.; Luo, M. *ACS Chem. Biol.* **2011**, *6* (7), 679.

(124) Islam, K.; Bothwell, I.; Chen, Y.; Sengelaub, C.; Wang, R.; Deng, H.; Luo, M. *J. Am. Chem. Soc.* **2011**, *134*, 5909.

(125) Wang, R.; Zheng, W.; Yu, H.; Deng, H.; Luo, M. *J. Am. Chem. Soc.* **2011**, *133* (20), 7648.

(126) Zhang, J.; Zheng, Y. G. *ACS Chem. Biol.* **2016**, *11* (3), 583.

(127) Fischle, W.; Schwarzer, D. *ACS Chem. Biol.* **2016**, *11* (3), 689.

(128) Wells, L.; Vosseller, K.; Cole, R. N.; Cronshaw, J. M.; Matunis, M. J.; Hart, G. W. *Mol. Cell. Proteomics* **2002**, *1* (10), 791.

(129) Zhang, H.; Li, X.-J.; Martin, D. B.; Aebersold, R. *Nat. Biotechnol.* **2003**, *21* (6), 660.

(130) Tian, Y. A.; Zhou, Y.; Elliott, S.; Aebersold, R.; Zhang, H. *Nat. Protoc.* **2007**, *2* (2), 334.

(131) Lewallen, D. M.; Bicker, K. L.; Subramanian, V.; Clancy, K. W.; Slade, D. J.; Martell, J.; Dreyton, C. J.; Sokolove, J.; Weerapana, E.; Thompson, P. R. *ACS Chem. Biol.* **2015**, *10* (11), 2520.

(132) Kim, S. C.; Sprung, R.; Chen, Y.; Xu, Y.; Ball, H.; Pei, J.; Cheng, T.; Kho, Y.; Xiao, H.; Xiao, L.; Grishin, N. V; White, M.; Yang, X. J.; Zhao, Y. *Mol. Cell* **2006**, *23* (4), 607.

(133) Zhang, J.; Sprung, R.; Pei, J.; Tan, X.; Kim, S.; Zhu, H.; Liu, C.-F.; Grishin, N. V.; Zhao, Y. *Mol. Cell. Proteomics* **2009**, *8* (2), 215.

(134) Hebert, A. S.; Dittenhafer-Reed, K. E.; Yu, W.; Bailey, D. J.; Selen, E. S.; Boersma, M. D.; Carson, J. J.; Tonelli, M.; Balloon, A. J.; Higbee, A. J.; Westphall, M. S.; Pagliarini, D. J.; Prolla, T. A.; Assadi-Porter, F.; Roy, S.; Denu, J. M.; Coon, J. J. *Mol. Cell* **2013**, *49* (1), 186.

(135) Ong, S.-E.; Mittler, G.; Mann, M. *Nat. Methods* **2004**, *1* (2), 119.

(136) Zhan, X.; Desiderio, D. M. *Anal. Biochem.* **2006**, *354* (2), 279.

(137) Egelhofer, T. A.; Minoda, A.; Klugman, S.; Lee, K.; Kolasinska-Zwierz, P.; Alekseyenko, A. A.; Cheung, M.-S.; Day, D. S.; Gadel, S.; Gorchakov, A. A.; Gu, T.; Kharchenko, P. V; Kuan, S.; Latorre, I.; Linder-Basso, D.; Luu, Y.; Ngo, Q.; Perry, M.; Rechtsteiner, A.; Riddle, N. C.; Schwartz, Y. B.; Shanower, G. A.; Vielle, A.; Ahringer, J.; Elgin, S. C. R.; Kuroda, M. I.; Pirrotta, V.; Ren, B.; Strome, S.; Park, P. J.; Karpen, G. H.; Hawkins, R. D.; Lieb, J. D. *Nat. Struct. Mol. Biol.* **2011**, *18* (1), 91.

(138) Rothbart, S. B.; Lin, S.; Britton, L.-M.; Krajewski, K.; Keogh, M.-C.; Garcia, B. a; Strahl, B. D. *Sci. Rep.* **2012**, *2*, 489.

(139) Kim, J. Y.; Kim, S. K.; Kang, D.; Moon, M. H. *Anal. Chem.* **2012**, *84* (12), 5343.

(140) Madera, M.; Mann, B.; Mechref, Y.; Novotny, M. V. *J. Sep. Sci.* **2008**, *31* (14), 2722.

(141) Xiong, L.; Regnier, F. E. *J. Chromatogr. B Anal. Technol. Biomed. Life Sci.* **2002**, *782* (1-2), 405.

(142) Geng, M.; Zhang, X.; Bina, M.; Regnier, F. *J. Chromatogr. B Biomed. Sci. Appl.* **2001**, *752* (2), 293.

(143) Yang, Z.; Harris, L. E.; Palmer-Toy, D. E.; Hancock, W. S. *Clin. Chem.* **2006**, *52* (10), 1897.

(144) Moore, K. E.; Carlson, S. M.; Camp, N. D.; Cheung, P.; James, R. G.; Chua, K. F.; Wolf-Yadlin, A.; Gozani, O. *Mol. Cell* **2013**, *50* (3), 444.

(145) Raasi, S.; Varadan, R.; Fushman, D.; Pickart, C. M. *Nat. Struct. Mol. Biol.* **2005**, *12* (8), 708.

(146) Dani, N.; Stilla, A.; Marchegiani, A.; Tamburro, A.; Till, S.; Ladurner, A. G.; Corda, D.; Di Girolamo, M. *Proc. Natl. Acad. Sci. U. S. A.* **2009**, *106* (11), 4243.

(147) Williams, B. A. R.; Diehnelt, C. W.; Belcher, P.; Greving, M.; Woodbury, N. W.; Johnston, S. A.; Chaput, J. C. *J. Am. Chem. Soc.* **2009**, *131* (47), 17233.

(148) Beaver, J. E.; Waters, M. L. **2016**, *11*, 643.

(149) Coleman, A. W.; Perret, F.; Moussa, A.; Dupin, M.; Guo, Y.; Perron, H. *Top. Curr. Chem.* **2007**, *277*, 31.

(150) Beshara, C. S.; Jones, C. E.; Daze, K. D.; Lilgert, B. J.; Hof, F. *ChemBioChem* **2010**, *11* (1), 63.

(151) Douteau-Guevel, N.; Coleman, A. W.; Morel, J.-P.; Morel-Desrosiers, N. *J. Chem. Soc. Perkin Trans. 2* **1999**, No. 3, 629.

(152) Pinkin, N. K.; Waters, M. L. *Org. Biomol. Chem.* **2014**, *12*, 7059.

(153) James, L. I.; Beaver, J. E.; Rice, N. W.; Waters, M. L. *J. Am. Chem. Soc.* **2013**, *135* (17), 6450.

(154) Beaver, J. E.; Peacor, B. C.; Bain, J. V; James, L. I.; Waters, M. L. *Org. Biomol. Chem.* **2015**, *13*, 3220.

(155) Gamal-Eldin, M. A.; Macartney, D. H. *Org. Biomol. Chem.* **2013**, *11* (3), 488.

(156) Petti, M. A.; Shepodd, T. J.; Barrans, R. E. J.; Dougherty, D. A. *J. Am. Chem. Soc.* **1988**, *110* (1), 6825.

(157) Ngola, S. M.; Kearney, P. C.; Mecozzi, S.; Russell, K.; Dougherty, D. A. *J. Am. Chem. Soc.* **1999**, *121* (6), 1192.

(158) Simpson, M. G.; Pittelkow, M.; Watson, S. P.; Sanders, J. K. M. *Org. Biomol. Chem.* **2010**, *8* (5), 1181.

(159) Corbett, P. T.; Leclaire, J.; Vial, L.; West, K. R.; Wietor, J.; Sanders, J. K. M.; Otto, S.; Furlan, R. L. E.; Sanders, J. K. M. *Drug Discov. Today* **2010**, *7* (2), 3652.

(160) Otto, S.; Furlan, R. L. E.; Sanders, J. K. M. *Current Opinion in Chemical Biology*. 2002, pp 321–327.

(161) Pinkin, N. K.; N. Power, A.; Waters, M. L. *Org. Biomol. Chem.* **2015**, *13* (44), 10939.

(162) Beaver, J. E. The Development of Small Molecule Receptors for Modified Amino Acids in Water, University of North-Carolina at Chapel Hill, 2014.

(163) Lin, S.; Garcia, B. A. In *Methods in Enzymology*; Elsevier Inc., 2012; Vol. 512, pp 3–28.

(164) Daze, K. D.; Ma, M. C. F.; Pineux, F.; Hof, F. *Org. Lett.* **2012**, *14* (6), 1512.

(165) Rappsilber, J.; Mann, M.; Ishihama, Y. *Nat. Protoc.* **2007**, *2* (8), 1896.

(166) George, J.; Norey, C. Use of CyDye Fluors for Improved FRET Protease Assays on BMG POLARstar Fluorescence Microplate Reader http://bmglabtech.customers.condeon.net/media/35216/1044070.pdf (accessed May 12, 2016).

(167) Tollervey, J. R.; Lunyak, V. V. *Epigenetics* **2012**, *7* (8), 823.